UC Davis

UC Davis Electronic Theses and Dissertations

Title

Functional Morphology and Evolutionary Pathways in the Locomotor System of Coral Reef Fishes

Permalink

https://escholarship.org/uc/item/3140t12p

Author

Satterfield, Darien Rose

Publication Date

2024

Peer reviewed|Thesis/dissertation

eScholarship.org Powered by the California Digital Library
University of California

Functional Morphology and Evolutionary Pathways in the Locomotor System of Coral Reef Fishes

By

DARIEN ROSE SATTERFIELD
DISSERTATION

Submitted in partial satisfaction of the requirements for the degree of

DOCTOR OF PHILOSOPHY

in

Population Biology

in the

OFFICE OF GRADUATE STUDIES

of the

UNIVERSITY OF CALIFORNIA

DAVIS

Approved:

Peter Wainwright, Chair

Kate Laskowski

John Stachowicz

Committee in Charge

2024

DISSERTATION ABSTRACT

Coral reef fishes represent one of the most morphologically and functionally diverse vertebrate groups. Reef fishes contain more than 70 families of ray-finned fishes including speciose groups that are most abundant on reefs like wrasses, butterflyfish, damselfish, surgeonfish, and angelfish. However, also present in the reef fish assemblage are species with unique morphologies and highly specialized ecologies like frogfishes, pufferfish, triggerfish, and moray eels. Reef fish occupy all levels of the trophic pyramid from detritivores and algivores, microbial specialists, planktivores, invertivores, and carnivores. The trophic diversity is matched by diversity in habitat usage from species which are highly coral associated to those that exist exclusively in the open water above and near the reef. Further, reef fish are highly variable in their locomotor styles with species that swim exclusively using their body and caudal fin undulation to those that use numerous combinations of the median and paired fins for propulsion. Broadly, my dissertation uses phylogenetic comparative methods to explore the relationships between morphological, behavioral, and functional diversity in coral reef fishes, and to determine the evolutionary pathways reef fish have taken to diversify into novel conditions.

It is widely believed that because of biomechanical trade-offs, fish body shape and the mode of propulsion are strong predictors of swimming performance, with the best cruisers, maneuverers, and accelerators having different body forms and emphasizing different propulsion mechanisms. This paradigm is regularly projected onto routine swimming behavior and dominates the ecomorphological literature, despite the paucity of field measurements. In my first chapter, I measure variation in swimming behavior among 48 species of Indian Ocean coral reef fishes using recordings from a remote stereo video system. I measured average swimming speed, average swimming bout distance, frequency of turns, and percent of time spent station-holding

and looked for the predicted trade-offs between them. I find little evidence of the expected relationships between swimming behaviors across species, little evidence that body shape affects swimming, and few differences between species that swim by undulating the body and those that emphasize the use of median and paired fins. Taxa widely thought of as archetypical maneuverers (*Chaetodon*) and cruisers (*Caranx*) were not outliers in any behaviors. My results indicate that swimming behavior is not easily predicted from simple measures of body shape and that alternative swimming modes can produce comparable behavioral profiles.

In my second chapter I further explore swimming diversity, though in this chapter I emphasize the effects of locomotor mode on fin shape evolution. In complex functional systems composed of many traits, selection can induce trait evolution by acting directly on individual components within the system, or indirectly through networks of trait integration. As a result, tension exists between the functional and developmental causes of trait integration and the capacity for diversification. I explore this dynamic in the evolution of fin shapes in 106 species from 38 families of coral reef fishes, a polyphyletic assemblage that shows exceptional diversity in locomotor function. Despite strong shared developmental pathways and expectations of a strong match between form and function, I find that species that share locomotor mode show substantial disparity in fin shape, and preferred locomotor mode is a poor predictor of fin shape. The evolution of fin shape is weakly integrated across the four functionally dominant fins and is weakened during transitions to derived swimming modes. As fin evolution is not strongly integrated there is substantial off-axis independent diversification, repeating a pattern found in many vertebrate systems. My study highlights the need for additional work on the functional consequences of fin shape in fishes and the diversifying impact of functions other than locomotion.

Trait integration and modularity have both been shown to be potent mechanisms in morphological evolution. While integration can provide access to morphologically novel phenotypes at the endpoints of axes of trait covariation, extreme phenotypes can also manifest via modular evolution producing novel trait combinations. It is unclear what the relative contributions of these two pathways are in accounting for the origins of novel or extreme forms. In my third chapter, I compare the importance of integration and modular evolution in generating novel forms in the body of coral reef fishes. I estimate novelty accommodating six morphological modules across the reef fish body and describe the evolutionary tendency of species to conform to axes of integration among modules. While just under a fifth of all reef fish species achieve extreme morphologies, evolution to the far reaches of integrated axes occurs slightly more often as the evolution of highly unique trait combinations. Through simulations, I show that strong evolutionary integration produces greater morphological novelty but only along axes of trait covariation, while weak integration allows species to enter the outer regions of morphospace with novel trait combinations but produces less extreme morphologies. Reef fishes closely match diversification under moderate integration, in which species evolve into novel regions of morphospace along integrated axes and through the evolution of extreme trait combinations facilitated by independence of modules.

ACKNOWLEDGEMENTS

I thought I wanted to be an astrophysicist, to explore worlds far beyond our own. I even applied to undergraduate astrophysics programs. Before the end of the summer between high-school and college I realized I would forever be behind a computer screen, when what I wanted was to explore new environments in a hands-on way. If you've ever seen an octopus or a crinoid it isn't hard to understand how otherworldly marine life can be. I switched to marine biology my first day on my undergrad campus. In ichthyology I met fish, and they taught me that there is no one way to exist, and that being different and weird is cool. So first and foremost, I would like to thank fish for inspiring me to be me and for being the perfect system for exploring all of my biggest questions.

I was three years old when I first met my dad, Kevin Goocher. I would not be where I am today if he had not openly embraced the trillions of questions I asked every hour. Where others simply did not have the answers, he always took the time to help me understand the world. The first question I remember asking was in response to Smash Mouth's *Walkin' on the sun* which made me wonder, "how are those people walking on the sun?" This may have been the moment when my dad realized my interest in science and took on the role of encouraging that interest. We watched sci-fi movies and talked all about how we might actually be able to communicate with aliens, we went to visit NASA, and when I struggled with English assignments like spelling (because it wasn't science) he sat with me for countless hours practicing. He continued to refuse to let me give up on myself, he didn't back down on my dreams even when I certainly gave my best effort to derail my path. Dad, when you chose mom, you also chose a little girl who loved science and you never stopped choosing her. I will never be able to express my gratitude for that choice you had no obligation to make.

My mom, Melanie Goocher, could have pursued her college dreams to become an architect, but at 18 years old she opted to give that up so that I could have the best life possible. Unfortunately, college and motherhood are still largely incompatible today, but I will do everything I can to change that for women like my mom. She once said to me, “if you are going to be a scientist you go all the way.” She always told me I could be anything I wanted to be, and though she had no academic background she helped me look into college programs and plan my course schedule. Alone she held me as a newborn. She held me when I flung myself into her lap and sobbed at 19 years old after failing a trigonometry exam. And alone she was the shoulder I slept on through the night in the emergency room when I unexpectedly needed an organ removed in the middle of grad school (because of course that would happen). Her love and support have been my only constant through my entire life. Today I can be a woman in science because of the sacrifices she made. Mom, I love you always, thank you.

Jeremy, you are my person. If I could’ve hand designed someone to be my main support system, my motivator, my life partner, and my adventure buddy that person wouldn’t have been as perfect as you are for me. You have stood by me and my dreams, encouraging me all along the way from undergrad, through masters, and even when I said I wanted to do MORE grad school to get my Ph.D. I feel like we have gotten to watch each other achieve milestones we could’ve never imaged. You always say I’m the only person that does everything I say I will do, and I’m telling you that I will always be the best wife I can be because you have always been the best husband, field work assistant, gear engineer, friend, and my biggest believer. I feel so lucky to share this life with you. Thank you for standing by me always, I love you.

Kota, you are so smart and passionate! I am inspired all the time by the way you see the world and your determination for making a stance to improve the lives of not just yourself but

for people who you've never met. Being a scientist requires being a good mentor and teacher. And you may not have enjoyed this much, but playing school with you was my first chance to learn how to teach. Being your big sister was my first chance to learn how to be an example and how to share my experiences with someone else. Thank you for always listening to my problems, being supportive and encouraging. I know you will do things for this world that are bigger than I could've ever dreamed of and I'm so thankful that I get to be a part of your life. I love you!

I have been blessed to have many maternal figures in my life. Nana, you are hands down the most kind and generous human I've ever known. You have taught me empathy and compassion. You have always been a safe place for me to turn when everywhere else felt tumultuous and uncertain. Thank you for loving me, and hearing my thoughts and opinions, and letting me express my emotions and concerns. Most relevantly, thank you for getting me the computer that all of my dissertation work was done on, and caring for Dixie and Mowgli while I did my field work. And thank you for coparenting Buster with me. Seyla, you are the most wonderful mother-in-law thank you for being a reliable shoulder to lean on as I've gone through school and grown up. LaRae, what would I have done without you?! Your selflessness and willingness to help me with the dogs, meals, and just being a comforting person while I've been away from my family has been a true foundation of how happy I've been during my Ph.D.

Peter Wainwright has seen potential in me that I didn't know existed. He has been the best advisor I could've ever asked for. Peter has taught me so much about science, and fish, and phylogenetic methods but I think most importantly I have learned from Peter how to be a good scientist. He has shown me how to be patient and supportive with students, how to think carefully, and be a good collaborator. Peter, looking back I can see times when you knew I needed a little push to keep moving forward and times when you knew I could handle the

demands of a Ph.D. I never could've imagined how much I would've had to overcome during my time in grad school and your ability to morph your advising style and support to the exact needs of each situation and each student is so inspiring. Thank you for giving me the space to learn and grow and not expecting me to be perfect but guiding me to my best self as a scientist. You changed my life by offering to be my advisor and I can't wait to pass that on to students of my own someday.

I have the best lab mates! Alexus Roberts-Hugghis, Katherine Corn, Nick Peoples, Khalil Russell, Mike Burns., Mike Mihalitsis, Dylan Wainwright, Ashley Adams, Sarah Friedman, Chris Martinez, Ed Burress, and Anthony Barley. I could not be luckier to have had you all as friends and collaborators. I'm so thankful our time in Peter's lab overlapped. I have learned so much from each of you and would not be the scientist I am today without your advice, help, collaboration, and friendship. I hope in 30 years the fish friends are still the life of all the conference outings. I had the help of three amazing undergraduate students Bernice Yin, Sam Hodges-Lisk, and Sky Jung. Without them the research in this dissertation would not have been possible. Thank you all for your time and enthusiasm for these projects! Being your mentor was such a joy.

The Population Biology Grad Group has been a home away from home for me. Each and every one of the students in the grad group means so much to me. My cohort mates are the most wonderful people. Anna Nagel, Brooke Benson, Danielle De La Pascua, Maddie Armstrong, Jasen Liu, Jeff Groh, and Tracie Hayes thank you all so much for being the welcoming, loving, supportive family that you are. To the EVE staff, Sherri Mann, Debbie Davidson, Ruby Wu, Yuliya Yarova-Yarovaya, Shelley Williams and Nick Enos you all are a godsend, I don't know what we would do without you. Thank you for helping to figure out the logistics of my dream

field work and conference travel and everything that you do. To my many professors, but especially the core instructors for 2019 and my QE and dissertation committee members (Louie Yang, Kate Laskowski, Phil Ward, Nann Fangue, and Jay Stachowicz) thank you so much for all you have taught me, and helping me to navigate grad school during a global pandemic and through major life changes. It's been a bumpy road but your genuine care for the pop bio students has made grad school a joy.

To my fieldwork gals and forever besties, Lorilyn Arnold, Meghan Holst, and Devon Ohlwiler thank you for being the greatest friends and marine bio buddies I could've ever asked for. Lori, you have been my emotional rock during grad school, and without your shoulder to lean on I would've been a mess. Devon, you are the most fair, loving, and kind mom and friend and I hope to be like you when I grow up. Meghan, you have been going through some of the toughest parts of grad school with me, and thank goodness I met you! I know we will make a great team for many years to come. I love you all very much and am so thankful to have amazing women as examples of how to be a great mom, a great scientist, and a great friend.

To all the teachers and professors who have believed in me and educated me from academy of the canyons to CSUN and CSULB, thank you for giving a first-gen kid with a passion for science the tools and the pathway to success. Specifically, Michele Siner, Sharon Garvar, Robert Walker, Jason Wilhelm, Mark Steele, Larry Allen, and Darren Johnson, you've all been such a huge part of the journey to this point and I'm so appreciative of what I have learned from you along the way.

Finally, to all of my nieces and nephews, Clarke, Weston, Chloe, Preston, Juliet, Logan, Ethan, Stella, and Max. Being your aunt is my greatest joy in life. Thank you for bringing so many smiles to my face. On my hardest days in grad school, I often would look at your pictures,

check in on your milestones, or use your birthdays as online shopping therapy. Spoiling you is one of the things I look forward to most. I hope I make you all proud, I know you all make me proud. I love you to the ends of the universe and back.

Thank you from the bottom of my heart,

Darien Satterfield

TABLE OF CONTENTS

Dissertation Abstract ii

Acknowledgements v

Table of Contents xi

Chapter 1: Body shape and mode of propulsion do not constrain routine swimming in coral reef fishes 1

Introduction *1*

Methods *6*

Results *10*

Discussion *13*

Figures and Tables *20*

Chapter 2: Weak evolutionary integration allows novel fin shapes and spurs locomotor diversity in coral reef fishes 28

Introduction *28*

Methods *33*

Results *37*

Discussion *44*

Figures and Tables *51*

Chapter 3: Diverse evolutionary pathways to morphological novelty in coral reef fishes 59

Introduction *59*

Methods *64*

Results *71*

Discussion *82*

Figures and Tables *90*

References 100

Appendix 1: Chapter 1 Supplementary Materials 130

Appendix 2: Chapter 2 Supplementary Materials 134

Appendix 3: Chapter 3 Supplementary Materials 144

Chapter 1: Body shape and mode of propulsion do not constrain routine swimming in coral reef fishes

Introduction:

Three axes of swimming performance have dominated thinking about locomotor ecomorphology in fishes: maneuverability, swimming endurance, and acceleration (Blake 2004; Lighthill 1975; Videler 1993). Biomechanical evaluations indicate that specific body shapes correspond to maximum performance on each of these three axes (Webb, 1984a,b). Because of their shape and distribution of fins around the center of mass, laterally compressed, deep-bodied fishes, such as butterflyfishes, are able to turn easily and thought of as highly maneuverable (Konow & Ferry-Graham, 2013; Larouche et al., 2020). In contrast, a body that is deepest in the middle but tapered towards the ends with a thin caudal peduncle, as seen in carangids and scombrids, is considered advantageous for sustained swimming due to low drag from its streamlined shape and low lateral forces at the caudal peduncle (Dewar & Graham, 1994; Donley et al., 2004; Larouche et al., 2020; Videler & Wardle, 1991). Finally, an elongate body with comparatively tall fins and a deep caudal peduncle, as is found in sand perch, supports short bursts of acceleration between periods of station holding because of the large lateral surface area near the posterior end of the fish and long body that can bend into high-amplitude curves (Porter & Motta, 2004; Tytell, 2010). Webb (1984a) originally called these three categories maneuverers, cruisers, and accelerators, respectively (Fig. 1).

These three archetypes represent specialization in their respective behaviors and are thought to reflect trade-offs that prevent fishes from simultaneously achieving high performance on all axes (Webb, 1984b). Fishes with intermediate body morphologies are considered generalists with intermediate performance on multiple axes. As such, generalist have poorer maximum

abilities than specialists on their respective axes but greater performance than specialists on the opposing axes (Fig. 1). This classic fish swimming paradigm is pervasive in literature on the ecomorphology of fish locomotion and generally characterizes how fish body form is thought to influence locomotion (de Barros et al., 2019; Villéger et al., 2017; Wikramanayake, 1990; Winemiller, 1991).

Despite the prominence and usefulness of this model (Astudillo-Clavijo et al., 2015; Bower and Piller, 2015; Ehlinger and Wilson, 1988; Fulton, 2007; Langerhans, 2009; Videler, 1993; Villéger et al., 2017), some empirical comparative studies of swimming performance have found surprising degrees of mismatch between fish morphology and swimming performance (Feilich, 2017; Gerstner, 1999; Pettersson, 2007; Sepulveda and Dickson, 2000; Walker et al., 2013), suggesting that the factors linking swimming ability and body shape can be complex (Hodge et al., 2018; Price et al. 2015). Others have noted that there are many challenges associated with measuring relationships between body shape and swimming efficiency, such as estimating drag, thrust, and energy consumption for a constantly undulating body, as well as accounting for differences in muscle composition, body size, and mode of propulsion (Bainbridge, 1958; Schultz & Webb, 2002; Tytell, 2007; Videler 1993). Due to these difficulties, there is still much debate over how strongly body shape limits performance capacities. Nevertheless, the proposed relationships between body shape and swimming performance are often used to substantiate predictions that body shape evolves in response to pressure for greater swimming performance. For example, the evolution of laterally compressed deeper bodies is often chalked up to an ecological need to turn more, and the evolution of an elongate, streamlined body is attributed to selection for faster or more efficient cruising (Costa and Cataudella, 2007; Ehlinger, 1990; Friedman et al., 2020, Larouche et al., 2020, Martinez et al., 2021, Rincón et al., 2007).

More generally, the body shape-swimming performance paradigm is often used as a justification that routine behavior can be predicted by body shape (Fig. 1). Where the paradigm asserts that a fish similar in morphology to a carangid should be able to achieve a high maximum swimming speed and sustainably swim for long distances, the parallel behavioral assumption is that these 'cruising' fishes are regularly using fast speeds and sustaining prolonged bouts of swimming (Blake, 2004; Villéger et al., 2017; Webb, 1994). For fishes similar in shape to butterflyfish, which are described as highly maneuverable, the behavioral expectation is that these fish use maneuvers or turns frequently (Villéger et al., 2017; Webb, 1994). Finally, elongate fish with a deep caudal peduncle, like sand perch and baracuda, are expected to be capable of rapid acceleration from a halt. As such, elongate fishes are expected to use sit-and-wait behaviors, or long periods of station holding between short, rapid burst-swimming, often used to catch prey or evade predators (Porter & Motta, 2004; Tytell, 2010; Villéger et al., 2017). Despite the longstanding use of the cruiser-accelerator-maneuverer paradigm to infer routine behaviors, many of these relationships between body shape, axes of swimming performance, and routine behaviors have yet to be tested, largely due to the difficulties of observing fishes undisturbed *in situ* and measuring these features of swimming.

Just as the paradigm suggests that body shape induces trade-offs in swimming performance, it is expected that suites of routine behaviors used by fishes will also trade-off (Table 1). The behavioral characteristic of a maneuverer is high turning frequency, which we would expect to trade-off with the traits of a cruiser - swimming speed and distance. In contrast, we expect speed and distance to be positively correlated as both behaviors are characteristic of cruisers. Accelerators are characterized by long periods of sit and wait behavior and achieve high speeds during burst starts, but do not sustain a high speed over a long distance or use turns frequently.

Thus, we expect the proportion of time a fish spends station holding will be negatively correlated with the traits that distinguish them from cruisers (swimming distance) and maneuverers (turning frequency).

A factor that potentially complicates the expected relationships between swimming behaviors and body shape is that the propulsive mechanisms used by swimming fishes differ among taxa. Two general locomotor modes are used for propulsion: body and caudal fin undulation (BCF) and median paired fin (MPF) swimming (Fulton, 2007; Sfakiotakis et al., 1999). Most species consistently use one of these modes for routine straight-line swimming (Blake, 2004; Fulton, 2007; Pink and Fulton, 2014). However, many fishes transition from MPF to BCF as swimming speed increases (Cannas et al., 2006; Feilich, 2017; Webb, 1994), and use different propulsors during bursts of acceleration and steady swimming. Nearly all fishes use median and paired fins to control turns, but straight-line swimming can be accomplished by both BCF and MPF swimming (Blake, 2004).

Biomechanical analyses suggest that BCF swimming is advantageous for long-distance and high-speed swimming, and MPF swimming is favorable for tight turns and fine directional control (Blake, 2004; Borazjani and Sotiropoulos, 2010; Lauder and Madden, 2007; Lauder and Tytell, 2005; Sfakiotakis et al., 1999; Webb, 1984a). As such, it has been argued that fishes that routinely use MPF swimming are more suited for maneuvering but incur the cost of lower swimming speeds, while routine BCF swimmers are expected to be capable of generating faster speeds but are less maneuverable (Borazjani and Sotiropoulos, 2010; Lauder and Madden, 2007; Lauder and Tytell, 2005; Sfakiotakis et al. 1999; Villéger et al., 2017). Like the body shape paradigm, this generalization has met with mixed results in comparative studies (Fulton, 2007; Fulton et al., 2013; Marcoux and Korsmeyer, 2019). Further, deeper levels of complexity within

locomotor modes can contribute variation in swimming behaviors. For example, in BCF swimmers it has been noted that modulation of body stiffness through muscle tension can increase the range of routine speeds that are accessible to a fish (Long and Nipper, 1996; McHenry et al., 1995). Additionally, MPF swimming acts as the mechanism allowing extremely stiff bodied fish to turn efficiently given their lack of bending potential (Walker, 2000; Webb, 2004; Weihs, 2002). Quickly it becomes clear that diversity in swimming behavior among fish species is likely to be driven by a more intricate set of kinematic related variables than body shape alone.

In the present study, I measure routine, daytime swimming behavior of coral reef fishes, focusing on four parameters: average straight-line swimming speed between turns, the distance covered in these bouts of straight-line swimming, the frequency of turns, and the percent of time spent station-holding. I use these data to explore several expectations from the fish ecomorphology literature. With a data set of 48 species, I first look for predicted trade-offs and positive correlations between these behaviors (Table 1, Fig. 1). I then test for an effect of species body shape on each of the swimming metrics. Finally, I contrast swimming behavior in BCF and MPF swimmers, testing for the expected differences in average swimming speed and turning frequency. If swimming behaviors are constrained by body shape, this should lead to the expected relationships between the behavioral axes. For example, a fish that turns frequently should not also be a high-speed cruiser. If BCF swimming results in better cruising performance and MPF swimming results in better maneuverability, I expect to find higher average swimming speeds in BCF swimmers and more frequent turning in the MPF swimmers.

Methods:

Behavioral Observation

I obtained videos from Thomas Claverie at the Centre Universitaire de formation et de recherche de Mayotte, recorded on coral reefs in the Mozambique channel in Mayotte in November 2018 and February 2021. The water temperature is similar in the months of November (26.5 to 29.5 ℃) and February (28.0 to 30.5 ℃). I selected videos in which water conditions were calm. The videos were recorded between 8:00 am and 4:00 pm and span 10 reef locations that range in depth from 2 to 81 meters. The recordings were taken using 5 camera rigs placed in position by snorkelers up to 5 m depth or directly from the boat and lowered with strings when depth was greater than 5 m and left to record for 2 hours before recovery. Cameras were set to film on full HD at a rate of 30 frames per second. Each Camera rig consisted of a pair of GoPros separated by 80 cm and oriented 8° inward to maximize field of view overlap (Letessier et al. 2015). Calibration was done before each recording session using a 2*2*1 m cubic contraption with 3D known coordinates positioned in two parallel planes for distances measurement and chess boards for camera distortion (Neuswanger et al., 2016). This set up allowed 3D video measurement of fish size and movement, including measurements of distance, speed, and changes in direction, all undisturbed by human presence. No fieldwork or animal ethics permits were required for the collection of videos.

I collected swimming behavior parameters from the videos on 48 fish species belonging to 16 families common on coral reefs. Sample sizes per species ranged from 7 to 31 individuals (Table 2), and the duration of each sample video was 29 seconds ± 35.1 sd, representing an average of 424.6 seconds of observation on each species. To ensure that each sample video was of a unique individual, I allowed for at least five minutes of video time between selected observation clips. I

began the measurements of behavior when the subject fish entered the field of view of both cameras and ended when the fish left the field of view of one of the cameras.

I used VidSync software (Neuswanger et al., 2016) to collect measurements of body size and behaviors of fishes swimming around the reef. I digitized behaviors manually by marking the position of the fish in both camera views when behaviors of interest occurred. During the observation interval, I calculated the **net frequency of turns** to characterize routine use of maneuvers, the percent of **time spent holding position** to characterize sit and wait behavior. The **average speed (cm/s)** and **distance traversed (cm)** among all bouts of straight-line swimming was measured to characterize routine swimming speeds and distances. Straight-line swimming was defined as the bout of swimming between two turns. Turns were defined here as a near-instantaneous change in direction larger than 45 degrees. Turn frequency was calculated as the number of turns made by a fish divided by the total amount of time that the fish spent moving (not when a fish was station-holding). A fish was labeled as station holding any time it was not swimming forward. Most often this looked like a fish physically resting on or hovering just above a coral structure. I only observed fish hovering high in the water column in a few instances. I also measured the standard length of each subject fish. Averaging across samples (i.e., individual fishes), I calculated the species mean values of four behavioral traits, including turning frequency, average straight-line swimming speed, average straight-line swimming distance, station holding proportion, and standard length.

I categorized species by locomotor mode based on behavior during routine straight-line swimming. Species were scored based on my observations and consultation of the literature. Median paired fin (MPF) swimming species used either their pectoral fins or dorsal and anal fins for locomotion and some taxa routinely mixed these (e.g., chaetodontids, tetraodontids). Body

caudal fin (BCF) swimmers used the undulation of the body and the caudal fin for locomotion, holding the paired fins against the body except during turns. The species of Chaetodontidae and Pomacentridae included in this study frequently mix median and paired fin propulsion with body undulations (Fulton, 2007). I placed these species in the MPF group because of their extensive use of paired fins during straight-line swimming.

Body Shapes

To examine body shape diversity among the 48 species in this study I utilized a publicly available dataset of eight body shape variables measured on museum specimen (Price et al., 2022). The body shape data set contains 37 of the 48 species in my study, and for the 11 species not in the body shape dataset I used closely related species as replacements. A list of replaced species and their substitutions can be found in the supplemental material (See Table S1 in the Supporting Information).

The first three of the body shapes variables I selected from this data set were standard length (SL), maximum body depth (BD), and maximum fish width (FW). From these variables I calculated body elongation (BE) as the BD divided by SL. Elongation is the primary axis of body shape diversity in reef fish (Claverie and Wainwright, 2014). Diversity along this axis of body shape is also thought to have a substantial impact on swimming ability. While, measuring hydrodynamic efficiency is difficult due to the challenges of estimating drag and energy consumption (see Schultz & Webb, 2002; Tytell, 2007), some hydrodynamic models suggest that elongate species may experience less drag and have a lower energetic cost of high-speed swimming (Lighthill, 1969) Meanwhile, other models find that body elongation alone is less predictive of swimming efficiency than when mode of propulsion and other axes of shape diversity such as caudal peduncle and fin shape are included (Tytell et al., 2010; Tytell and

Lauder, 2004). Additionally, I calculate cross sectional area, which accounts for lateral compression which is expected to have significant impacts on turning ability as deep-bodied fishes experience greater drag and are less efficient cruisers but can make more acute turns (Eloy, 2013; Sfakiotakis et al., 1999; Tytell et al., 2010, Tokić and Yue, 2012; Webb, 1984a).

Additionally, I calculated size standardized head depth (HD), lower jaw length (JL), mouth width (MW), minimum caudal peduncle depth (CD), and maximum caudal peduncle width (CW) by dividing each of these variables by SL. Additionally, I calculated the second moment of area ($[\frac{\pi * BD * FW^3}{4}]$; Porter et al., 2009; abbreviated as SMA), a factor contributing to body stiffness. I size corrected SMA by transforming the variable to be the residuals of the linear regression between Ln(SMA) and Ln(SL).

Analyses

Behavioral variables were natural log-transformed to achieve normal distributions. However, normalization was not possible for the proportion of time spent station-holding; thus, no transformation was applied. Average swimming speed and distance were strongly positively correlated with fish body length, and turning frequency was negatively correlated with fish body length (Fig. 2A, B, &C). As these linear relationships with size were strong ($p < 0.001 – 0.008$), I removed size effects by using residuals from linear regressions of the log-transformed behavioral variables versus the log of fish standard length: $X' = \ln(X) - k \ln(L) - b$, where X' is the residual size corrected behavioral variable such as size corrected swimming speed, L is body length, and k and b are the coefficients from the regression. I used the residuals in place of the behavioral variables in all subsequent analyses. I found no relationship between the time spent

station holding and fish standard length, so no size correction was performed on this variable (Fig. 2D).

For my phylogenetic analyses, a phylogeny including the species in my study was trimmed from a larger time-calibrated phylogeny of ray-finned fishes (Rabosky, Chang, Title, al. et Alfaro, 2018). The larger phylogeny did not include *Gomphosus caeruleus*, *Oxycheilinus orientalis*, or *Scarus caudofasciatus*. I used *Gomphosus varius*, *Oxycheilinus arenatus*, and *Scarus festivus,* respectively, as proxies. I tested for significant correlations between the swimming variables using phylogenetic generalized least squares regressions (PGLS; *Caper* [Orme et al., 2013]). Additionally, I used phylogenetic ANOVAs (*GeoMorph* [Baken et al., 2021; Adams et al., 2022]) to test if BCF and MPF swimmers differ in each swimming variable. To test for the effects of body shape on swimming behavior, I ran PGLS regressions for each of the eight body shape variables against each of the four swimming variables (Table S2). To examine the combined effects of body shape variation on multiple axes on swimming behavior, I ran a PCA on the eight body shape variables (body shapes PCA). I then tested for the relationships between PC1 of the body shapes PCA and my swimming behaviors using PGLS regressions.

Results:

Relationships between Swimming Variables

If body shape induces behavioral trade-offs, we would expect to find negative correlations between behaviors that typify the maneuverers, accelerators, and cruisers, and positive correlations between behaviors that are both associated with one archetype. Using phylogenetic generalized least squares (PGLS), I first tested the suspected trade-off between the use of

maneuvers versus distance and swimming speed (i.e., between maneuverers and cruisers, Fig. 1, Table 1). Opposite of expectations, I found a positive correlation between the average swimming speed and turning frequency (p:0.0004, r:0.49, Fig. 3A). This result indicates that fish which turn frequently also use high speeds. I also found a positive correlation between swimming distance and average swimming speed (p: 0.002, r: 0.43, Fig. 3B), as predicted. In line with expectations, I found swimming distance and turning frequency to be negatively correlated (p: 0.002, r: -0.44, Fig. 3C). Thus, there may be a trade-off between the rate of turns and the distance covered in bouts of swimming without turns.

I also expected trade-offs between swimming speed and distance vs the amount of time spent not swimming (between cruisers and accelerators, Fig. 1, Table 1). However, my test for a correlation between the proportion of time spent station holding and swimming distance was not significant (p: 0.63, r: 0.07, Fig. S1). Furthermore, I did not detect a significant correlation between the proportion of time spent station holding and swimming speed (p: 0.24, r: 0.17, Fig. S1). Fishes that used station-holding were diverse in swimming speeds and distances. However, this relationship should be interpreted with caution as only 33% (16) of the species in my data set had a non-zero amount of time spent station holding and only 12.5% (6) of species spent more than 10% of the time station holding (Fig. 2D).

Finally, I tested for a trade-off between the frequency of turns and the percent of time spent in sit and wait behavior (maneuverers vs accelerators). I found that the proportion of time spent station holding was weakly negatively correlated with turning frequency (p: 0.04, r: -0.30, Fig. S1). This indicates that station holding fish turned less frequently when they were swimming, but the relationship was not strong and with a limited number of station-holding species in the data, this result should be interpreted with caution.

Swimming Behaviors and Body Shape

The PGLS analyses used to independently compare the body shape variables and swimming behaviors showed no significant relationships (Fig. 4, Table S2). The body shape variables used in this study were modified from Price et al., (2022). As such, that the patterns of body shape diversity in the body shapes PCA (Fig. 4A) reflect the patterns Price et al. report among their larger set of species. Among the species in this analysis, PC1 accounts for 45% of the variation in body shape and is predominantly composed of cross-sectional area (CS), body elongation (BE), and head depth (HD). Deep-bodied and laterally compressed species are at the positive end of PC1 while elongate-bodied fish are at the negative end of PC1. PC2 accounts for 19% of the variation in body shape and represents diversity in caudal peduncle shape, specifically peduncle depth (CD) and peduncle width (CW). Fish with deep and narrow caudal peduncles are on the negative end of PC2 and those with short but wide peduncles are at the positive end of PC2. Using PGLS regressions I tested for relationships between PC1, PC2, and average swimming speed, swimming bout distance, and turning frequency (Fig. 4). I found no effects of PC1, PC2 or their interaction on average swimming speed or swimming bout distance (Fig.4 B,C). There were also no effects of PC1 or PC2 individually on turning frequency, however there was a weakly significant interaction effect (*p:* 0.043; Fig. 4D). This trend is driven by the presence of *Parapercis hexophtalma*, which has the highest body elongation and a very low turning frequency. When this data point is removed the significant interaction effect is lost (*p:* 0.141).

The fish in my data set that was most emblematic of the "cruiser" body form, *Caranx melampygus*, had a relatively low average swimming speed. The species that best matched the deepest-bodied "maneuverer" specialist body shape in my data set were the 5 species of *Chaetodon*, along with *Zanclus cornutus*, and the acanthurid *Zebrasoma scopas.* All but one of

these deep-bodied species were intermediate in turning frequency (Fig. 3A); *Chaetodon lunula* had a high turning frequency. *Parapercis hexophtalma* was the most elongate species, most similar to the specialist "accelerator" archetypal shape. *P. hexophtalma* had the highest station holding proportion. However, the two next most elongate species were both labrids, and neither used station holding. The *Paracirrhites spp.,* which were also high in their proportion of time spent station holding, were average in body elongation. Finally, the three species with the fastest average swimming speed spanned the range of the elongation ratio (e.g., *Chromis fieldi*, *Paracirrhites forsteri*, and *Thalassoma hardwicke*).

Locomotor Mode and Swimming Behaviors

The phylogenetic ANOVAs comparing BCF and MPF swimmers showed no significant differences in average swimming speed (p: 0.72, F: 0.11, df: 1,46), straight-line distance (p: 0.58, F: 0.30, df: 1,46), or turning frequency (p: 0.36, F: 0.87, df: 1,46). BCF swimmers spent more time station holding than MPF swimmers (p: 0.03, F: 5.69, df: 1,46; Fig. S1). The six species that spent greater than 10% of the time station holding are all BCF swimmers. However, eight BCF swimmers did not use station holding at all. Four of the top five species in turning frequency were BCF swimmers. Of the top five species in average swimming speed, three were MPF swimmers, and two were BCF swimmers. For straight-line distance, four of the top five species were BCF swimmers.

Discussion:

This study assessed the validity of projecting widely used linkages between swimming mode, fish body form and swimming performance onto routine swimming behavior. The expectations that deep bodied fish are maneuverable, streamlined fish are efficient cruisers, and elongate fish

can achieve fast accelerations, in addition to the assumption that body shape induces swimming performance axes have metamorphosed in the literature into the concept that body shape predicts routine behavior (Costa and Cataudella, 2007; Ehlinger, 1990; Friedman et al., 2020; Larouche et al., 2020; Martinez et al., 2021; Rincón et al., 2007; Villéger et al. 2017). I found limited evidence of the expected trade-offs between turning frequency, average swimming speed and distance, and station-holding as manifestations of maneuverers, cruisers, and accelerators. I also found little impact of body shape or mode of propulsion (BCF vs MPF swimming) on swimming behavior. My results have important implications for studies of fish locomotion, as they indicate that classic and widely used ecomorphological expectations from the literature cannot be used to predict the diversity of routine swimming behavior in coral reef fishes.

Trade-offs and Correlations between Behavioral Axes

A key concept in the classic fish swimming paradigm (Webb, 1984a) is that high abilities on one of the performance axes – maneuvering, cruising, or accelerating – will incur tradeoffs with the other axes. The behavioral analog of these predictions is the expectation of trade-offs between suites of behaviors that would distinguish maneuverers, cruisers, and accelerators (Fig. 1, Table 1). I did not observe strong evidence of the expected relationships between my four differentiating behaviors: average swimming speed, swimming bout distance, turning frequency, and the proportion of time spent station holding.

Only two of the six expected relationships between behaviors matched the classic expectations with significant correlations in the predicted direction. First, I observed a positive correlation between average swimming speed and swimming bout distance, as expected. Second, I observed a negative correlation between turning frequency and swimming distance, a pattern that confirms a classic expectation related to cruising and maneuvering. However contrary to

expectations, there is a significant positive correlation between turning frequency and swimming speed. This result was unexpected, as the notion that fish can optimize body shape to perform well at either maneuvering or at high sustained swimming speed, but not both, is likely the most prevalent in swimming ecomorphology literature (see Astudillo-Clavijo et al., 2015; Bandyopadhyay et al., 1997; Ellerby and Gerry, 2011; Gaston et al., 2012; Rincón et al., 2007; Villéger et al., 2017; Weihs, 2002).

It is commonly expected that fish which use sit-and-wait behavior swim fast over short distances and do not turn frequently when they are swimming (Higham, 2007; Villéger et al., 2017). I observed that fishes that use sit-and-wait behavior are no more or less inclined to swim fast or travel far than fishes which are constantly swimming. I found a negative relationship between turning frequency and the proportion of time spent station holding. However, as this relationship is weak and highly sensitive to the inclusion of one species, *Parapercis hexophtalma,* I view it as weak if any evidence of a trade-off between these two variables.

While it may be that trade-offs prevent high performance on the key swimming traits that distinguish cruisers, maneuverers, and accelerators, I found little evidence that these distinctions are appropriate for describing diversity in routine behaviors. A possible explanation for why my findings did not match expectations is that peak performance may not be a strong predictor of routine swimming behavior. It is possible that the use of maximum performance is uncommon in the daily life of animals and routine behaviors may usually fall well below maximum capacity. While many studies find that maximum swimming performance and routine behavior are significantly correlated (Fisher and Bellwood, 2003; Plaut, 2001; Wainwright, 1987) this need not always be the case and there is evidence that the degree of the match varies by locomotor mode (Fulton, 2007). Thus, it may be that adaptations for high performance on each of the three

traditional locomotor axes yield trade-offs among the performance traits, but that peak performance is a weak guide to routine swimming behavior in reef fishes, so that these relationships are not manifested in average swimming profiles.

Effects of Body Shape on Swimming

Body shape is classically expected to underly the expected trade-off between axes of swimming performance (Webb, 1984a; Blake, 2004). It is intuitive that to maintain low fitness costs, fishes would be unlikely to routinely use behaviors that are energetically expensive and that the routine behaviors used by a fish would reflect the body shape. However, I found that variation among species in most routine swimming behaviors cannot be attributed to body elongation, cross sectional area, caudal peduncle shape, head and mouth shape, or second moment of area. Thus, it is not the case that for routine behavior fish can neatly be categorized as cruisers, maneuverers, or accelerators based on body shape. Rather, I observe fish of all shapes using many combinations of routine speeds and distances, turning frequencies, and periods of rest. Both elongate and deep-bodied species can be found along most of the range of all behavioral axes (Fig. 3). One of the many examples of the lack of morphological similarity among fishes in the same region of behavior-space (high-distance/low-turning frequency) can be found between *Zanclus cornutus,* the most deep bodied species in the data set (BE: 0.83) and a more elongate fish, *Parupeneus macronemus* (BE: 0.33). Finally, I observe that fishes of similar body shape can vary substantially in behavior. My findings demonstrate that carangiform fish such as *Caranx* and *Caesio* are not necessarily prone to using higher speeds routinely than chaetodontiform fish such as *Chaetodon* and *Zebrasoma*. The labrids and acanthurids in this study are also a good example of how much behavior variation can exist among closely related

species despite similarities in overall morphology. As such, I recommend that body shape should not be used to estimate routine swimming behaviors.

While theory suggests that maximal swimming performance is limited by body shape, my observations show that routine behaviors do not appear to be constrained by body shape. As discussed above, one possible explanation for the mismatch is that maximal performance profiles do not translate to routine behaviors. However, a second possible explanation is that the mapping of morphology to swimming performance in fishes is more complex than previously thought.

While there is positive evidence of the correlation between body shape and variation in swimming performance capacity from a number of laboratory studies (Blake et al., 1995; Ellerby and Gerry, 2011; Gerry et al. 2012; Langerhans et al., 2009; Oufiero et al., 2011) these studies usually focus on variation within species rather than comparative patterns. These studies have found consistent support for the expected morphological responses to greater use of sustained swimming (Aguilar-Medrano and Barber, 2016; Friedman et al., 2016; Jastrebski et al., 2004), increased maneuvering (Ellinger and Wilson, 1988; Mittelbach 1981; Robinson, 2000), and threats of predation (Ghalambor et al., 2003; Langerhans, 2009). However, studies of swimming performance require intensive laboratory effort and have therefore not been generated in a comprehensive way for large numbers of species. Those comparative studies that do exist often do not find the expected relationships between morphology and swimming performance (Feilich, 2017; Gerstner, 1999; Walker et al., 2013). This literature suggests that the mapping of body shape to swimming performance is complex, in part because descriptors of body shape do not account for the extensive variation found in the anatomical basis of locomotion (Aguilar-Medrano et al., 2016; Donatelli et al., 2021; Feilich, 2017; Gerstner, 1999; Walker et al. 2013), the mechanics of propulsion (Long and Nipper, 1996, Wainwright et al. 2002; Walker, 2000;

Walker and Westneat, 2002) or flexibility in the mode of propulsion (Feilich, 2017). Indeed, I suggest that descriptions of the anatomical diversity that supports locomotor capabilities are needed if we are to build a realistic and meaningful picture of swimming ecomorphology for fishes.

Effects of Locomotor Mode on Swimming

In addition to body shape, the primary locomotor mode used for propulsion has been thought to limit the range of behaviors available to fish. Biomechanical analyses suggest that MPF swimming offers maximum control during slow-speed maneuvering (Lauder and Madden, 2007; Weihs, 2002) while BCF swimming is thought to allow for higher sustained speeds, and provide higher power during bursts, and thus has been suggested to perform best during sustained swimming or burst starts (reviewed by Blake, 2004; Colgate and Lynch, 2004; Korsmeyer, 2002; Lauder and Tytell, 2005; Sfakiotakis et al., 1999; Webb, 1984a). Though numerous species have been shown to transition from MPF to BCF as swimming speed increases (Cannas, 2006; Druker, 1996; George, 2019; Korsmeyer, 2002), most species adopt a single locomotor mode that is used for routine travel. I have attempted to clarify if a species' standard locomotor mode shapes its behavioral profile while swimming.

I found no significant difference between the behavioral profiles of MPF and BCF swimmers. Further, species that emphasize either locomotor mode can achieve behavioral extremes in turning frequency, average swimming, and straight-line distance (Fig. 3 & 4). Thus, I find no support for the idea that MPF swimmers are routinely slower swimmers or that they turn more frequently. These patterns suggest that the locomotor modes are surprisingly comparable in behavior and support the previous findings that MPF swimmers can be highly efficient over a wide range of speeds (Korsmeyer et al. 2002). Further my findings indicate

behaviors are not sensitive to the additional drag experienced by BCF swimmers due to the undulating body, as compared to the fixed body of a MPF swimmers (Lighthill, 1969; Lighthill and Blake 1990). My findings are consistent with observations that MPF swimmers can thrive in environments where exceptional swimming endurance is needed such as high flow conditions and strong wave exposure (Bellwood and Wainwright, 2001; Fulton and Bellwood, 2004; 2005).

Conclusion

With the advancing tools available to study fish undisturbed *in situ*, it is likely that my data set is only the beginning of what will become a large and diverse record of routine behavior in fish. Analyses of the effects of factors other than body shape and locomotor mode will help to elucidate predictors of diversity in routine behavior. In the present there is limited evidence that it is valid to project the proposed relationships between body shape and swimming performance onto routine swimming behavior. As such, inferring routine behavior in fishes based on body shape should be avoided.

Figures and Tables:

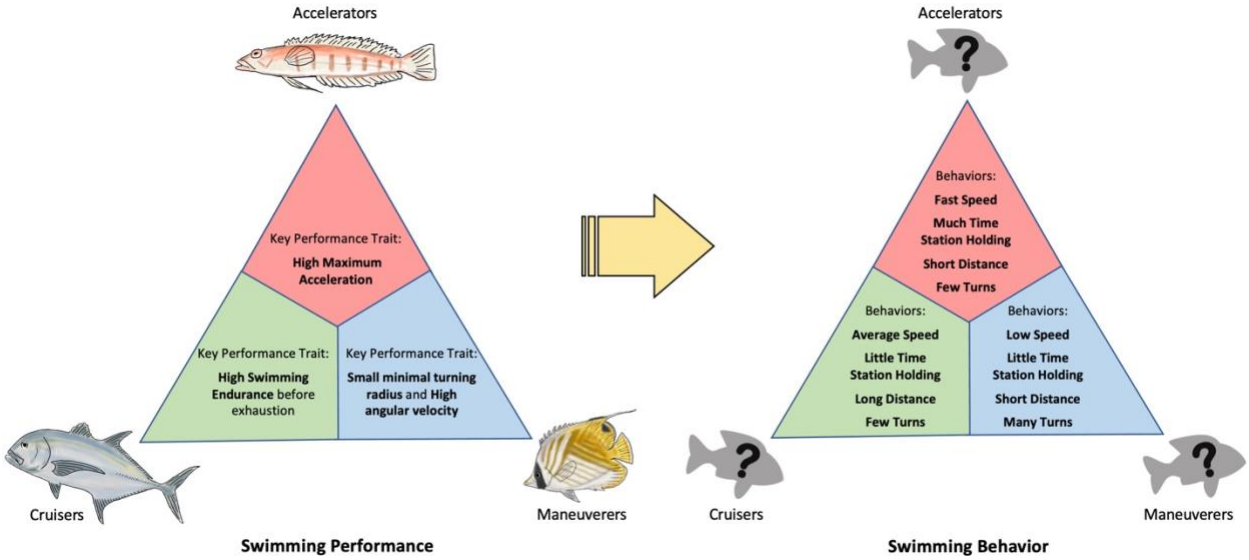

***Figure 1*. Fish Swimming Paradigm.** An adaptation of Webb (1984a, Fig. 1). On the left-hand triangle, corners represent swimming specialists while generalists have intermediate traits. Webb classifies swimming variation in terms of key performance traits. His hypothesis was that high performance in each swimming trait is best achieved by a particular body design. These body shape archetypes are shown in the corners. Accelerators which have a high maximum acceleration are elongate but have uniform body depth. Cruisers have a high sustained swimming speed and endurance, and have average elongation but have tapered bodies. Maneuverers are highly maneuverable with small minimal turning radius and can achieve high angular velocity. Maneuverers are deep bodied and laterally compressed. These hypotheses regarding swimming performance and body shape are often projected onto routine swimming behavior. On the right triangle, I show how four behaviors axes can be used to distinguish routine behaviors for the three swimming archetypes. The proportion of time spent station holding is expected to be highest for accelerators. Average swimming speed is expected to be low for maneuverers but higher for accelerators and cruisers. Straight-line distance should be greatest for cruisers. Finally, turning frequency should be highest for maneuverers. Here I use these behaviors to test for relationships between routine behavior and body shape.

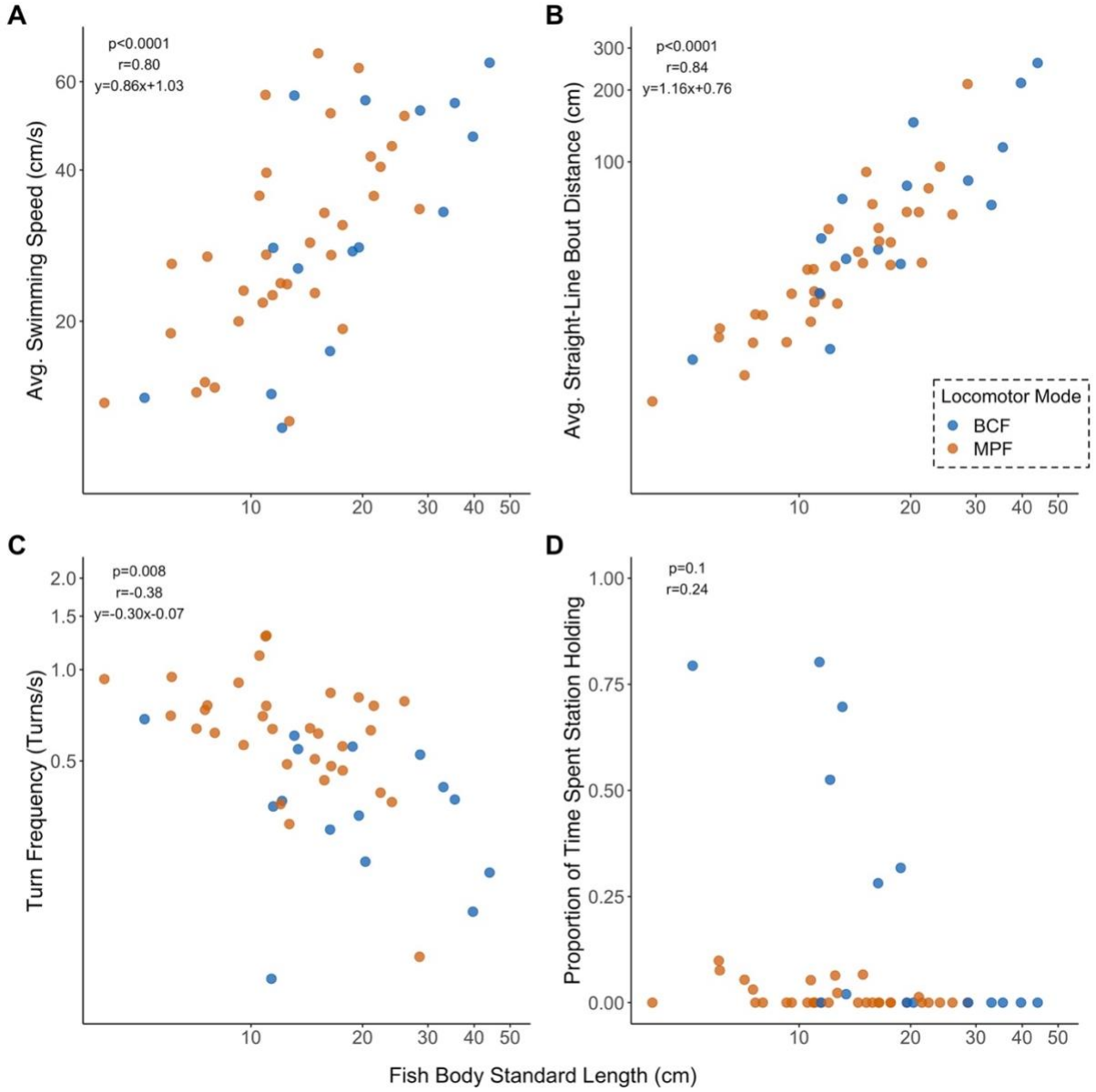

Figure 2. **Body Size is Correlated with Most Swimming Behaviors.** The relationships between the average standard length of each species and A) the average swimming speed during bouts of straight-line swimming, B) the of average distance traveled during bouts of straight-line swimming, C) the of average number of turns made per second, and D) the proportion of time spent holding position to total observation time. Species are color coded by locomotor mode. Blue points represent body caudal fin swimmers (BCF), orange points represent median paired fin swimmers (MPF). *P*-values, *r*, and equations were calculated using phylogenetic general least squares regression.

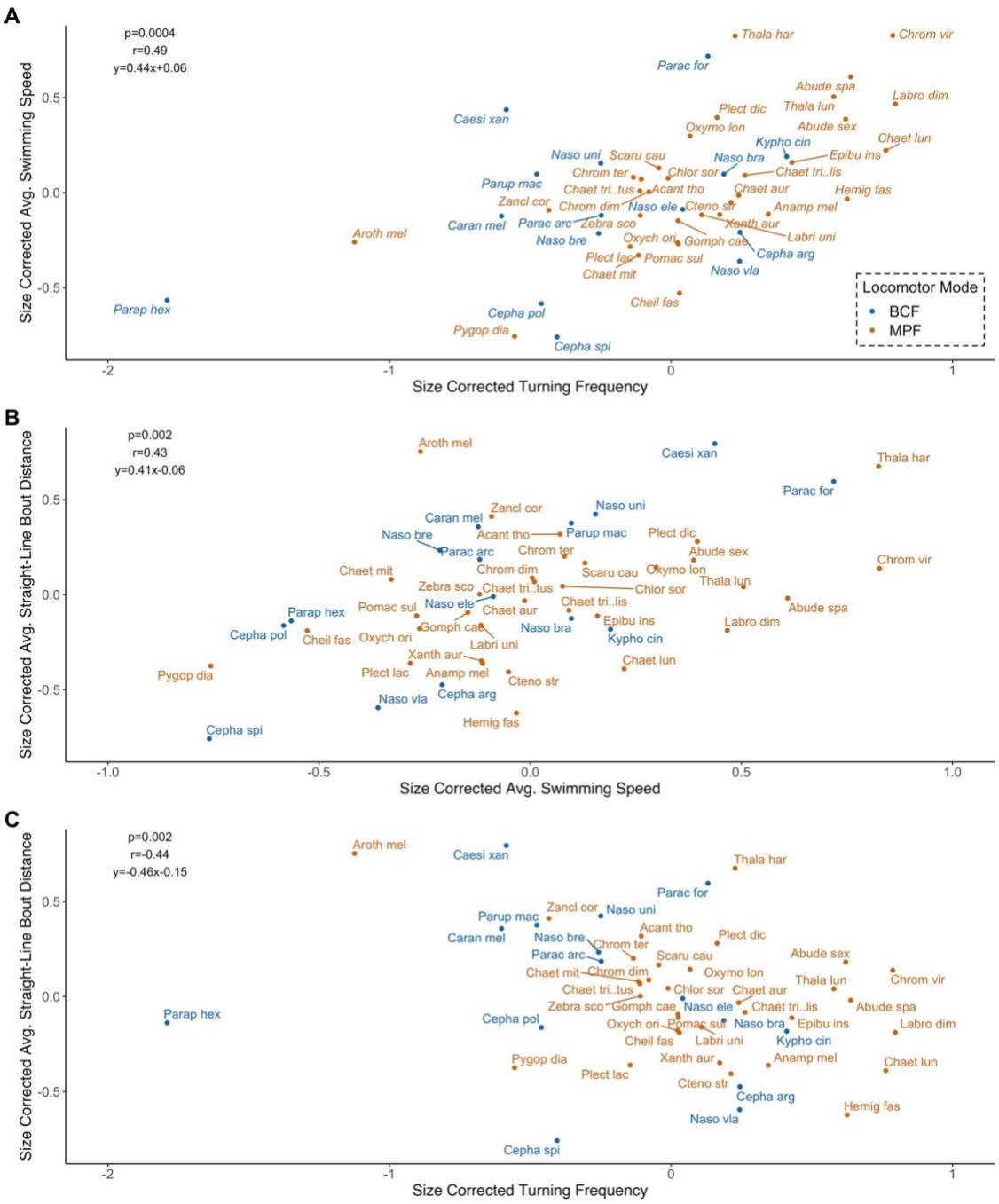

Figure 3: **Behavioral distributions and relationships.** A) The relationship between turn frequency and average swimming speed, B) The relationship between average swimming speed and average straight-line distance, C) The relationship between average straight-line distance and turn Frequency. Points are labeled by the first 5 letters of the genus and first 3 letters of the species. For very similar species, the last 3 letters are also provided. Average swimming speed

values are the residuals of the relationship between the natural log of the species average swimming speed during bouts of straight line swimming (cm/s) and the natural log of the average fish body length (cm), shown in Fig. 2A. Turning frequency values are the residuals of the relationship between the natural log of the species average for number of turns per second and the natural log of the average fish body length (cm), shown in Fig. 2B. Average straight-line distance values are the residuals of the relationship between the natural log of the species average for distance traveled during straight line swimming and the natural log of the average fish body length (cm), shown in Fig. 2C. Species are color coded by locomotor mode. Blue points and bars represent body caudal fin swimmers (BCF), orange points and bars represent median paired fin swimmers (MPF). *P*-values, *r*, and equations were calculated using phylogenetic general least squares regression.

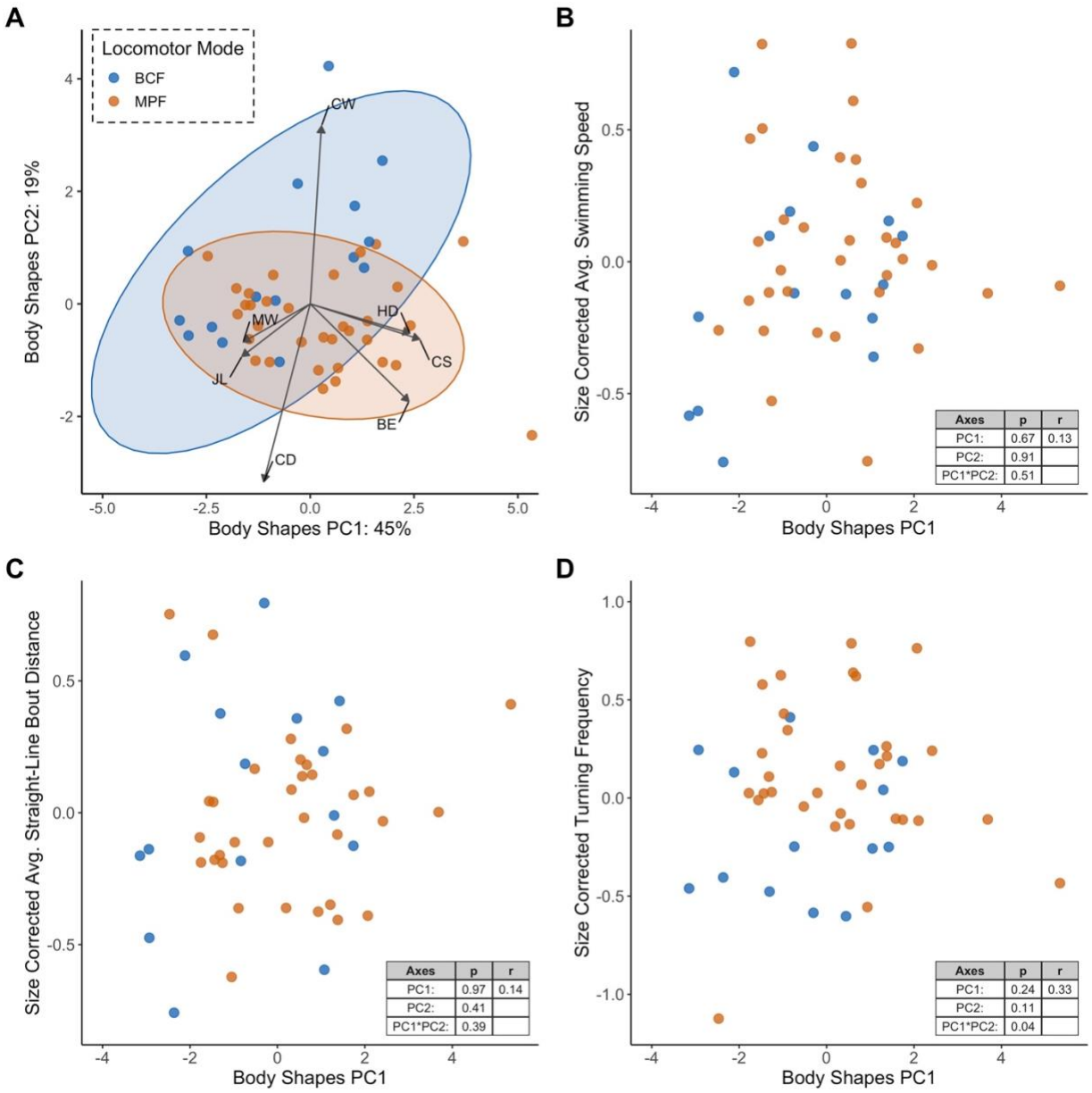

Figure 4. **The effects of Body Shape on Swimming Behaviors.** A) A morphospace PCA modified from Friedman et al., (2021) and Price et al., (2022), where of species scores are plotted on the first two principal components axes, PC1 vs PC2. Body shape ratios included as loadings are Body Elongation (BE), Cross Sectional Area (CS), Head Depth (HD), Minimum Caudal Peduncle Depth (CD), Maximum Caudal Peduncle Width (CW), Mouth Width (MW), and Lower Jaw Length (JL). B) Average swimming speed vs. PC1. Average straight-line distance values are the residuals of the relationship between the natural log of a species' average

distance traveled during straight-line swimming and the natural log of the average fish body length (SL; cm). C) Average straight-line distance vs. PC1. Average straight-line distance values are the residuals of the relationship between the natural log of the species average for distance traveled during straight line swimming and the natural log of SL. D) Turning Frequency vs. PC1. Turning frequency values are the residuals of the relationship between the natural log of the species average for number of turns per second and the natural log of SL. Species are color coded by locomotor mode. Blue points represent body caudal fin swimmers (BCF), orange points represent median paired fin swimmers (MPF). The ellipses contain 95% of the points in their respective locomotor mode, showing the significant interaction of PC1*PC2 and locomotor mode. Tables in the lower right corner of panels A, B, and C show the *P* and *r* values from the phylogenetic general least squares regressions of the swimming behaviors vs. the body shape PCs.

***Table 1*. Predicted Correlations between Swimming Variables vs Observed Relationships.** Predicted pairwise relationships among four variables that describe swimming behavior, as measured in this study. Expected correlations (positive or negative) are based on interpretation of properties of specialist swimmers as discussed in the Introduction. The results column reports the results from PGLS regressions that test for each relationship. Results were counter to predictions in four of six cases.

Behavior 1	Behavior 2	Expected Correlation	Results
Swimming Speed	Turning Frequency	-	+
Swimming Speed	Swimming Bout Distance	+	+
Swimming Speed	Proportion of Time Station Holding	+	0
Turning Frequency	Swimming Bout Distance	-	-
Turning Frequency	Proportion of Time Station Holding	-	- / 0
Swimming Bout Distance	Proportion of Time Station Holding	-	0

***Table 2*. Species List.** Videos (N) is the number of individual video sequences sampled for each species. Body Elongation (BE) is calculated as the body depth / standard length. Cross Sectional Area (CS) is the body depth / fish width.

Species	Videos (N)	BE	CS
Acanthuridae			
Acanthurus thompsoni	20	0.47	3.03
Ctenochaetus striatus	13	0.52	2.96
Naso brachycentron	9	0.43	3.59
Naso brevirostris	13	0.39	2.79
Naso elegans	31	0.44	2.79
Naso unicornis	25	0.44	3.09
Naso vlamingii	17	0.40	2.61
Zebrasoma scopas	12	0.60	3.89
Balistidae			
Xanthichthys auromarginatus	30	0.47	2.60
Caesionidae			
Caesio xanthonota	15	0.37	2.31
Carangidae			
Caranx melampygus	14	0.36	2.64
Chaetodontidae			
Chaetodon auriga	10	0.59	4.10
Chaetodon lunula	11	0.66	3.85
Chaetodon mitratus	23	0.60	3.49
Chaetodon trifascialis	12	0.54	3.00
Chaetodon trifasciatus	9	0.61	3.69
Epinephelidae			
Cephalopholis argus	13	0.34	1.74
Cephalopholis polleni	28	0.36	1.70
Cephalopholis spiloparaea	25	0.35	2.02
Kyphosidae			
Kyphosus cinerascens	7	0.44	1.94
Labridae			
Anampses meleagrides	13	0.28	2.14
Cheilinus fasciatus	12	0.40	2.00
Chlorurus sordidus	7	0.35	1.98
Epibulus insidiator	12	0.47	2.50
Gomphosus caeruleus	11	0.27	2.13
Hemigymnus fasciatus	10	0.39	2.03
Labrichthys unilineatus	15	0.34	2.26
Labroides dimidiatus	12	0.24	2.04
Oxycheilinus orientalis	10	0.36	2.36
Scarus caudofasciatus	26	0.38	2.11
Thalassoma hardwicke	11	0.33	2.21
Thalassoma lunare	11	0.31	2.17
Monacanthidae			
Oxymonacanthus longirostris	11	0.41	3.00
Mullidae			
Parupeneus macronemus	9	0.33	2.12
Cirrhitidae			
Paracirrhites arcatus	13	0.42	2.56
Paracirrhites forsteri	11	0.37	1.98
Pinguipedidae			
Parapercis hexophtalma	12	0.20	1.04
Pomacanthidae			
Pygoplites diacanthus	14	0.53	2.98
Pomacentridae			
Abudefduf sexfasciatus	14	0.54	2.85
Abudefduf sparoides	10	0.55	2.67
Chromis fieldi	15	0.56	2.51
Chromis ternatensis	15	0.49	2.84
Chromis viridis	11	0.48	2.72
Plectroglyphidodon dickii	9	0.56	2.68
Plectroglyphidodon lacrymatus	12	0.52	2.49
Pomacentrus sulfureus	12	0.47	2.34
Tetraodontidae			
Arothron meleagris	12	0.29	1.00
Zanclidae			
Zanclus cornutus	14	0.83	5.23

Chapter 2: Weak integration allows novel fin shapes and spurs locomotor diversity in reef fishes.

Introduction:

Evolutionary integration between anatomical traits, the tendency of traits to covary through deep time scales, can arise through genetic, developmental, and functional pathways (Evans, 2023; Klingenberg, 2008; Zelditch & Goswami, 2021). In the case of strong integration among traits, morphological changes in one trait induce shifts in any integrated traits. For example, the radius and ulna display strong covariation in most tetrapods because these bones articulate with the humerus at their proximal edge and the carpals at their distal edge (Chamero et al., 2013; Fabre et al., 2014). Consequently, a lengthening of the radius would not be feasible without a tandem lengthening of the ulna. Such axes of trait covariation can act as evolutionary pipelines, or pathways of least resistance, along which diversity can accumulate as selection on any one trait in an evolutionarily integrated system can tow associated traits into new trait space along axes of trait covariation (Du et al., 2019; Eliason et al., 2023; Evans et al., 2021). Traits which are not integrated (evolutionarily independent) do not have access to these evolutionary pipelines and must experience direct selection to reach novel morphospace. Meanwhile, traits in integrated systems may be more prone to diversification, as the sources of selection on many traits will be greater than for a single trait. However, trait integration can also inhibit diversification, as strong stabilizing selection on any one trait in an integrated system can prevent the evolution of associated traits into novel regions of trait space (Evans 2017; Goswami & Polly, 2010; Larouche et al., 2018; Marroig et al., 2009). While no integration (evolutionary independence) and strong integration may both limit accessible trait space (Goswami et al., 2014), moderate trait covariation (often referred to as weak integration) in which there is a primary axis of trait

covariation but with substantial off-axis variation, may facilitate the greatest diversification (Burns et al., 2023; Felice et al., 2018, Hansen 2003). Thus, an emerging theory is that weak evolutionary integration may be a common mechanism underlying diversification in highly diverse functional systems (Burns et al., in Review).

Locomotor variation is an axis of functional diversity that has direct consequences for ecological diversity, as locomotor range is generally a limiting factor determining access to resources in an environment (Bellwood & Wainwright, 2001; Citadini et al., 2018; Crumière, 2016; Essner 2007; Fulton et al.,2001; Granotsky 2018). In most vertebrate locomotor systems, the ancestral condition is that all limbs work in cooperation to produce movement, creating functional integration but also commonly showing genetic and developmental integration (Gatesy & Dial, 1996; Goswami et al., 2014; Hallgrímsson et al., 2002; Petit et al., 2017; Wimberley et al., 2021). Within vertebrate clades, the evolution of novel locomotor styles often occurs through functional decoupling of limb modules. For example, we observe locomotor expansion in mammals associated with the decoupling of fore- and hindlimbs, such as in climbing in bipedal marsupials and primates, and flight in bats (Bell et al., 2011; Goswami et al., 2014; Yong et al., 2010). Similarly, functional decoupling of the limbs was the necessary precursor for the locomotor expansion from quadrupedal archosaurs to bipedal theropods to avian flight (Gatesy and Dial 1996; Gatesy and Middleton 1997).

In each case of vertebrate limb decoupling, a reduction of morphological covariation between the fore- and hindlimbs relative to quadrupedal ancestors has been observed, which suggests developmental disintegration (Bell et al., 2011; Garland et al., 2017; Goswami et al., 2014; Kelly & Sears, 2011; Young & Hallgrímsson 2005, Young et al., 2010). While studies demonstrating a reduction of intraspecific (developmental) limb integration with locomotor

diversity are plentiful, studies that examine interspecific (evolutionary) integration are rare. A notable exception is that in birds, the presence of independent evolution of up to three locomotor modules (the forelimb, the hind limb, and the tail) has been observed (Eliason et al., 2023; Orkney et al., 2021). While these studies do not directly test for relationships between evolutionary independence of the limbs and locomotor diversity, the evidence for division of locomotor modules supports the hypothesized pathway to flight via increasing modularity in traits involved in locomotion (Gatesy and Dial 1996; Gatesy and Middleton 1997).

Fishes, the most diverse group of vertebrates, have extensive locomotor diversity (Breder 1926; Lindsey 1978; Webb 1984). Numerous classification systems are available to categorize locomotor mode in fish; one of the more common methods is identifying the fins used for routine propulsion at average speeds (reviewed by Blake 2004; Breder 1926; Lindsey 1978; Fulton, 2007; Sfakiotakis, 1999). Many fish swim primarily with the undulation of their body and caudal fin (BCF), while others use the flapping, rowing, or undulation of their median and paired fins (MPF). Within MPF swimming, propulsion can be achieved predominantly by the pectoral fin (labriform) or by the dorsal and anal fins in concert (tetraodontiform). Finally, some species spend most of their time resting on the substrate and swim only occasionally or "hop" between resting places; herein referred to as "benthic." Historically, many studies have subcategorized BCF swimming by the proportion of the body used in undulation (from anguilliform to thunniform). However, a recent study indicates that these subcategories are not kinematically meaningful (Di Santo et al., 2021).

It is important to note that all fish will use BCF locomotion at their maximal speeds, such as during pursuit or escape responses, and will use MPF swimming to support slow swimming and fine-scale maneuvers (Blake, 2004; Sfakiotakis, 1999; Webb 1984). Further, while the

predominant mode of locomotion may be accomplished with a single fin, this does not preclude species from regularly using all of their fins. For example, many BCF swimmers make constant fine-scale adjustments with their median and paired fins, thus while the caudal fin is supporting forward movement, the paired fins are stabilizing and steering the fish. Meanwhile, Labriform swimmers will use their pectorals for propulsion and maneuvers and only utilize BCF undulation at extremely high speeds or accelerations. Despite their reliance on dorsal and anal fins for propulsion, tetraodontiform swimmers will also use their pectorals frequently in steering and will employ caudal flaring and undulation to accomplish maneuvers such as backing out of tight spaces. Thus, across these main swimming categories, there is variation in functional integration in the use and cooperation of the fins. As such, shifts in patterns of fin integration with expansion into new locomotor mode could be expected. However, equally plausible is that fins are always integrated, because most species use all fins in some capacity to access the full spectrum of locomotion from slow maneuvers through routine swimming to high-speed modes. While functional integration alone can induce evolutionary covariation, fins are also subject to common developmental origins in shared epidermal fin folds and mutual genetic pathways that produce fin buds, fin supports, cartilage and soft tissue, and fin rays (Ahn et al., 2002; Crotwell et al., 2001, 2004; Crotwell & Mabee, 2007; Dahn et al., 2007; Freitas et al., 2006; Goodrich, 1906; Huede et al., 2014; Letelier et al., 2018; Mabee et al., 2002; Neumann et al., 1999; Sordino et al., 1995). Thus, all fins share locomotor roles, genetic pathways, and developmental origins, which all may lead to strong evolutionary integration among fins.

Despite the many sources of evolutionary integration between fins, there is some evidence that independent fin evolution reflects locomotor diversity. For example, studies have explored the evolutionary integration and modularity of *fin position* relative to the body of fishes, as the

ability to independently adjust fin positions is considered instrumental in locomotor specialization (Druker & Lauder, 2002; Harris, 1937; Lauder & Druker, 2004). The two independently evolving modules of fin position that are most supported are the trunk region, which includes dorsal, anal, pectoral, and pelvic fin insertions, and the caudal region which includes the caudal peduncle and the caudal fin insertions (Aguilar-Medrano et al., 2016; Larouche et al., 2018). The positionings of fins in the trunk region were found to evolve at rates 3 to 5 times faster than the caudal module (Larouche et al., 2018) suggesting independent evolution of the modules. The independent evolution of the trunk module relative to the caudal module parallels the functional distinction between MPF swimming, in which the median and paired fins are most important, and BCF swimming in which the caudal fin is most important.

In addition to fin position, fin shape is considered particularly important in the ecological filtering of reef fish communities. For example, wrasses with high aspect ratio (AR) pectoral fins are found more often in high-exposure environments with more wave energy (Bellwood & Wainwright, 2001). Additionally, high AR caudal fins are associated with depth-generalists, many of which swim over greater distances in depth migrations (Bridge et al., 2015). High AR fins experience less drag than low AR fins and are likely cost efficient in conditions requiring continuous swimming. In contrast, low AR fins such as rounded caudal fins are more common on shallow reefs, presumably because higher surface area fins are beneficial in drag production needed for maneuvering in complex reef structure (Blake, 2004; Bridge et al., 2015; Sfakiotakis, 1999; Lindsey, 1978; Webb, 1984). These studies suggest that fin shape is functionally important to the swimming capacity of fishes and that changes in fin shape may have significant functional costs in locomotor ability.

The combination of plausible integration among fins, independent evolution in the caudal module, and ecomorphological specialization in fins, begs the question of how morphological and functional diversity evolve within the complex locomotor system of reef fishes. Each fin may individually experience functional constraints on patterns of evolution and accumulation of diversity. However, as components in an integrated system, functional constraints on a single fin may influence the evolution of each other fin in the system. Thus, painting a complete picture of the diversification of the reef fish locomotor system requires uncovering the impact of axes of integration on functional and morphological diversification. In this study I ask, 1) what are the effects of locomotor mode on fin shape morphospace occupation and rates of fin evolution, 2) what is the effect of transitions in locomotor mode on patterns of evolutionary integration among fins?

Methods:

Fin Morphology Data Collection and Processing

I photographed 321 cleared and stained specimens (Dingerkus & Uhler, 1977), representing 106 species from 38 families of coral reef fishes (Burns et al., In Review). My sampling covers most of the ecological diversity of reef fishes, and about half of all families found on reefs. For each specimen, I fully extended and pinned the pectoral, caudal, dorsal, and anal fins onto thin foam sheets permeable to light. I opted not to photograph the pelvic fin, as it is absent in some species in my data sets and is not considered an essential fin for generating thrust in any locomotor category I use. I used photographs from the John E. Randall Fish Photo Collection at the Bishop Museum and Google image searches as a guide for ensuring accurate fin posture and extension. I used clay block supports where needed to position the fish's body so the fin could

lay flat against a level light box surface. I took images of the specimens in lateral view with a Canon DSLR camera mounted to a level fixture such that the lens was parallel to the light box.

Shape of the pectoral, caudal, dorsal, and anal fins was digitized in the statistical software R (version 4.2.0; R Core Team, 2022) using the package *StereoMorph* (version 1.6.7; Olsen & Westneat, 2015). I placed a single fixed landmark at the anterior-most (dorsal and anal) or dorsal-most (pectoral and caudal) insertion of the fin to anchor a sliding semi-landmark curve placed around the fin's perimeter. As for most cleared and stained specimens the connective tissue between fin spines or rays is transparent, I placed the outlining curve along the tips of spines and rays. To generate a matrix of coordinates representing the shape of each fin, the perimeter curves were sampled at evenly spaced intervals. I selected curve sampling intervals to produce the most detailed outline of fin shape possible while remaining near the ideal one landmark per three specimen ratio (Zelditch et al., 2012). More sampling points were needed to fully capture the shape of larger fins and those with more extreme shape variation (range was N=95 pectoral to N=150 Dorsal).

Categorization of Locomotor Mode & Phylogeny

Each species in my data set was categorized into locomotor groupings by their predominant mode used during routine straight-path swimming (Table S1). I used four locomotor categories: the first contains fishes that move via the undulation of their body and caudal fin (BCF), the second group consists of fish that rely heavily on the rowing of the pectoral fin, which I call labriform locomotion. Labriform locomotion is named after Labriformes which are the most exemplar clade of pectoral fin swimming, though many reef fish outside of Labrifomes also use labriform swimming. However, a single clade in my species set, the Tetraodontiformes, use the undulation of the dorsal and anal fin in concert to swim, a mode I call tetraodontiform

swimming. Finally, the fourth group includes benthic species which are periodic swimmers that spend most of their time resting in direct contact with the substrate. Species were classified using published records of swimming modes (Fulton, 2007; Korsmeyer et al., 2002; Webb, 1984; Lindsey, 1978; Breder, 1926).

In preparation for phylogenetic analyses, I created a time-calibrated phylogeny of the 106 species in my data set by trimming a larger phylogeny of fishes (Rabosky et al., 2018). In cases where species in my dataset were not present in the larger phylogeny, I used the most closely related species present in the larger phylogeny based on other phylogenetic analyses as a substitution (Table S1). I used an ancestral state reconstruction to map the history of locomotor mode transitions onto the phylogeny (Fig. 1) using *phytools* (version 1.9.16; Revell, 2012) and *ape* (version 5.7.1; Paradis & Schliep, 2019). Specifically, I generated 100 stochastic character maps, with the highest likelihood estimated transition matrix (Q), and calculated locomotor mode transition probabilities at nodes.

Analyses of Fin Shape and Locomotor Mode

Fin shape coordinates were scaled and aligned using a Generalized Procrustes Analysis (GPA) in the R package *geomorph* (version 4.0.5; Adams et al., 2022; Baken et al., 2021) to remove the effects of size and rotation on fin shape variation. I generated fin shape morphospaces (Fig. 2) using a Principal Components Analysis (PCA) on the variance-covariance matrix of fin shape coordinates. For each fin, I used *geomorph* and *RRPP* (version 1.3.1; Adams & Collyer, 2018;2021) to test for differences in mean fin shape between locomotor groups with Phylogenetic ANOVAs (*procD.pgls, 1000 iterations for permutations*) and post-hoc comparisons (*pairwise,* Table 1), and to estimate shape disparity within each locomotor group (*morphol.disparity, 10,000 iterations for permutations*; Table S2).

I further explored regions of fin morphospace uniquely occupied by a single locomotor group and the degree of morphospace overlap between locomotor groups using fin shape hypervolumes generated in the R package *hypervolume* (version 3.1.3; Blonder et al., 2023). For each fin I generated a hypervolume for each of the four locomotor groups, as well as what I refer to as "non-focal group" hypervolumes, which contain all species not in one of the four locomotor groups (for example, all species that are not BCF swimmers). This process produced a total of 10 hypervolume comparisons for each fin: 6 which compare the locomotor groups in a pairwise manner (Table S3), and 4 which compare a locomotor group to a non-focal group hypervolume (of all species not in that locomotor group; Table 2). I used a broken-stick method to determine the number of principal component axes for each fin shape that explained a great enough proportion of overall shape variance to warrant inclusion in the hypervolume construction (the first 3 PCs for pectoral fins and 4 PCs for all other fins). I determined unique morphospace occupation by calculating the fraction of the volume that did not overlap with the other hypervolume in comparison. To validate whether the unique morphospace occupation was more or less extreme than expected under a null model, I generated 10,000 permutations for each comparison in which the data for the two original hypervolumes were combined and randomly redistributed into the hypervolume assignment. I created null distributions by calculating the unique morphospace occupation of each hypervolume for each permutation. I calculated P-values as the fraction of the permuted distributions that were greater than the observed unique morphospace occupation from the true data. Thus, I deemed p-values of less than 0.025 to indicate that the hypervolume has significantly more unique morphospace occupation than would be expected under null conditions and a p-value of greater than 0.975 to mean that the hypervolume occupies less unique morphospace than would be expected under a null model.

I evaluated the evolutionary correlation between fins with calculations of phylogenetic integration and rates of fin shape evolution in *geomorph.* To determine if transitions between primary locomotor mode co-occurs with a reduction in fin integration, I estimated integration within each locomotor group (Table 3; Fig. 3) and for all species (Table S4). To visualize the fin shapes that commonly occur together, I plotted the fin-by-fin comparisons from non-phylogenetic two-block partial least squares (PLS) regressions (Fig. 3). This is helpful as plotting the PLS axes of the fins from the phylogenetic integration tests would instead show relationships between residual variation in fin shape once the phylogeny is accounted for and thus does not easily translate to the original fin shapes. In summary, I used non-phylogenetic PLS axes for visualization, but statistical interpretations of the evolutionary integration are taken from phylogenetically corrected analyses (*phylo.integration, 1000 iterations*). To compare overall rates of evolution between the fins for all species, I used '*compare.multi.evol.rate*' to estimate the multivariate Brownian rates for each set of fin landmarks with 1000 iterations to test for significance. To assess the effects of locomotor mode on Brownian rates of fin shape evolution, I estimated the rates among species within a locomotor group for each fin using the function '*compare.evol.rate'* in *geomorph* (Fig. 4), again with 1000 iterations.

Results:

Evolutionary History of Locomotor Mode

Of the 106 species in my fin data set, I categorized 44 as BCF, 15 as benthic, 34 as labriform, and 13 as tetraodontiform. The average number of transitions between locomotor modes from 100 stochastic character maps (simmaps) was 17.26 transitions. The most common ancestral state was BCF in 86.6% of the simmaps, followed by benthic at 10.5% of the simulations, and only 1.4% for both labriform and tetraodontiform. The most common transition was from BCF to

benthic with an average of 7.99 transitions, followed by 6.25 transitions from BCF to labriform, 1.35 from benthic to BCF, and finally 1.01 from BCF to tetraodontiform (Figs. 1, S1). The simmaps recovered no other transitions between modes, for example, there were no transitions from labriform swimming back to BCF swimming.

Effects of Locomotor Mode on Fin Shape Diversity in Reef Fish

The fin shape morphospaces I have constructed represent the first comparative dataset of fin shape diversity across reef fish (Figs. 2, S2). The first axis of pectoral fin diversity (PC1) separates fins by what is commonly referred to as aspect ratio, or an axis of narrow, wing-like fin shapes to deep, paddle-like fin shapes. The elongation of the pectoral fin at the lower half of PC1 is possible through a lengthening of the leading edge, trailing edge, or central rays of the fin. This variation in which parts of the fin are lengthened falls out on the second axis of pectoral fin variation, which reflects the ratio between the length of the leading and trailing edges of the fin. Here, species that score high on PC2 have longer trailing edges of the fin, and species with low PC2 scores have longer leading edges. I detect a significant effect of locomotor mode on mean pectoral fin shape (Table 1; $p=0.003, F=3.475, df=3,105$). Specifically, the mean BCF pectoral shape is more wing-like (low PC1) than other locomotor groups. Benthic species almost exclusively occupy the region of morphospace with elongated trailing edges (high PC2). The MPF categories, labriform and tetraodontiform, occupy the mid to upper region of PC1 and lower region of PC2, with generally more paddle-like fins where the leading edge is more elongate. Labriform swimmers are more central in pectoral fin shape than tetraodontiform swimmers; note, however, that the MPF swimming categories are the only pair without statistically different mean pectoral shapes. Benthic species have the greatest disparity (Fig. 4; Table S2; 0.052) in pectoral shape, while labriform swimmers have the lowest disparity (0.022).

The first two axes of caudal fin shape diversity separate fins that are 1) rounded (low PC1) to forked (high PC1) and 2) deep (low PC2) to narrow (high PC2). When corrected for number of landmarks and species, caudal fin disparity is similar across all locomotor modes (Table S2; 0.031-0.034). The locomotor groups highly overlap in the caudal fin morphospace, showing no differences in mean fin shape (Table 1; *p=0.102, F=1.760, df=3,105*). BCF, benthic, and labriform swimmers occupy a wide array of shapes, spanning both PC1 and PC2. However, the tetraodontiform caudal occupies a very narrow region of PC1 in which the caudal fins are slightly more rounded than square, though mean shape is not significantly different from the mean of the other locomotor groups. It should be noted that of the 34 labriform species and 15 benthic species, only 6 labriform and 2 benthic species have heavily forked caudal fins. In contrast, BCF swimmers more evenly occupy the array of caudal fin shapes.

The dorsal fin morphospace is the most intricate, and the primary axes of diversity are the most complex. PC1 represents both the gradient in dorsal fins that are elongate and low-lying (low PC1) to those that are short and deep (high PC1), and dorsal fins with longer posterior rays (low PC1) relative to longer anterior spines (high PC1). PC2 separates fins that have a significant separation between the spiny and soft dorsal (low PC2) and continuous fins (high PC2). Most species lay in the low PC1, mid-PC2 region of elongate continuous dorsal fins, with a subtle dip where the spines and rays meet. Many of the locomotor groups have a large degree of overlap in dorsal fin morphospace, however, I do detect a significant effect of locomotor group on mean dorsal shape (Table 1; *p=0.007, F=2.421, df=3,105*). Namely, the tetraodontiform swimmers have a mean dorsal shape significantly shorter and deeper (high PC1) than other locomotor groups. However, they span the range of a single continuous dorsal (Tetraodontidae) to a split between the spiny dorsal and soft ray dorsal (Balistidae & Monacanthidae). Interestingly, dorsal

fin disparity is similar for BCF, benthic, and labriform swimmers (0.043-0.047); however, tetraodontiform dorsal fins display nearly 3x the disparity of the other locomotor groups (0.126), making the tetraodontiform dorsal the most diverse of any fin shape (Fig. 4; Table S2).

Like the dorsal fin, the first axis of diversity in the anal fin distinguishes species that have elongate, low-lying anal fins (low PC1) and those that have short, deep anal fins (high PC1). PC2 represents a ratio of the length of the anterior-most spines (or rays in the absence of spines) of the fin to the length of the rays at the posterior of the fin, separating species with longer anterior length (low PC22) to longer posterior length (high PC2). Locomotor groups are not distinct in mean anal fin shape (Table 1; *p=0.220, F=1.426, df=3,105*). However, tetraodontiform swimmers do not occupy the low PC1 region. Labriform swimmers have anal fin shapes nested within the diversity of the other locomotor modes and are more central in the morphospace. Benthic species span most of PC1 but occupy only a narrow region of PC2 where the anterior and posterior spine/ray lengths are uniform. Tetraodontiform swimmers have the greatest anal fin disparity (0.066), while labriform swimmers have the lowest disparity (0.029).

Effects of Locomotor Mode on Unique Fin Morphospace Occupation

While the analyses in the previous section allow us to address the impacts of locomotor mode on the mean fin shape, using hypervolumes demonstrates whether the diversity of fins within locomotor groups occurs within unique or shared regions of morphospace (Table 2, S3). The range of significant results observed when comparing unique morphospace occupation of a focal locomotor group to all species not in that locomotor group (non-focal group species) were that a) the focal group occupied more unique morphospace than expected under a null model, b) the focal group occupied less unique space than expected, and c) the non-focal group occupied more

unique space than expected. I did not observe any cases where the non-focal group was less unique than expected.

I find that for the pectoral fin, the volume of morphospace that benthic species occupy is more unique than would be expected under a null model (68% unique, $p=0.0019$); meanwhile, the labriform morphospace occupation is far less than would be expected under a null model (only 2.3% unique, $p=0.9989$). These results indicate that benthic species have expanded into more novel morphospace than expected, and labriform species have diversified less than expected. I also find that non-BCF, non-labriform, and non-tetraodontiform are more unique than expected from their respective focal locomotor groups. In other words, there are significant regions of the focal group morphospace that species outside of the focal group do not occur in, indicating more exclusion from focal group regions than would be expected under a null model (see Table 2 for p-values on non-focal group hypervolumes).

I find one significant result for the caudal fin: non-tetraodontiform swimmers are significantly excluded from the tetraodontiform morphospace ($p=0.0125$). In the dorsal fin, tetraodontiform swimmers occupy 93% unique morphospace ($p<0.0001$), and non-labriform swimmers are significantly excluded from the region occupied by labriform swimmers (82% unique; $p=0.007$). Finally, for the anal fin, labriform species occupy less unique morphospace than expected under a null model (only 6.9% unique, $p=0.9801$) and non-labriform swimmers occupy a large region that is non-overlapping with labriform morphospace ($p<0.0001$). Additionally, the tetraodontiform occupation of anal fin morphospace is highly unique at 67.7% ($p=0.0069$).

The possible outcomes of pairwise hypervolume comparisons between locomotor groups were that a) one locomotor group shared less morphospace with the other than expected, b) both

shared less morphospace than expected, or c) neither was significantly unique in morphospace occupation (see Table S3 for proportions of the hypervolumes that were unique in morphospace and the associated p-values). I did not observe cases where either locomotor group occupied more shared morphospace than expected.

For the pectoral fin, the benthic species hypervolume shared less morphospace than expected with BCF, labriform, and tetraodontiform swimmers (see Table S3 for statistics). Additionally, the BCF pectoral hypervolume had a large region that was significantly unique from tetraodontiform swimmers. The labriform occupation of pectoral fin morphospace was never statistically unique, indicating labriform swimmers had a large volume nested within the BCF, benthic, and tetraodontiform hypervolumes. The BCF hypervolume was largely unique relative to tetraodontiform swimmers in the caudal fin (Table S3). Tetraodontiform swimmers shared little dorsal fin morphospace with any of the other three locomotor groups. Finally, for the anal fin, BCF swimmers and benthic species both occupied much unique space relative to labriform and tetraodontiform swimmers. Tetraodontiform swimmers also had a large proportion of morphospace unique from BCF, benthic, and labriform swimmers. However, the labriform morphospace was not significantly independent from BCF, benthic, or tetraodontiform swimmers. All other pectoral, caudal, dorsal, or anal comparisons not explicitly mentioned above were highly overlapping in hypervolume space.

Effects of Locomotor Mode on Fin Shape Evolutionary Integration and Rate of Evolution

To determine if patterns of fin evolutionary integration vary with locomotor mode, I tested for phylogenetic integration among the fins of species within locomotor groups (Table 3). To understand overall patterns of fin evolutionary correlation, I tested for phylogenetic integration among all species (Table S4). I find that fin modules among fishes in the most likely ancestral

locomotor mode, BCF swimming, are more integrated than any of the derived locomotor modes. In BCF swimmers, all fins are integrated except for the pectoral and dorsal (*p=0.338*), with the most substantial integration being between the dorsal and anal fins (*r = 0.72, Z=4.09, p=0.001*). Aside from the dorsal-anal integration, the BCF fin integrations are significant but relatively weak, with a correlation coefficient (*r*) ranging from 0.45 to 0.52 and effect sizes (*Z*) from 1.69 to 2.28 (*p = 0.009 – 0.045*). The dorsal and anal remain integrated in the three derived locomotor modes, though with a weaker signal (*r=0.65-0.89, Z=1.98-2.48, p=0.005-0.022*). Labriform species have lost all other integration except for a weak integration between the caudal and anal (*r=0.50, Z=1.78, p=0.037*). Tetraodontiform swimmers have no other significant integration. In benthic species, the only other significant integration is between the pectoral and dorsal (*r=0.73, Z=1.67, p=0.043*), though *r* is quite high here, the significance is weak due to there being relatively few benthic species.

Overall patterns of fin integration are similar to patterns within BCF swimmers but stronger, showing that all fins are integrated (*r=0.33-0.62, Z=2.10-4.92, p=0.001-0.016*) except for the pectoral and dorsal (*r=0.28, Z=0.82, p=0.195*; Fig. 3; Table S4). Elongate, wing-like pectorals typically occur with more forked caudals and elongate, low-lying anal and dorsal fins, while rounded, paddle-like pectorals occur with rounded caudals and short and deep anals and dorsals (Fig. 3A, B, C). Low-lying, elongate dorsals are more common with more forked caudals and elongate, low-lying anal fins (Fig. 3D, E). Rounded caudals occur with deeper, short anal fins, while more forked caudals occur with elongate, low-lying anal fins (Fig. 3F). In all cases, there is plentiful variation that falls off the main integration axes, and much of the off-axis variation represents diversity within locomotor groups. Notably, for the dorsal-anal and caudal-anal

integration, locomotor mode variation is more constrained to the overall integration axes than other fin combinations.

Evidence for independent evolution of the fins among reef fish comes from comparing their respective rates of evolution. When comparing the Brownian rates of fin shape evolution for all species, I find a rate ratio of 3.6 (*Z=21.66, p=0.001*), where the dorsal fin is evolving the fastest (rate = $3.62x10^{-4}$) and the pectoral has the slowest rate (rate=$1.00x10^{-4}$). The caudal (rate=$2.20x10^{-4}$) and anal ($1.73x10^{-4}$) are intermediate in the Brownian rate of evolution. Much of the high rate in the dorsal fin comes from the vast morphological disparity acquired by tetraodontiform fishes in a relatively short amount of time (Fig. 4, *p=0.001*). In addition to the dorsal fin, the caudal fin also shows a significant effect of locomotor mode on the rate of evolution, where BCF and labriform swimmers have caudals that evolve faster than tetraodontiform or benthic species (*p=0.004*). While I detected no significant effect of locomotor mode on the rate of evolution in the pectoral fins (*p=0.083*), it is notable that BCF and labriform swimmers have lower rates of evolution relative to tetraodontiform and benthic species. BCF, benthic, and tetraodontiform swimmers have similar rates of evolution of the anal fin, and the rate is lower for labriform swimmers though not statistically so (*p=0.069*).

Discussion:

Locomotor diversity relates broadly to reef fish ecology, including feeding, habitat use, and reproduction. However, the locomotor system in reef fishes is complex and comprises many fins, all of which may directly and indirectly be subject to selection for locomotor specialization. Previous studies have described varying levels of functional cooperation between the fins of reef fishes (Blake, 2004; Fulton, 2007; Sfakiotakis, 1999), ecological specialization of the fins (Bellwood & Wainwright, 2001, Bridge et al., 2015), and shared physical and genetic

developmental pathways among fins (Ahn et al., 2002; Crotwell et al., 2001, 2004; Crotwell & Mabee, 2007; Dahn et al., 2007; Freitas et al., 2006; Goodrich, 1906; Huede et al., 2014; Letelier et al., 2018; Mabee et al., 2002; Neumann et al., 1999; Sordino et al., 1995). Each of these factors has the potential to strongly influence the macroevolutionary patterns of fin diversification and points toward an expectation of strong integration among fins. In contrast to this expectation, I find only a weak relationship between swimming mode and fin shape and unexpected diversity of fins within each locomotor mode category. In their ancestral locomotor condition, BCF swimming, reef fishes exhibit significant but weak integration among fins. With the introduction of derived locomotor modes the integration among fins is further weakened. These findings illustrate that a general lack of tight functionally induced fin shape restrictions and the presence of mild integration allow for high morphological and locomotor diversity in reef fishes.

Weak signals of locomotor mode in fin morphospace occupation and evolutionary rate

Relationships between form and function are often the core focus for evolutionary biologists aiming to describe mechanisms driving the accumulation of diversity in highly diverse functional systems. In locomotor systems, variation in routine locomotor mode is often related to diversity in limb anatomy (Berman, 1985; Buttimer et al., 2020; Citadini et al., 2018; Martín-Serra et al., 2014; Wainwright et al., 2002). However, in reef fishes I find locomotor mode diversity is not easily described by variation in fin shape. In each fin type I measured, there are large areas of overlap where multiple locomotor groups occupy similar fin shapes. Further, the range of fin shapes that each locomotor group contains is often quite expansive. For example, the caudal fins of benthic species, BCF, and labriform swimmers span the full axis of rounded to forked, and the dorsal and anal fin diversity of benthic and labriform swimmers is almost entirely nested inside

the diversity of BCF swimmers. As such, if one selected a caudal, dorsal, or anal fin shape at random, it would be a challenge to identify which locomotor group the fin belonged to.

Pectoral fins show the strongest signal of swimming mode effects, as many of the locomotor groups have different mean pectoral shapes (Fig. 2, Table 1), and the hypervolumes show that many regions of pectoral fin morphospace are only accessible to a single locomotor group (Table 2). In particular, the average BCF pectoral is significantly more elongate and has rays that are longest in the middle of the fin relative to the labriform and tetraodontiform groups that have more rounded pectorals where the longest ray is along the leading edge. Note that the pectoral fin is the most important fin in labriform propulsion, and the finding that the labriform pectoral fin occupies less unique space than expected under a null model (Table 2) and the low Brownian rate of evolution and low disparity (Fig. 4) suggests that the functional role of the pectoral in labriform swimming may constrain its morphospace diversification. Additionally, there is a large region of pectoral morphospace uniquely occupied by benthic species, in which the trailing edge rays are lengthened relative to the leading edge. In contrast to labriform species in which the pectoral is the predominant propulsor and shows reduced rates of evolution and disparity, benthic species use their pectoral fins for substrate contact and these fins evolve relatively rapidly with high morphological disparity. Benthic species have pectoral fins that therefore appear released from the functional constraints of locomotion.

Tetraodontiform locomotion is highly reliant on the cooperation between the dorsal and anal fins. In this group I find that generally both fins are typically short in base length but deep. However, there is substantial morphological disparity in the tetraodontiform locomotor fins, in part because the families Balistidae and Monocanthidae have evolved a split dorsal fin in which the spiny region of the fin is not used in locomotion but is rather a predominant anti-predator

defense mechanism. The disparity in the tetraodontiform anal fin reflects diversity in the lengthening of different regions of the anal fin. Specifically, balistids and monacanthids have longer anterior edges which may reflect a genetic or developmental lack of independence with the elongation of the spiny first dorsal (Sorenson, 2007). It is plausible that if one examined the rate of evolution and morphological disparity of only the soft ray dorsal fin in tetraodontiform swimmers, it would be more reflective of the rate and disparity in the anal fin. Future work should be done to investigate the functional decoupling of the first and second dorsal fin and the implication of that decoupling for locomotor evolution. Interestingly, the caudal and pectoral fins in tetraodontiform swimmers occupy narrow regions of morphospace. Most species in this group feed on benthic invertebrates, requiring the ability to navigate complex benthic structures. Thus, the confinement to narrow morphospace in the tetraodontiform caudal and pectoral could reflect their constraints induced by their essential role in maneuvering and stabilization (Blake, 1978; Dornburg et al., 2011) for this group in which most species feed on benthic invertebrates, requiring the ability to navigate complex benthic structures (Corn et al., 2022; Turingan, 1994). Alternatively, if these fins are generally used less by tetraodontiform swimmers, there may be little selective pressure to evolve outside of the existing diversity in this clade.

Evolutionary integration between fins is lost with locomotor expansion

Evolutionary integration has been debated as either a facilitator or hinderer of diversification in complex functional systems (Burns et al., 2023; Du et al., 2019; Eliason et al., 2023; Evans et al., 2017, 2021; Felice et al., 2018; Goswami & Polly, 2010; Hansen 2003; Larouche et al., 2018; Marroig et al., 2009). In the vertebrate locomotor system, the typical ancestral condition is one of functional cooperation among the limbs, which, in combination with shared genetic and developmental limb origins, can induce evolutionary integration (Gatesy & Dial, 1996; Goswami

et al., 2014; Hallgrímsson et al., 2002; Petit et al., 2017; Wimberley et al., 2021). Reef fish appear to follow this general rule as I find that the most likely ancestral state is body-caudal fin (BCF) swimming, which makes use of all fins regularly. Further, I observe that generally (and specifically for BCF swimmers) almost all fin combinations are integrated, as expected given the shared genetic and developmental pathways among the fins, and likely functional cooperation. However, while significant integration exists across reef fish fins (Table S4), integration is generally weak and there is a large amount of off-axis diversity in fin shape ($r = 0.28 – 0.62$). Further, the different rates of fin shape evolution and the spectrum of accumulated morphological disparity (Fig. 4) suggest considerable independent evolution in fin shape. Together, these findings indicate that for reef fishes, weak integration has acted as an evolutionary pathway of least resistance, providing a backbone for diversification. At the same time, the ability to independently evolve in some capacity allows for further expansion into disparate regions of morphospace.

I additionally find that reef fishes experience locomotor expansion through lability in evolutionary integration (Table 3, Fig. 4). I find that within each novel locomotor mode (labriform, tetraodontiform, and benthic) that arises out of BCF swimming, there is a loss of detectible evolutionary integration between most of the fins. My findings mirror patterns observed in birds and mammals in which locomotor expansion into bipedal walking and flight consistently co-occur with reduction in morphological correlation between limbs (Bell et al., 2011; Garland et al., 2017; Goswami et al., 2014; Kelly & Sears, 2011; Young & Hallgrímsson 2005, Young et al., 2010). Such lability in evolutionary integration suggests that either underlying genetic ties between traits must first be broken prior to locomotor expansion, or that evolution into novel ecological niches and selection for new locomotor capacities releases

functional constraints on diversification off of axes of integration. Further, I also see that fin shape variation within locomotor groups typically falls off the primary axis of integration (Fig. 3A-D), with the exception being the integration between the dorsal and anal fin, which remains present in all locomotor groups (Fig. 3E). As such, variation within locomotor groups is more parallel to the primary integration axis between dorsal and anal fins (Fig. 3E). The same is true of the caudal and anal integration (Fig. 3F), though when phylogeny is accounted for, this integration is not significant for tetraodontiform swimmers and benthic species (Table 3). Comparing off-axis diversity within a locomotor group when integration is weak versus strong demonstrates that weak axes of integration and lability in that integration are integral in the diversification of the reef fish locomotor system.

The retained integration between the dorsal and anal across locomotor groups, even with phylogeny accounted for, is likely driven by their similar developmental and genetic origins in addition to the tendency of these fins to functionally cooperate more directly than any other fin combination. In contrast, there is no detectable integration in the pectoral and dorsal fins, except for a very weak trend for benthic species that is actually counter to the primary axis of shape diversity in the other species (Fig. 3A, Table 3). Such lack of integration between the pectoral and dorsal is not surprising given that they develop from independent fin folds. Additionally, the dorsal fin, perhaps more than any other fin, has functional roles outside of locomotion, such as predation defense. This functional independence may promote greater evolutionary independence. In fact, the developmental isolation of the pectoral fin on the body makes the evidence for evolutionary integration between the pectoral and caudal and the pectoral and anal (overall and in the ancestral swimming condition) surprising. This finding demonstrates that the

predominant function of each of these fins in locomotion is a strong enough factor to induce evolutionary integration despite some developmental independence.

Conclusion

The effect of locomotor mode on reef fish fin morphospace is limited, as there is high diversity in fin morphology within locomotor groups. The many to one mapping of fin shape to locomotor mode demonstrates that no single fin shape is most suited to satisfying the demands of any specific locomotor style. While locomotor mode does not map strongly to fin shape, I do observe that evolutionary integration between fins is lost with each transition to a novel locomotor mode. This functional expansion into new locomotor modes is likely encouraged due to weak integration with extensive off-axis diversity in the ancestral swimming condition, BCF swimming. Future work should address whether relationships between evolutionary integration and functional novelty in comparative phylogenetic frameworks hold across diverse vertebrate taxa and functional systems.

Figures and Tables:

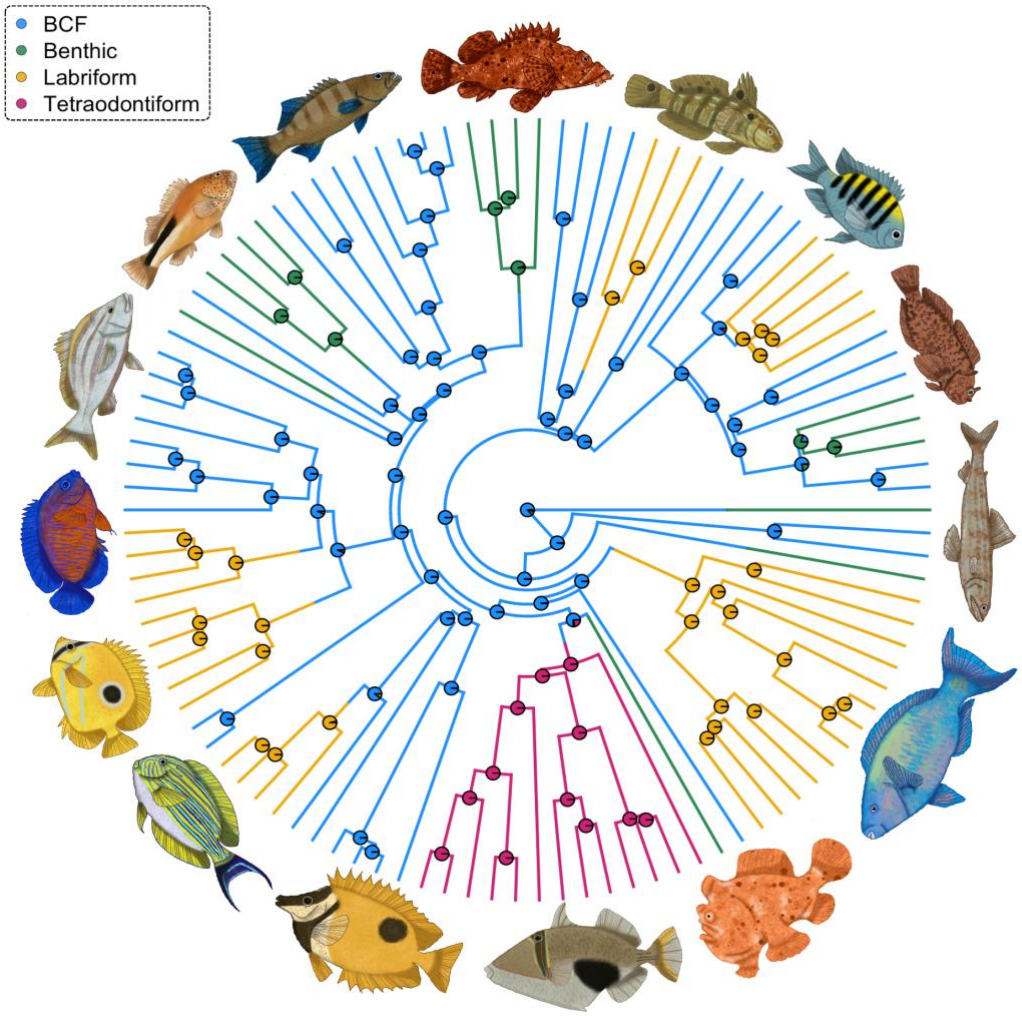

Figure 1. **Stochastic character map of the history of locomotor styles**, with pie charts indicating the node state percentage out of 100 maps. Blue represents body caudal fin (BCF) swimmers, which use the undulation of their body and caudal fin to move forward. Yellow lineages use pectoral fins as the predominant propulsor (labriform), and pink lineages use the dorsal and anal fin for propulsion (tetraodontiform). Green represents benthic species.

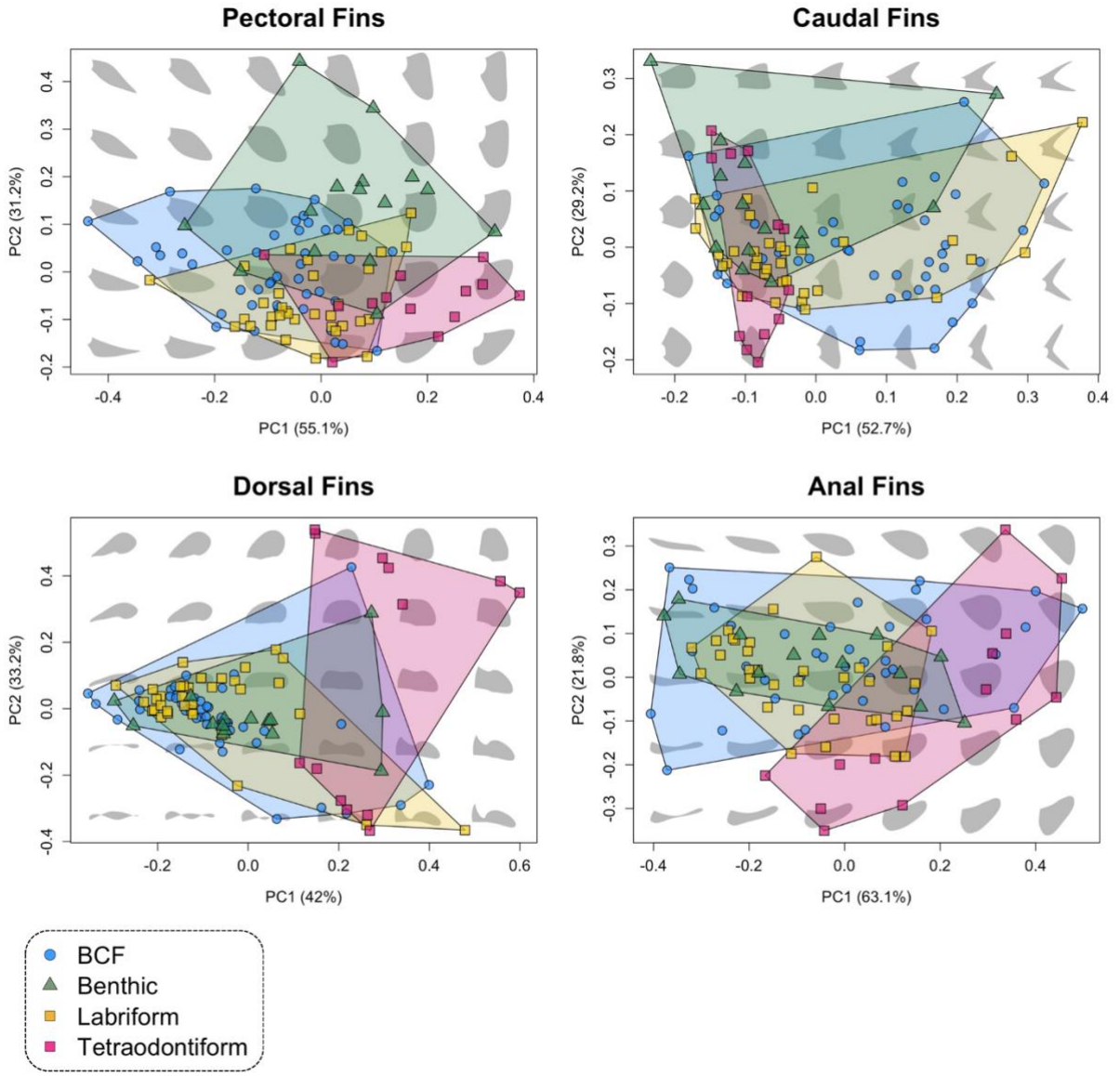

Figure 2. **Fin Shape Diversity by Locomotor Mode.** A) Fin shape morphospaces for the pectoral, caudal, dorsal, and anal fins. Each point represents the average Procrustes superimposed fin shape for a species. Blue circles represent body caudal fin (BCF) swimming species. Green triangles are benthic species. Squares represent median paired fin (MPF) swimming species. MPF labriform species in yellow, and pink are MPF tetraodontiform swimmers.

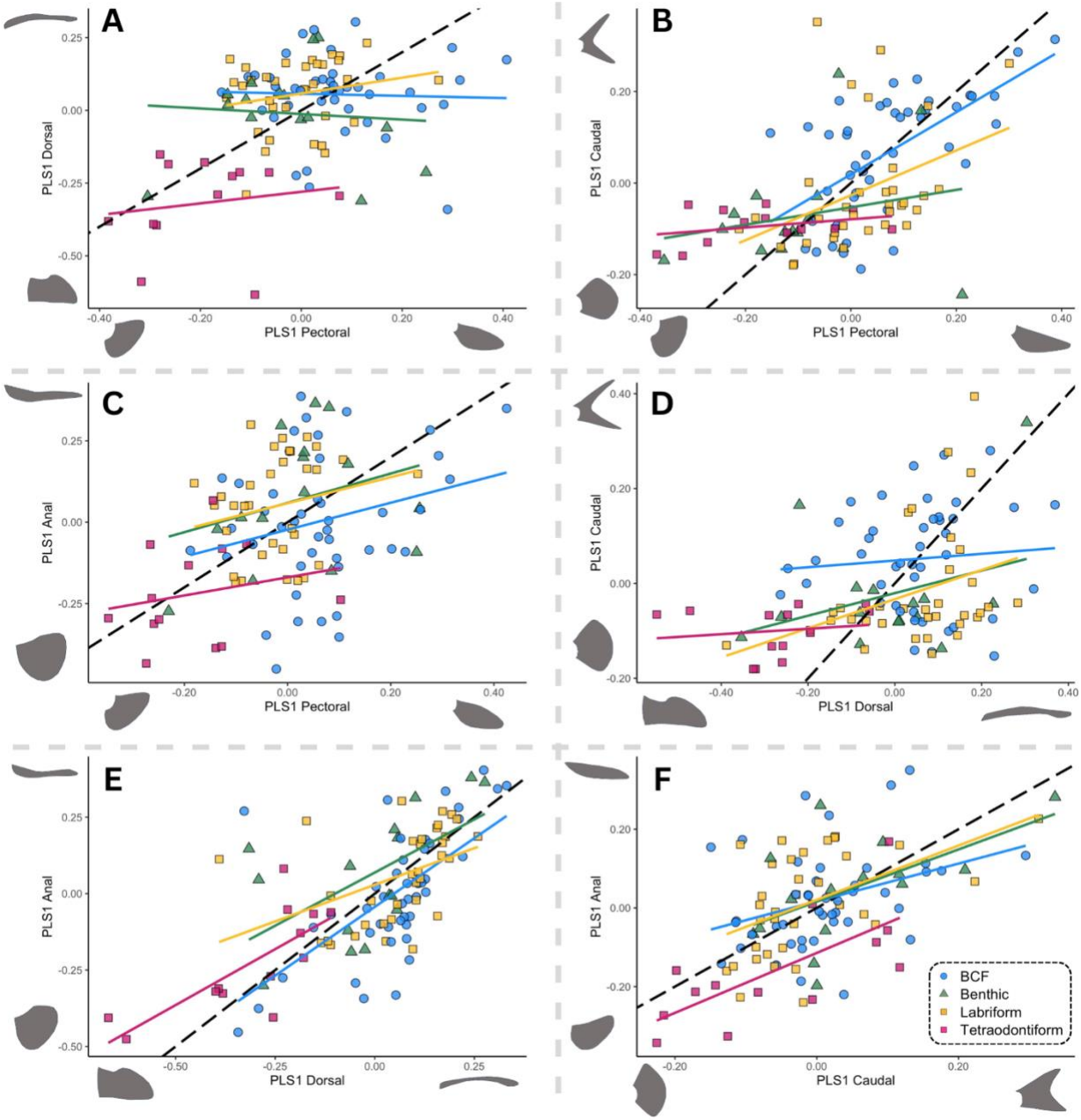

Figure 3. **First partial least squares regressions depicting morphological correlation between fin shapes.** Linear relationships showing non-phylogenetically corrected morphological integration between fins: A) dorsal vs. pectoral, B) caudal vs. pectoral, C) anal vs. pectoral, D) caudal vs. dorsal, E) anal vs. dorsal, F) anal vs. caudal. Each point represents the first partial least squares (PLS1) score for a species. Blue circles represent body caudal fin (BCF) swimming species. Green triangles are benthic species. Squares represent median paired fin (MPF)

swimming species. MPF labriform species in yellow, and pink are MPF tetraodontiform swimmers. Dashed black line is the overall integration trendline for all species. The trendline for integration within each locomotor group is also displayed as a solid line matching the color of the points.

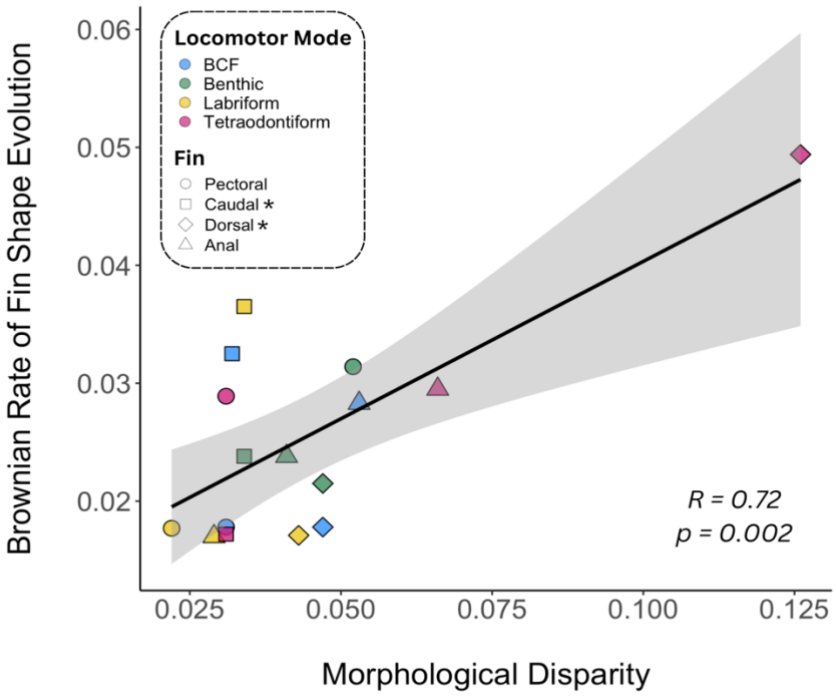

Figure 4. **Brownian Rate of Fin Shape Evolution versus Morphological Disparity**. For each fin the Brownian rate of fin shape evolution and morphological disparity were calculated within locomotor mode groups using *geomorph (v 4.0.5; R)*. Rates have been multiplied by 10,000. Blue shapes represent body caudal fin (BCF) swimmers, green are benthic species, yellow represents labriform swimmers, and pink represents tetraodontiform swimmers. Circles are pectoral fins, squares are caudal fins, diamonds are dorsal fins, and triangles are anal fins. The correlation coefficient (R) and the associated p-value for the relationship between rate and disparity are provided. Disparities have been corrected for the number of landmarks for each fin. Asterisks next to the fin labels indicate significant effect of locomotor mode on the rate of evolution (Caudal: *p=0.004*, Dorsal: *p=0.001*).

Table 1. **Mean fin shape by locomotor mode ANOVAs.** *P*-values and *F* statistics where mean fin shape significantly differs by locomotor mode are bolded. For fins with different mean fin shape by locomotor mode the pairwise least squares comparisons are provided to indicate which locomotor groups differ in shape from each other.

Phylo. ANOVA	Pectoral	Caudal	Dorsal	Anal
p	**0.003**	0.102	**0.007**	0.220
F	**3.475**	1.760	**2.421**	1.426
Pairwise Comparison				
BCF : Benthic	**0.012**		0.607	
BCF : MPF - Lab.	**0.031**		0.105	
BCF : MPF - Tet.	**0.004**		**0.002**	
Benthic : MPF - Lab.	**0.003**		0.074	
Benthic : MPF - Tet.	**0.009**		**0.010**	
MPF - Lab. : MPF - Tet.	0.318		0.094	

Table 2. **Hypervolume results.** Comparisons of the hypervolumes of species within a locomotor group against the hypervolume of all other species. The table contains the fraction of the hypervolume space which is unique to each hypervolume, and the p-values calculated as the proportion of 10,000 permutations (hypervolume identity was randomly assigned to average fin shape landmarks) in which the unique hypervolume space was more extreme than observed. P-values less that 0.05 (bolded) indicate the real hypervolume occupies more unique space than expected relative to a null distribution. Real hypervolumes and random permutations were generated in *Hypervolume (v 3.1.3; R).*

Hv1	Hv2	unique frac. Hv1	Prop. Of permuted Dist. > unique frac. Hv1	unique frac. Hv2	Prop. Of permuted Dist. > unique frac. Hv2
Pectoral					
BCF	Not BCF	0.163	0.7366	0.559	**0.0059**
Benthic	Not Benthic	0.679	**0.0019**	0.236	0.7138
Labriform	Not Labriform	0.023	**0.9989**	0.679	**0.0002**
Tetraodontiform	Not Tetraodontiform	0.362	0.2471	0.759	**0.0064**
Caudal					
BCF	Not BCF	0.330	0.3277	0.384	0.2573
Benthic	Not Benthic	0.210	0.5819	0.704	0.0535
Labriform	Not Labriform	0.247	0.5094	0.530	0.0958
Tetraodontiform	Not Tetraodontiform	0.453	0.2311	0.816	**0.0125**
Dorsal					
BCF	Not BCF	0.163	0.7967	0.661	0.0530
Benthic	Not Benthic	0.231	0.6238	0.618	0.2451
Labriform	Not Labriform	0.111	0.8825	0.820	**0.0070**
Tetraodontiform	Not Tetraodontiform	0.930	**0.0000**	0.587	0.3042
Anal					
BCF	Not BCF	0.388	0.1862	0.296	0.4266
Benthic	Not Benthic	0.238	0.5533	0.573	0.1634
Labriform	Not Labriform	0.069	**0.9801**	0.805	**0.0000**
Tetraodontiform	Not Tetraodontiform	0.678	**0.0069**	0.675	0.0770

Table 3. **Fin by fin comparisons of phylogenetic integration.** Results generated using *Geomorph (v 4.0.5; R).* Statistically significant integrations were determined based on 1000 iterations and are denoted by p-values (*P)* which are bolded.

Fin By Fin Phylo. Integration	**Body Caudal Fin (BCF)**			**Labriform (MPF)**			**Tetraodontiform (MPF)**			**Benthic**		
	***r*-PLS**	**Effect (*Z*)**	***P***	***r*-PLS**	**Effect (*Z*)**	***P***	***r*-PLS**	**Effect (*Z*)**	***P***	***r*-PLS**	**Effect (*Z*)**	***P***
Pectoral - Dorsal	0.40	0.39	0.338	0.51	1.09	0.140	0.46	-0.50	0.692	0.73	1.67	**0.043**
Pectoral - Caudal	0.45	1.69	**0.045**	0.43	1.12	0.145	0.45	0.04	0.479	0.70	1.45	0.079
Pectoral - Anal	0.49	2.19	**0.011**	0.36	0.05	0.482	0.61	0.92	0.185	0.52	2.42	0.413
Dorsal - Caudal	0.52	1.80	**0.034**	0.51	1.33	0.104	0.70	1.46	0.076	0.65	0.80	0.650
Dorsal - Anal	0.72	4.09	**0.001**	0.65	2.40	**0.008**	0.89	2.48	**0.005**	0.74	1.98	**0.022**
Caudal - Anal	0.52	2.28	**0.009**	0.50	1.78	**0.037**	0.67	1.37	0.096	0.51	0.19	0.444

Chapter 3: Diverse Evolutionary Pathways to Morphological Novelty in Coral Reef Fishes.

Introduction:

Understanding the processes that give rise to morphological diversity is a major focus of evolutionary research. One major factor is that morphological systems are evolutionarily integrated, with traits that covary through deep timescales (Goswami et al., 2014; Felice et al., 2018; Larouche et al., 2018; Evans et al.,2021;2023). For example, in quadrupedal tetrapods, changes in the forelimb typically co-evolve with changes in the hindlimbs such that if the radius and ulna lengthen, the fibula and tibia also lengthen (Schmidt & Fischer, 2009; Villmoare et al., 2011; Foster et al., 2018; Mallet et al., 2020). These evolutionary correlations may be caused by shared functional demands, genetic pathways, and developmental origins (Klingenberg, 2008; Zelditch & Goswami, 2021; Evans, 2023).

When morphological systems are evolutionarily integrated, shapes can evolve by following axes of covariation between traits (Goswami et al., 2014). In such cases, selection on one trait can induce shared responses in associated traits (Marroig & Cheverud, 2005). For example, the caudal fin and pectoral fin are both important in fish locomotion, and pleiotropic genes can regulate development of both fins (Webb, 1984; Akimenko et al., 1994;1995; Freitas et al., 2006; Fulton, 2007; Heude et al., 2014). As such, selection for a pectoral fin with high surface area and a rounded shape to enhance maneuverability may tow the evolution of the caudal fin to a higher surface area, rounded shape. Similarly, selection for drag-reducing high aspect ratio caudal fins can pull the pectoral fin into a more wing-like high aspect ratio shape (Fig. 1a; Satterfield et al., In Review). More generally, as selection on any one trait in an integrated system will bring correlated traits into novel morphospace, we can think of the axis of

trait covariation as an evolutionary pathway of least resistance, a pipeline to morphological and functional extremes (Schluter, 1996; Du et al., 2019; Evans et al., 2021; Eliason et al., 2023).

Additionally, studies show that with increasing strength of covariation between traits, extreme phenotypes along the integrated axis are more likely to be reached (Goswami et al., 2014). However, strong integration limits off-axis diversification (Marroig et al., 2009; Goswami & Polly, 2010; Evans et al., 2017; Larouche et al., 2018). Off-axis diversification occurs when traits evolve independently and is facilitated by modularity of body regions that permits relatively independent diversification (Klingenberg, 2008; Zelditch and Goswami, 2021). One can think of the extreme morphologies that arise through off-axis evolution as evolutionary mismatches that may reflect selection for functional decoupling or novel trait combinations. For example, a caudal fin that is high aspect ratio and experiences less drag and is thus advantageous for efficient swimming endurance paired with a low aspect ratio pectoral fin that allows for more drag and is better for maneuverability (Fig. 1a).

Extreme off-axis phenotypes, as much as extreme integrated phenotypes, represent morphological and functional novelty but are thought to be less likely achieved relative to extreme traits along an integrated axis. This is because an integrated system of traits can respond to selection on one trait by pushing the entire system into novel morphospace, while traits evolving independently will only enter the outer regions of morphospace if all traits experience selection individually (Goswami et al., 2014; Zelditch & Goswami, 2021). Nevertheless, both strong integration and strong modularity are seen as different pathways to extremes of morphospace. While examples of both are common in the literature, there is no consensus on their relative importance across large sections of the tree of life.

One framework for identifying the evolutionary pathway that has led to morphological novelty is to calculate 1) the morphological difference of species from average morphology as a measure of morphological novelty and 2) estimate the phylogenetically corrected covariation between traits (evolutionary integration) as well as the amount of off-axis variation not explained by trait covariation (the residuals from an axis of integration between modules). The morphological difference from average is informative of which species have evolved the most extreme morphologies. The residual variation around an integration axis tells us to what degree traits are evolutionarily mismatched. By plotting these two variables against each other, we can construct a two-dimensional space in which we can isolate species into a) those with typical morphologies that fall along an axis of integration, b) those with typical morphologies through independent evolution, c) those which have evolved traits at the extreme ends of an axis of integration, and d) those which have evolved extreme phenotypes through independent evolution of traits (Fig. 1b). In theory, when integration among modules is very strong, few if any species will have access to extreme morphologies through off-axis evolution but will reach farthest in the morphological diversity. When there is no integration, we expect most species to have trait combinations that evolve independently but rarely to morphological extremes (Goswami et al., 2014). Thus, we expect morphological novelty to be most common when integration is present but weak enough to allow for some off-axis evolution. We can apply this framework to simple two-trait integrated systems, or it can be advanced to apply to complex multidimensional systems.

A prominent example of one of the most functionally diverse systems among vertebrates is the coral reef fish feeding system. Among over 70 families which began interacting with reefs as long as 150 Mya (Bellwood & Wainwright, 2002; Ghezelayagh, 2022), reef fish now

encompass vast trophic diversity from lower levels such as detritivores, algivores, and planktivores, to mid-level invertivores feeding on prey such as corals, worms, and echinoderms, and finally high-level carnivores feeding on fish, large mollusks, cephalopods, and crustaceans (Randall, 1967; Wainwright & Bellwood, 2002; Bellwood et al., 2005; 2010; Mouillot et al., 2014; Clements et al., 2016, Tebbett et al., 2017; Mihalitsis & Bellwood, 2019; Mihalitsis et al., 2022). Descriptions of the morphological basis of feeding diversity in reef fish have primarily emphasized adaptations in the skull, mouth, and jaws (Kotrschal, 1989; Wainwright & Bellwood, 2002; Wainwright et al., 2004; Barnett, 2006; Konow et al., 2008; Cooper & Westneat, 2009; Konow & Bellwood, 2011; Huertas & Bellwood, 2020). For example, diversity in the jaws of reef fish reflects an axis of integration in jaw traits that reflect diet categories at one extreme that primarily require suction to overtake prey versus the other extreme requiring physical removal of benthically attached prey (Burns et al., in Review). Even so, a substantial amount of functional variation exists in the reef fish feeding system that cannot be explained by diversity in the jaws alone.

While fish must, of course, use their jaws to capture and process prey, their body and fins are responsible for positioning the fish to capture prey as well as providing leverage and stability (Webb, 1984; Rincón et al., 2007; Mihalitsis & Bellwood, 2019; Friedman et al., 2020; Larouche et al., 2020; Perevolotsky et al., 2020; Corn et al., 2022). Thus, the jaws, body, and fins likely comprise a more complex and integrated network of traits contributing to feeding performance. However, the body and fins are also crucial in functions unrelated to feeding, such as courtship and defense against predation, and therefore, likely benefit from the ability to evolve with some independence from their role in the feeding system (Amundsen & Forsgren, 2001; Robinson et al., 2011; Aguilar-Medrano et al., 2013; Price et al., 2015). Therefore, it is plausible that some

modules of the feeding system, like the jaws, may be more predictive of functional diversity than others.

However, any integration between the jaws, body, and fins could be the basis of specialized diversification in the feeding system, where combinations of integrated and independent evolution of traits in a broader network explain greater functional variance than the jaws alone. Specifically, integration among structures in the feeding system may act as pipelines of functional diversification that may the mechanism facilitating the vast trophic diversity in reef fishes. For example, benthic invertivory is thought to require laterally compressed bodies for maneuverability and robust jaws for removing hard from the reef (Corn et al., 2023; Burns et al., In Review). If robust jaws were correlated with deep bodies, fish may follow this axis of integration towards extreme optimal phenotypes for this diet. However, other diet types may not require such demands on the morphology, and we may expect to see a higher degree of modularity in such cases.

In this paper, I aim to first present a method for determining the relative importance of integrated axes versus off-axis independent trait evolution in the evolution of extreme morphologies in complex functional systems. I then evaluate the importance of these two pathways for the evolution of novel extreme phenotypes in reef fishes as a model of a highly diverse complex morphological system. Additionally, I illustrate the effects of variable strength of integration on access to morphological extremes through simulations of morphological evolution under varying strengths of integration among modules. To demonstrate that the underlying integration structure among modules regulates the areas of extreme morphospace that are accessible I compare diversification in the reef fish morphological complex to my theoretical simulations. Finally, I explore functional implications of diversity in reef fish morphology and

module integration structure through the lens of diet asking 1) does morphological diversity in the jaws, body, and fins map equally to diversity in diet, and 2) are evolutionary pathways to morphological novelty affected by diet?

Methods:

Data Collection and Processing

Morphological module assembly.—To characterize morphological diversity in functional modules of the reef fish feeding system, I utilized a collection of 294 specimens from 93 species and 37 families (Tab. S1; Burns et al., In Review). This collection represents an ecologically diverse set of species and covers about half of all reef fish families, including all of the major groups. I took a series of measurements on the fresh specimens before formalin fixation. I then cleared and stained (Dingerkus & Uhler, 1977) the collection, and took lateral photos of the body, pectoral fin, caudal fin, dorsal fin, anal fin, and jaws (Burns et al., In Review; Satterfield et al., In Review).

On the lateral body images, I marked the location of 15 homologous geometric morphometric fixed landmarks (Tab. S2) that capture the diversity in the shape of the post-cranial region of the body and the orbit. Landmarks were digitized in the statistical software R (version 4.2.0; R Core Team, 2022) using the package *StereoMorph* (version 1.6.7; Olsen & Westneat, 2015). Geometric morphometric sliding semi-landmark shape outlines were previously digitized for the pectoral, caudal, dorsal, and anal fin images (Satterfield et al., In Review). To correct for size and rotation, I scaled and aligned landmark coordinates for the body and the fins using a Generalized Procrustes Analysis (GPA) in the R package *geomorph* (version

4.0.5; Baken et al., 2021; Adams et al., 2023). I calculated the average shape of the body and fins for each species.

Additionally, 12 linear traits that capture diversity in the oral raw of reef fishes, a combination of nine traits measured digitally from the lateral images of the jaws and three traits measured on fresh specimens (Tab. S3), were previously collected for a larger set of 110 species (Burns et al., In Review). The original jaw data set includes head depth, which I have excluded to maximize independence between the body and jaw modules. I trimmed the species averages of this jaw data set to the species for which body and fin shape data were available.

Phylogeny.—I pruned a large time-calibrated phylogeny of ray-finned fishes (Rabosky et al., 2018), using the associated R package *fishtree* (version 0.3.4; Chang et al., 2019), to a tree containing the 93 species in my morphological data set. I used the nearest available relative as a substitute for species in the morphological data not present in the larger phylogeny (see Table S1). I use this trimmed reef fish phylogeny in all phylogenetic analyses (Fig. S1).

Data Analysis

Within module diversity by diet.—To characterize functional diversity related to the reef fish feeding system species in my collection, I used the diet categorization from Burns et al. (In Review), modified from Siqueira et al. (2020): Herbivore-Detritivores, Planktivores, Sessile Invertivores, Biting Mobile Invertivores, Suction Feeding Mobile Invertivores, Omnivores, and Generalized Carnivores. Diet classifications for my species can be found in Table S1. To determine whether diet affects the mean morphology of any of the six empirical morphological modules, I use phylogenetic ANOVAs (*ProcD.pgls* in *geomorph*) and posthoc pairwise comparisons (*RRPP package;* version 1.3.1; Collyer & Adams, 2018;2024). The response

variable in these ANOVAs is the raw Procrustes aligned shapes in the case of the body and fins, and the 12 linear traits in the case of the jaws. Using these full data sets allows us to retain all the variation in morphology and to detect any effect of diet on morphology. However, to visualize how diet maps onto each morphological module's primary axes of diversity, I implemented principal component analyses (PCA) and constructed morphospaces of the first and second axes of diversity (PC1 and PC2) for each module, where species are color-coded by diet. These PCAs reduce the dimensionality in the data sets allowing for easier viewing of the main axes of variation among species.

Estimating morphological novelty in a multi-module system.—One of the primary aims of this study is to illuminate the relative importance of following lines of least resistance versus off-axis diversification in allowing reef fish to reach novel morphospace. In a simple two-trait integrated system, we can measure the distance of the two traits from the morphological average as a metric of morphological novelty (Fig. 1a). However, many functional systems are complex with many modules, each containing many traits that influence performance. Producing a similar metric of morphological novelty for complex systems requires approaches that capture morphological diversity within and across modules.

Our approach to estimating morphological novelty accommodating many modules begins with creating a morphospace encompassing axes of variation in all the modules. For our collection of reef fish, the body was measured as 15 geometric morphometric landmarks and the fins as sliding semi-landmark curves with 90-150 sampled coordinates, with more coordinates sampled for more complex fins (see chapter 2). In these geometric morphometric modules, the data takes the form of a 3-dimensional array where each species has a matrix of 15-150 rows (depending on the number of landmarks) of X-Y coordinates. Meanwhile the jaw data is a matrix

where each species is a row, and the columns are the 12 linear jaw variables. If the coordinate arrays were transformed so that each species was a row, there would be a column for each x and y position of each landmark in each geometric morphometric module. These X and Y columns plus the 12 linear jaw traits would total over 900 columns. With only 93 species we do not have the power to perform a PCA with that many loading variables. Thus, we need an alternative approach to combining morphological data across modules into an overall morphospace when modules have been measured incommensurately. One option is to first reduce dimensionality within each module. Thus, I first created individual module morphospaces (a PCA of the traits for a single module which can be done on geometric morphometric coordinates or linear traits independently; Figs. 2a, 3).

Then, I calculated the number of PCs required to account for 95% of the variation within each module, which turned out to be 4 PCs unanimously. As there is a range of variances across modules, and we do not want one module to contribute more heavily to the overall morphospace than another, I scaled the 24 PC scores (four from each of the six modules) using a z-score transformation. However, as the first PCs are the primary axes of diversity and account for a larger proportion of variance in the individual morphospaces than PC2 (and PC2 more than PC3 and so on), we want earlier PCs to contribute more heavily to the overall morphospace. I weighted each of the 6 PC1 components by using the average proportion of variation that the PC1s account for in the individual modules as a multiplier. Similarly, I calculated an average of the proportion of variance captured by the PC2s and so on, and used those averages as multipliers for the respective components. After weighting all 24 PC components I supplied them as data to an overall PCA (hereafter "overall morphospace"; Figs. 2b, 4).

Once I created the overall morphospace, I estimated the number of PC axes needed to account for 95% of the variation in the overall morphospace (k). I then used the corresponding number of PC axes to calculate the 'k'-dimensional Euclidean distance of each species from the center of the morphospace (Fig. 2c). I use this distance as a measure of morphological novelty, as a species' distance from the center of the overall morphospace is equivalent to its difference from the morphological average. Note that a species that is unique in one module but not others will, on average, have a shorter distance from the center of morphospace than species that are unique in many modules. I test for differences in morphological novelty in the reef fish feeding system among diet groups using a phylogenetic ANOVA.

Estimating evolutionary tendency in a multi-module system.—Evolutionary tendency can be described as the amount of mismatched evolution of traits or the amount of residual variation around an axis of integration (Fig. 1a). Similarly to morphological novelty, evolutionary tendency is relatively simple to measure in a two-trait system, as you can easily estimate the integration between the traits and calculate the phylogenetically corrected residual of each species from that integrated axis (Fig. 1a). However, complex functional systems again require a more complicated set of procedures to attain a species' general evolutionary tendency in a network of integrated axes. My approach was first to calculate pairwise phylogenetic integration (evolutionary correlation) between each of the six modules using the *phylo.integration* function in *geomorph* (Fig. 2d). Then I calculated residuals from each of the 15 pairwise combinations (Fig. 2e). Those 15 residuals variables were supplied to a PCA (hereafter "residuals PCA"; Fig. 2f) for which I estimated the number of PCs needed to account for 95% of the variation in the residuals (j). Finally, to assess the overall evolutionary tendency of a species, I calculated the 'j'-dimensional Euclidean distance from the centroid of the residuals PCA for each species (Fig.

2g). Species that have high distances from the centroid have high residuals (significant evolutionary mismatches) around at least one axis of integration. However, species with high residuals around more integrated axes will be, on average, further from the centroid. I test for differences in evolutionary tendency among diet groups in the reef fish feeding system using a phylogenetic ANOVA.

Visualizing evolutionary pathways to morphological novelty in multi-module systems.—To demonstrate the effects of evolutionary correlation among modules in a complex functional system on the morphological diversification of species, I plot the species' distance from the centroid of the residuals PCA against the distance from the centroid of the morphospace. Plotting these two variables against one another provides a two-dimensional space that, when divided into equal quadrants, highlights species that are morphologically common from those that are morphologically extreme and separates species that evolve extreme morphologies via integrated axes versus those that diversify through evolutionary mismatch (Fig. 2h). In this case I opted to divide the axes by the half-range as this evenly splits axes by the full range of possible morphological outcomes and evolutionary outcomes. Doing so ensures four equally sized quadrants that allow us to infer which species have morphological and evolutionary distances from the centroid that are greater than the halfway mark of all possible values. I test for diet's effects on species distribution in this two-dimensional evolutionary tendency versus morphological novelty space using a phylogenetic MANOVA.

Simulated correlated modules.—To describe the effect of correlation strength among modules in a complex functional system on morphological diversification, I simulated Brownian trait evolution under four levels of correlation in a six-module system (to reflect my six morphological modules in reef fish). The first three levels represent 1) no integration (r=0), 2)

weak integration (r=0.5), and 3) strong integration (r=0.9) among modules. The levels used for simulations were chosen to cover the range seen in reef fish (0.331-0.852) but also to extend to what is biologically and mathematically possible (0-1). I used the respective *r*-level for every pairwise combination in the six-module correlation matrix for these first three simulations. I additionally calculated an observed correlation matrix for my six morphological modules in reef fish using two-block partial least squares analyses to estimate pairwise *r* statistics between modules (Tab. 1a). I then ran a fourth simulation of trait evolution under this observed correlation matrix from the reef fish data set. Using my trimmed reef fish phylogeny, I did simulations with the *sim.corrs* function in the R package *phytools* (version 1.9.16; Revell, 2012). I repeated each of the four simulations 100 times.

After each simulation I combined data from the six-modules into an overall morphospace similar to the overall morphospace generated for the empirical reef fish data set in step b of Figure 2. One difference is that here each of the six modules is simulated identically and each module is a single simulated value for each species, as such the data is commensurate and less complex. Thus, an overall morphospace is more easily constructed by supplying the values of all the simulated modules directly to a principal components analysis (PCA), reducing the dimensionality through shared axes of variation among traits without the need to first create PCA morphospaces for each module individually.

For each simulation, I calculated the 'k'-dimension Euclidean distance from the center of the overall morphospace as the estimate of morphological novelty. To compare the effects of module integration strength on the accumulation of morphological novelty, I produced density distributions of the distances from the centroid of the overall morphospace using the 100 iterations of each simulated module system. I estimated the density distributions' mean, variance,

skew, and maximum. I tested for statistical differences between means using an ANOVA and between variances using a Levene's test. Further, I tested for differences in the shapes of the distributions or the skew using an Anderson-Darling test (Table S4).

I generated residuals PCAs for each iteration of the simulations following the same procedure used on the empirical reef fish data set and shown in Figure 2d-f. I also calculated the 'j'-dimensional Euclidean distance of each species from the center of each of the simulated residuals PCAs as the estimate of evolutionary tendency. I plotted the distance from the centroid of the residuals PCA versus the distance from the centroid of the overall morphospace for each simulation with all 100 iterations at each *r*-level. I divided the four quadrants by the half-ranges of the x and y axes and then calculated the percentage of occurrences in the four quadrants within each *r*-level. I compare these simulated results to those observed in coral reef fishes to determine how closely reef fish diversification in nature approximates simulated expectations, and to what degree the strength of integration among reef fish modules regulates access to extreme morphologies.

Results:

Evolutionary Pathways to Diversification in the Reef Fish Feeding System

Morphospace Descriptions—I created morphospaces for each of the six morphological modules of the reef fish feeding system (Jaws, Body, Pectoral Fin, Caudal Fin, Dorsal Fin, Anal Fin) using PCAs. Note my morphospace for the jaw module (Fig. 3a, S2a, S3) is modified from Burns et al. (Fig. 2, In Review). As I have removed the head depth variable and constructed the morphospace on a subset of species presented in the original, there are slight differences between the two versions. On the lower end of the first principal component axis ($PC1_{jaws}$) are fish with

short, robust jaw elements, a jaw joint positioned anteriorly to the orbit, and small gapes. The upper end of $PC1_{jaws}$ represents elongate jaws, with thinner elements where the joint is positioned posterior to the orbit and wide gapes. $PC2_{jaws}$ separates species in which the jaw elements are in front of and in line with the orbit with small adductor masses to those that are lower and underneath the orbit with large adductor masses. Together, $PC1\&2_{jaws}$ explain 58.2% of the variance in jaw morphology.

The body morphospace is presented for the first time here (Fig. 3b, S2b). Lower $PC1_{body}$ body shapes are deep-bodied and short, while high $PC1_{body}$ shapes are elongate and thin. Low $PC2_{body}$ body shapes have shorter distances between the lower point of the pectoral girdle and the anterior insertion of the anal fin resulting in a body plan that is increasingly narrow towards the caudal fin in a tapered fashion. Meanwhile, species at the upper end of $PC2_{body}$ have large spans between the tip of the pectoral girdle and the insertion of the anal fin, which creates a stockier square body form. Together, $PC1\&2_{body}$ account for 63.9% of body shape variation.

The fin morphospaces presented here (Fig. 3c-f, S2c-f) are a subset of those provided in Satterfield et al. (In Review). Thus, for a more detailed description of these morphospaces, I will direct the reader to their original presentations (see chapter 2). However, here I present the fin morphospaces with species color-coded by diet.

Integration between modules.—All modules have significant axes of covariation (Tab. 1a), with the strongest being between the body and dorsal fin (r=0.782, Fig. 4a) and the body and anal fin (r=0.852. Fig. 4b). These axes generally reflect that elongate bodies are paired with more low-lying elongate dorsal and anal fins. The caudal fin also has a moderately high covariance with the anal fin (r=0.613) and pectoral fin (r=0.556), where rounded caudal fins generally co-occur with shorter and deeper anal fins and rounded pectorals in contrast to forked caudals with

elongate anal fins (Fig. 4c) and pointed pectorals (Fig. S5a). The body and jaws covary as well (r=0.553), where elongate bodies co-occur with long, thin, posterior jaws and deep bodies pair with short, robust, anterior jaws (Fig. cd). The weakest axes of covariation are between the anal fin and the jaws (r=0.331), the dorsal and pectoral (r=0.361), and the dorsal and caudal (r=0.363). All other axes of covariation are mild (r=0.380-0.520). Integration plots not included in Figure 4 can be found in the supplemental Figures S4-S6.

I phylogenetically corrected axes of covariation to reflect correlation over deep-time scales (evolutionary integration) using phylogenetic integration tests (Tab. 1b). Most axes of covariation remain evolutionarily significant and the dorsal and anal integrations with the body are still the strongest (r=0.626 & 0.771 respectively), the exceptions are that the dorsal fin evolves independently of the jaws, pectoral, and caudal, and the caudal evolves independently of the jaws and body. These axes of evolutionary integration (regardless of statistical significance) are the backbone for my calculations of residual variation around the baseline evolutionary trend. In cases where the integration axis is insignificant, it simply means that there are large residuals and that the primary axis describes relatively little variation in morphology through time.

Overall morphospace.—Many of the axes of diversity from individual morphospaces contribute strongly to the first two axes of diversity in the overall morphospace ($PC1_{overall}$ and $PC2_{overall}$). $PC1_{overall}$ generally reflects distinctions between fish with elongate and high aspect ratio fins versus those with deep rounded fins. The first axis of diversity of the dorsal fin is the strongest loading on $PC1_{overall}$ (loading = 0.51; Fig. 5a), such that species at the low end of $PC1_{overall}$ have, on average, more elongate dorsal fins relative to the deep-fin species at the high end of $PC1_{overall}$. The first axes of diversity in the anal fin (0.44) and pectoral fin (0.42) load similarly strongly on $PC1_{overall}$. Where low $PC1_{overall}$ species have anal fins that are elongate and

pectoral fins that are more wing-like, high $PC1_{overall}$ species have anal fins that are deep and rounded and pectoral fins that are round. .

$PC2_{overall}$ is primarily an axis of body and jaw shape diversity. The strongest loadings on $PC2_{overall}$ are the 1st axis of diversity in the jaws (-0.59) and the 1st axis of diversity in the body shape (-0.59). Low $PC2_{overall}$ species are generally more elongate, and rounder bodied with longer and wider jaws relative to their fin shape position on $PC1_{overall}$. High $PC2_{overall}$ species are deeper laterally compressed bodied with very short, narrow, and robust jaws. Together, $PC1\&2_{overall}$ cover 45.5% of the variation in the overall morphological diversity. However, to account for 95% of the variance in the overall morphospace 9 PCs were required in total, given the vast range of morphologies that reef fish possess.

Closely related species generally occupy similar spaces in the overall morphospace (Fig. 5b). For example, the acanthurids, chaetodontids, pomacanthids, and siganids which make up the lower left quarter of the phylogeny (Fig. S1) all occur in the high $PC2_{overall}$, central $PC1_{overall}$ region. The balistids occupy the upper end of $PC1_{overall}$ and $PC2_{overall}$. However, there are regions of morphospace in which distantly related species with similar morphologies converge. For example, *Ecsenius midas*, *Hoplolatilus cuniculus*, and *Parapercis tetracantha*, which are all elongate-bodied and have long ribbon-like dorsal and anal fins, all occur at the lowest reaches of $PC1_{overall}$ and are average on $PC2_{overall}$. There are also cases where closely related species with divergent morphologies have large areas of separation for example, the non-Balistid tetraodontiforms such as *Arothron manilensis*, *Canthigaster solandri*, and *Sphoeroides spengleri* occur much lower on $PC2_{overall}$ than the Balistids do.

Residuals PCA.—The first axis of diversity in the PCA of residuals ($PC1_{residuals}$) primarily accounts for residual variation around axes of integration that the anal fin shares with the other

modules (Fig. 5c). For example, the anal fin integration residuals with the jaws (loading = 0.42), and with the body (0.27) load positively on $PC1_{residuals}$ and the residuals with the caudal fin (-0.37), pectoral fin (-0.36), and dorsal fin (-0.26) load negatively with $PC1_{residuals}$. The integration residuals of the dorsal fin with the pectoral (-0.32) and the jaws (-0.32) also negatively load with $PC1_{residuals}$. These results suggest that species vary greatly in their evolutionary trends and patterns of covariation between the anal fin and other modules. In contrast, the residuals of the integration between the body and pectoral fin load very weakly (-0.06) with $PC1_{residuals}$, indicating that species do not vary greatly in the evolutionary trend between the body and pectoral fin.

$PC2_{residuals}$ distinguishes patterns of residual variation between the caudal fin and other modules (Fig. 5c). The four most substantial loadings on $PC2_{residuals}$ are the residuals between the caudal and the dorsal fin (-0.47), the jaw (-0.43), the pectoral (-0.43), and the body (0.40). Thus, species have an extensive range in how independent their caudal fins are from other modules, where species at the center of $PC2_{residuals}$ have caudal fins that are evolving in an integrated manner with the other modules and species at the extremes of $PC2_{residuals}$ have caudal fins that are evolving independently of at least one other module. $PC1\&2_{residuals}$ combined account for 54.7% of the variance among species in their integration residuals. The most substantial loadings of $PC3\&4_{residuals}$ are residuals from integration combinations of the body, jaws, and pectoral fin; they account for an additional 25% of the variation. In total, 7 PCs are needed to account for 95% of the variance among species.

The residuals PCA separates closely related species with large differences in some aspects of morphology (Fig. 5d). For example, *Chromis multilineata* is low on both $PC1\&2_{residuals}$. Within the pomacentrids, it is the most elongate-bodied and has fins that are more

elongate and high aspect ratio than its relatives. Meanwhile, *Dascyllus trimaculatus* is at the pomacentrids' deep-bodied, rounded fin extreme and occurs at the upper ends of $PC1\&2_{residuals}$. The sizeable morphological distance along shorter phylogenetic branches results in high residuals and represents strong off-axis trait evolution.

Evolutionary pathways to morphological novelty in coral reef fishes.—To determine the evolutionary pathways that lead to the morphological novelty found among reef fish, I plotted the distance from the centroid of the residuals PCA (evolutionary tendency/trait mismatch) against the distance from the centroid of the overall morphospace (morphological novelty; Fig. 6). I divided this plot into four equal quadrants at the half-range of each axis. These divisions are somewhat arbitrary but allow us to isolate species where evolutionary and morphological novelty is more extreme than the halfway point of all possible outcomes. Another potential method is to divide quadrants by the means of both axes. However, the distributions of the morphological and evolutionary distances from their respective centroids are heavily positively skewed. As such, dividing axes by their means would obscure that most species are not extreme in morphology or evolutionary tendency.

Most species (71.0%) retain near-average morphologies and evolve along integrated axes (Fig. 6). Some species have a high degree of trait mismatch but traits that are not far from the mean morphology (9.7%). *Chromis multilineata* and *Dascyllus trimaculatus,* in the upper left quadrant, illustrate nicely how species end up with average morphology but high residuals. Recall from above that *C. multilineata* is the elongate-bodied extreme of pomacentrids, and *D. trimaculatus* is the deep-bodied extreme. While their overall morphology is not novel relative to the entire species set, the evolution of their distinct body shapes relative to one another over short timescales manifested as large residuals on axes of integration with body shape.

Out of the 93 species included in this study, only 18 (19.4%) exceed morphological novelty beyond the half range of possible outcomes. Some species reach extreme morphologies by following integrated axes to outer morphospace (10.8% of species). Fewer species reach the extremities of morphospace through evolutionary independence of modules (morphological mismatch; 8.6%). In summary, morphological novelties at the extreme ends of axes of integration arise 1.25 times as often as extremely modular phenotypes do.

Simulations under Varying Strength of Integration among Modules

The effect of module correlation strength on the evolutionary pathways to morphological novelty.—The module correlation structure had the anticipated impact that under stronger correlation greater morphological novelty was reached (Fig. 7a&b; Tab. S4). Specifically, when there was a strong correlation (r=0.9), the maximum morphological novelty (9.23) was 1.26X greater than the maximum morphological novelty under weak integration (r=0.5, max. = 7.28) and 1.64X greater than under no integration (r=0, max. = 5.63). However, mean morphological novelty was greatest under no integration among modules (2.34), followed by weak integration (2.20) and strong integration (1.94; p<0.0001, F=356.6, df=2). There was much higher variance (σ^2=1.82) in morphological novelty under strong integration than weak integration (σ^2=0.84) or no integration (σ^2=0.47; p<0.0001, F=1422.7, df=2). Overall, the skew of morphological novelty becomes more positive with increasing integration (p<0.0001, AD=1486.5, df=2) but with a more significant jump from no integration (skew = 0.37) to weak integration (skew = 0.99) than to strong integration (skew = 1.03). Under strong integration, 4.5% of species surpass the half-range of morphological novelty; this number declines to 1.9% under weak integration and 0.2% under no integration. These results indicate that while even moderate amounts of integration heavily reduce the average tendency for morphological novelty, the number of species that will

diversify into the most novel regions of morphospace increases with integration. In other words, though greater morphological extremes along integrated axes are achievable under strong integration, it is always relatively uncommon for species to reach outer regions of morphospace.

A species' distance from the centroid of the residuals PCA represents its tendency to evolve counter to axes of integration among modules (mismatch). Under strong integration, by definition, large residuals do not occur. The mean centroid distance in my simulations under a correlation of r=0.9 was 1.57. This value almost doubled (3.03) when integration was weaker (r=0.5). Interestingly, though, when there is no integration (r=0), evolutionary tendency is similar (3.51) to when integration is weak, indicating that though very large residuals can occur under no integration, evolutionary mismatch, though greater, does not, on average, get much more extreme than what is allowable under a correlation of r=0.5 (Fig. 7a&c).

Theoretical pathways to morphological novelty in the coral reef fish feeding system.—I additionally simulated evolution of traits under the correlation matrix empirically calculated for the six reef fish feeding system modules (Table 1a). This simulation informs us of the possible pathways to morphological novelty in this system if traits evolve according to Brownian motion. The range of correlations between modules was r=0.332 – 0.852, with an average value of r=0.505. Under this correlation matrix, the mean simulated morphological novelty was 2.25 (σ^2=0.87, max. = 7.81, skew = 0.96), which is very similar to the simulated morphological novelty distribution where all *r=0.5 (*Fig. 7b). This suggests that despite a range of integration strengths among modules in a system, the general morphological tendency will theoretically follow expectations according to the average integration. Further, the distribution of distances from the centroid of the residuals PCA closely matches that of the simulation in which all r=0.5 (Fig. 7c). As such, we can anticipate that in a system with some strong integration and some

weak integration, species which have evolved morphological novelty will likely be doing so primarily via off-axis evolution.

The Effects of Diet on Morphology and Evolutionary Diversification

Does diet map to morphological diversity in reef fishes?—Diet significantly explained differences in mean shape for the jaws (Fig. 3a, p=0.001, F=2.55, df=6), body (Fig. 3b, p=0.017, F=1.76, df=6), caudal fin (Fig. 3d, p=0.001, F=2.89, df=6), and dorsal fin (Fig. 3e, p=0.013, F=1.77, df=6). Note that we used the raw shape data as opposed to the PC scores in these analyses to avoid missing the effects of diet on less prominent axes of diversity than those displayed in the morphospaces. I will highlight some significant pairwise comparisons between diet groups. The full spectrum of pairwise comparisons for all morphological modules by diet can be found in Table S5. Generalized carnivores and planktivores tend to be characterized by elongate, wide-gape jaws, but planktivores have smaller adductor mandibulae than carnivores (*p=0.024*). Meanwhile, herbivore-detritivores have significantly shorter and more anterior jaws than either carnivores (p=0.029) or planktivores (p=0.041). Omnivores also generally have smaller, more robust anteriorly positioned jaws than carnivores (p=0.041). The invertivore groups are all central in the jaw morphospace with significant spread and overlap with other groups.

Planktivores typically have more heavily forked caudal fins on average than most other diet groups (p=0.001-0.026), except suction-feeding mobile invertivores, which have significant spread into the forked caudal region. The caudal fins of the other feeding groups are broadly spread widely over regions of space from slightly forked to rounded caudal fins. Omnivore dorsal fins are shorter and deeper than most other groups (p=0.001-0.015); however, suction-feeding mobile invertivores and sessile invertivores also spread into deep dorsal fin regions.

Most dorsal fin shapes are elongate, low-lying fins, and a few species in each diet group evolve split dorsal fins. Although the mean body shape overall is significantly different by diet, none of the pairwise comparisons revealed different means statistically, suggesting that differences in body shape were not substantial enough to be retained in the pairwise comparisons. Visually, the herbivore detritivores generally occupy the lower end of $PC1_{body}$ and $PC2_{body}$ where body shape is deeper and more tapered towards the caudal. That said there is a large amount of overlap and spread in body shape in most of the diet categories. Diet categories are also highly overlapping and spread over many shapes for both the pectoral fin and the anal fin.

I detect more distinctions between diet categories in the overall morphospace than in any individual module morphospace (Fig. 5a&b; Tab. S5; p=0.001, F=3.12, df=6). Generalized carnivores are more present in the lower half of $PC2_{overall}$ reflecting their longer jaws and bodies. The mean carnivore morphology differs significantly from herbivore-detritivores, omnivores, planktivores, and sessile invertivores (p=0.001-0.040). Planktivores are generally confined to the lower halves of $PC1_{overall}$ and are central on $PC2_{overall}$, with few exceptions. Planktivores have more elongate and high aspect ratio fins than every other diet group (p=0.001-0.008). Suction-feeding mobile invertivores are central in morphospace with very neutral traits, they overlap in morphology with all groups (p=0.062-0.326) except planktivores (p=0.008) and herbivore detritivores (p=0.031). Herbivore-detritivores overlap heavily with sessile invertivores (p*=0.658)*, biting mobile invertivores (p=0.177), and omnivores (p=0.104) but are typically higher on $PC2_{overall}$ than most other groups (p=0.002-0.031) and have short jaws with laterally compressed bodies, but neutral fins. Omnivores and sessile invertivores are typically high on $PC1_{overall}$ and are also generally higher on $PC2_{overall.}$ They have more rounded and short fins with laterally compressed bodies and short jaws. Some omnivores do have a more elongate body and

jaw. Biting mobile invertivores differ in morphology only from planktivores (p=0.003) and omnivores (p=0.010) and are extremely widespread on both axes.

Are evolutionary pathways to morphological novelty affected by diet?—Diet groups vary in position in the space of evolutionary tendency (aka the residuals PCA; Fig. 5c&d; Tab. S5; p=0.003, F=2.522, df=6). Most notably, planktivores, on average, occupy a lower region of $PC2_{residuals}$ than all other diet groups. They have caudal fins that are more forked than expected, given their other module anatomy (p=0.001-0.024). Omnivores also differ in mean residual tendency from generalized carnivores, herbivore-detritivores, biting mobile invertivores, and planktivores (p=0.001-0.049). Specifically, omnivores generally occupy higher $PC1_{residuals}$ than those other diet groups and have anal fins that are, on average, more rounded than would be expected given the anatomy of the other modules. Omnivores are also slightly elevated on $PC2_{residuals,}$ and their average tendency is that the caudal fin is more rounded than would be predicted by the anatomy of the other modules. Otherwise, diet groups are widespread in the residuals PCA with a large amount of overlap.

I also find that diet groups vary in their average position in the space of evolutionary tendency versus morphological novelty (Fig. 6, p=0.002, F=4.188, df=6). Of the 17 species that fall above the half-range of the centroid distance from the residuals PCA (evolutionary tendency), 7 are planktivores, which is 58% of all the planktivores in the study. The remainder are generalized carnivores (5), omnivores (3), a biting mobile invertivore, and a sessile invertivore. The converse is that 93% of the invertivores (MIB, MIS, and SI) evolve along integration axes and do not have significant off-axis trait mismatch. Of the 18 species that are above the half-range of morphological novelty, 5 are biting mobile invertivores, 4 are generalized carnivores, 3 are omnivores, 3 are planktivores, 2 are sessile invertivores, and 1 is a

suction feeding mobile invertivore. Note that 100% of the herbivore-detritivores fall within the quadrant denoting species with average morphology evolving along integrated axes.

Discussion:

Strong trait integration and the ability of modules to evolve independently have both been described as crucial factors enabling integrated morphological systems to diversify into novel regions of morphospace. However, the relative frequency at which these mechanisms lead to morphological extremes in nature is not well known. In this study, I have described a pipeline for distinguishing novel morphologies that arise by following axes of least resistance from those that come about through off-axis evolution of novel trait combinations. I characterize morphological novelty, or a species' distance from the average morphology, in a manner that encompasses traits within many morphological modules that may or may not have been measured similarly. Additionally, I outlined how residual variation around axes of evolutionary integration among morphological modules can be used to describe whether traits are co-evolving along pathways of evolutionary least resistance or are moving through morphospace via independent responses to selection. My measures of reef fish morphological novelty and evolutionary tendency, supported by simulated trait evolution under increasingly strong integration, reveal that moderate integration among modules is key to allowing species to access extreme morphologies following integrated axes *and* through modular evolution resulting in novel trait combinations. However, just under a fifth of my species ever reached my definition of an extremely novel phenotype and did so through axes of integration slightly more often as extremely unique trait combinations were evolved. Below, I further discuss diversity within individual morphological modules and the evolution of the reef fish morphological complex into novel extreme phenotypes.

The Effects of Integration Strength on Access to Morphological Novelty

Do the jaws, body, and fins of reef fishes form an evolutionarily integrated complex?— There are many axes of covariation between the jaws, body, and fins in reef fishes, and I find evidence of evolutionary integration among these modules (Tab. 1). Among some module pairs, the integration is relatively weak ($r<0.5$). Among other modules, integration is strong ($0.5<r<1$), and on average, integration among modules is moderate (near $r=0.5$). The average integration among modules was 0.505, which agrees with the estimated average trait covariation in vertebrates of 0.5 (Conner et al., 2014).

The integration between fins has been previously noted in Satterfield et al. (In Review), and its presence is not surprising given the known genetic and developmental pathways that fins have in common and their mutual involvement in locomotion. However, what is more profound is that the jaws are moderately integrated with each fin. Shared genetic linkages between the jaws and fins aren't impossible but have not been well studied to date, and given the amount of isolation between the jaws and fins, it's less likely that common developmental pathways lead to this integration. The most plausible explanation is that there is a correlated function among the jaws and fins, and their evolution trajectories may both be driven by feeding optimization.

Do reef fishes evolve morphological novelty along evolutionary pathways of least resistance or through the independent evolution of traits?— Traits can evolve to extreme morphological phenotypes in two ways. The way that has been more commonly emphasized by functional morphologists is independent trait evolution in response to direct directional selection (e.g., Malhotra & Thorpe, 1991; Wainwright, 1996; Clegg et al., 2002; Shuai et al., 2018; Hadj-Hammou et al., 2021). A complex of multiple traits can evolve unlimited combinations of trait values through this mechanism. However, when there is evolutionary integration, the covariation among traits through deep timescales, selection on any one trait in the complex can induce

morphological evolution on covarying traits (Du et al., 2019; Evans et al., 2021; Eliason et al., 2023). Yet, morphological evolution through integration will follow the axis of covariation, and as such, there is a limit on the trait combinations that will arise through evolutionary integration (Fig. 1a; Goswami et al., 2014; Felice et al., 2018; Burns et al., 2023). Moreover, traits evolving along an integrated axis with a fixed rate can reach further into distant morphospace, generating greater morphological novelty, than independently evolving traits evolving at the same rate (Goswami et al., 2014). In this study, I aimed to determine the relative importance of trait integration or modular evolution of traits to extreme novel phenotypes in nature.

In the coral reef fish morphological complex, most species do not evolve morphologies far from the center of morphospace; 80.6% of species in my study have relatively average morphologies. For the 19.4% of species that do evolve extreme morphologies, it is 1.25 times more common that extreme morphospace is accessed along axes of integration than via modular evolution of traits into extreme novel trait combinations (Fig. 6). This pattern of diversification in the empirical reef fish morphological complex closely reflects simulated module evolution under a moderate correlation structure of r=0.5 (Tab. S4; Fig. 7). In fact, my simulations reveal that the only case in which novel phenotypes are accessible via both evolutionary pathways simultaneously is when integration is present but moderate. When integration is overwhelmingly strong, species cannot diversify into off-axis regions of morphospace, and when integration is too weak, traits do not have access to covariation as a pathway of least resistance into outer morphospace (Fig. 7a). Therefore, the moderate integration that is present in coral reef fishes in nature is the key facilitator of diverse evolutionary pathways to morphological novelty.

Species that have evolved unique morphologies along integrated axes (10.8%) fall in the lower-right quadrant of Figure 6. Some of the species in this region have reached unique

morphologies along the integrated axis between the jaw and body module (Fig. 4d). For example, *Balistoides conspicillum* has a very large adductor mass that supports strong biting and a deep laterally compressed body, and *Synodus saurus* is at the other extreme of jaw and body morphology with a large gape, high protrusion, and a dorsoventrally compressedelongate. Though these species are quite different in jaw and body morphology, they are similarly morphologically extreme and have low evolutionary residuals.

Species that have evolved unique morphologies through independent evolution of the modules (8.6%) fall in the upper-right quadrant of Figure 6. Only eight species of the 93 in my data set have evolved extreme morphologies this way. Three of those are elongate-bodied species: *Ecsenius midas, Hoplolatilus fronticinctus,* and *Valenciennea strigata.* I can identify which modules are evolutionarily mismatched relative to the rest using Figure 5c. *E. midas* has a caudal fin that is far more forked and narrower, and *V. strigata* has a caudal fin that is far more rounded than would be expected relative to the other modules. *V. strigata* also has a split dorsal fin, which occurs more typically on deep-bodied species. *H. fronticinctus* has an anal fin that is not very elongate relative to the dorsal, jaw, and body shape. *H. fronticinctus,* is slightly deeper bodied than some of the other elongate species and it's dorsal fin is actually a bit more elongate than expected for its jaw and body shape.

Each other species in this region is also morphologically extreme due to odd fin and body combinations. *Pterois russelii* spends much of its time resting on the substrate and has pectoral fins that are primarily decorative and rounded, and though I corrected for size in my shapes, it is notable that the pectoral fins in this species are huge relative to the body. Meanwhile, the *P. russelii* caudal fin is narrower and squarer than expected for a species with its body depth. *Caranx ruber* is a fish that spends most of its time cruising the reef and has fins that are different

from most other fish in the data set as they appear adapted for maximal drag reduction; its pectorals are very high aspect ratio and thin, its dorsal and anal have a short section of the leading edge that is triangular and deep, and the trailing edge is elongate and low-lying, and its caudal is very forked and very thin. *Acanthostracion quadricornis* has a very atypical box-shaped body, *Canthigaster solandri* is a small pufferfish with a spineless short rounded dorsal and anal fin, and both species have short, robust jaws relative to how wide-bodied they are. Finally, *Pempheris schomburgkii* is a short, deep-bodied species with a very long anal fin, a very short dorsal fin, and jaws that are much larger than would be expected for its body shape.

As other vertebrate groups also have, on average, moderate trait covariation (Conner et al., 2014) and should also have the flexibility to evolve morphologically novel phenotypes via both evolutionary pathways, it would be interesting to explore whether axes of integration are unanimously the more common pathway to extreme phenotypes.

The Effects of Diet on Morphological Diversification in Reef Fishes

Does morphological diversity in the jaws, body, and fins map equally to diet of reef fishes?—The jaws, caudal, and dorsal fin were the modules where I detected significant variation in mean morphologies between diet groups. The body was weakly predictive of diet overall, though not with enough strength to retain distinctions in pairwise groups. The pectoral and anal fin showed no significant effect of diet (Tab. S5, Fig. 3). Interestingly, the significant effect of diet on jaw morphology relates to distinctions between generalized carnivores, herbivore-detritivores, planktivores, and omnivores. These distinctions primarily reflect the slight tendency towards larger gape, more protrusion, and longer jaws that carnivores and planktivores have versus the tendency towards smaller, high adductor mass jaws that herbivore detritivores have. Meanwhile, the jaw morphology of each invertivore group (MIB, MIS, SI) is not distinguishable

from any other diet category. This result likely reflects the vast diversity among invertebrates and the fact that separating these categories by where the invertebrates are found and how they are captured is not a fine enough comb to describe the functional role of diversity in invertebrate jaws.

The only detectable distinctions between the diet groups in the caudal fin were between planktivores and all other diet groups except for suction-feeding mobile invertivores. Planktivores generally have more forked caudal fins than other diet groups. Meanwhile, omnivores make up most of the detectible distinctions in the dorsal fin shape, where omnivorous species occupy some of the more unique dorsal fin regions where the dorsal has a significant reduction between the spines and rays or a full split. Alternatively, some omnivores exist in the areas where the spines are absent altogether, and the ray dorsal is very short and rounded. Other diet groups aren't excluded from these more unique dorsal regions, but notably, omnivores very rarely have the standard elongate continuous and uniform dorsal.

Our findings suggest that specific morphology is essential to successful planktivory and omnivory, though surprisingly, most diets can be achieved with a wide array of jaw, body, and fin shapes. In particular, the pectoral fin and anal fin are not significantly linked to diet distinctions individually or in the overall morphospace, which is unexpected given their essential roles in locomotion and maneuverability.

Are evolutionary pathways to morphological novelty in reef fishes affected by diet?— Though the body and fins are not overwhelmingly predictive of diet diversity in reef fish, patterns of covariation between the body and fins and jaws are underlying the unequal access to morphological novelty and the diverse pathways to diversification in different diet groups. Specifically, diversity among herbivore-detritivores is accumulated exclusively along axes of

integration and never expands into the extremities of morphospace. In the three invertivore groups (MIB, MIS, SI), some species evolve extreme morphologies but only along integrated axes. The one exception is *A. quadricornis*, a sessile invertivore and the only invertivore with extreme morphology through independent evolution of modules. These findings indicate strong functional costs to off-axis evolution and mismatched morphologies for these diet groups.

Meanwhile, planktivory is more common in species with independent evolution among modules than in species that evolve strictly along integrated axes. Most of the planktivorous species in this set are not closely related, and it is plausible that transitions to planktivory from other diets occur most commonly when species can adapt the jaws and fins to the midwater environment and planktivorous feeding mode independently of body shape and one another. Carnivores and omnivores have a proportional presence in each of the four quadrants of Figure 6. As such, it seems that fish in these diet groups occupy many evolutionary pathways and a range of morphologies, from a typical shape to extreme conditions. Further work is needed to clarify whether diet transitions or functional expansions are possible after a weakening in morphological integration or if transitions to certain diets occur and lessen the functional costs of independent evolution among modules, encouraging a reduced evolutionary covariation among traits. My findings here suggest that the strength of integration between the body, jaws, and fins does not apply equally to all diet groups, but I am limited in the ability to empirically test for differences in integration strength between groups due to within-group sample sizes. However, future efforts should focus on building more speciose multi-module morphological data sets and developing a finer scale gradient of trophic niche to assess shifts in the evolutionary pathways to morphological novelty with functional expansion in the reef fish feeding system.

Conclusion.—The strength of evolutionary covariation among morphological modules in complex functional systems determines the available evolutionary pathways to the most extreme regions of morphospace. When integration is very strong, species may diversify further into morphospace but only into areas that align with axes of covariation between traits. Species typically won't diversify into extreme morphospace in systems without integration or complete evolutionary independence. However, when integration is present but weak species can explore disparate regions that align with the covariation axes *and* where morphologies have evolved independently. Exploring the complex reef fish body as a unit reveals patterns of diverse evolutionary pathways between diet groups that are not initially obvious in individual module variation. The coral reef fish system exemplifies morphological diversification in a system with weak to moderate integration. Axes of integration are an equally common pathway to morphological extremes as modular evolution and are important sources of novel phenotypes that should not be ignored when considering morphological diversification.

Figures and Tables:

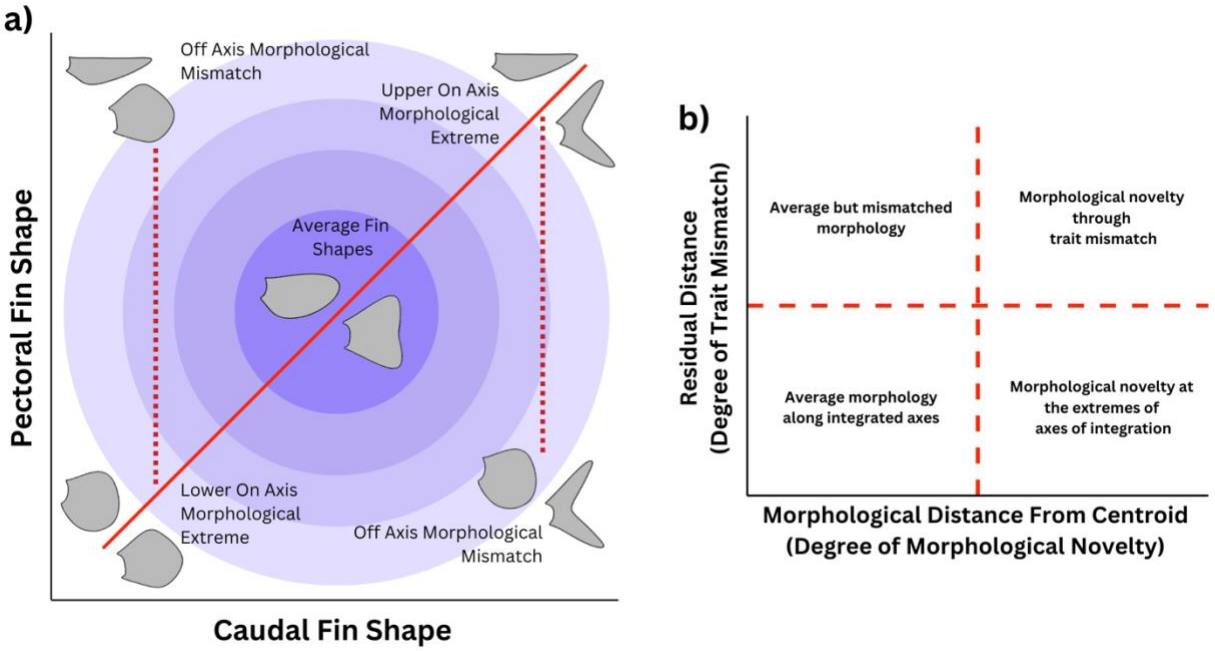

Figure 1. **Evolutionary pathways to morphological novelty.** a) an example of a hypothetical integrated axis between two morphological modules, the pectoral fin vs the caudal fin. The solid red line represents the axis of evolutionary integration between these fins. The dashed red lines represent residuals from the main axis of integration. The purple circles represent increasing distance from the average fin shapes, such that the dark purple is very close to mean fin shape and light purple is very different from mean fin shape. Species can reach morphological extremes in two ways: 1) by evolving along the axis of integration or 2) evolving off axis resulting in evolutionary mismatched fins. b) a plot showing that the pathway to morphological novelty can be illustrated by comparing species residuals from the axis of integration versus the morphological distance from the centroid of fin shape space.

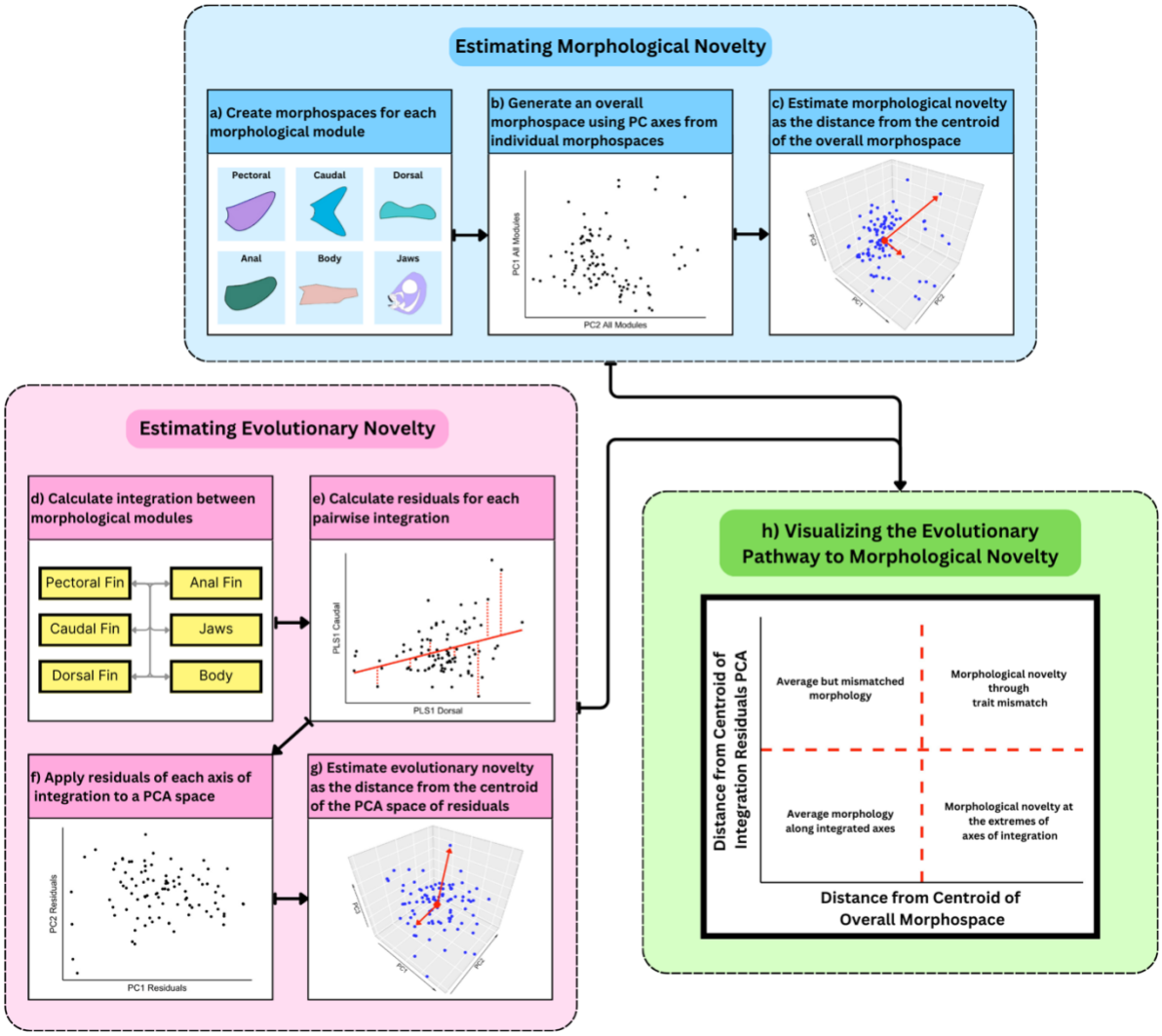

Figure 2. **The pipeline to visualizing evolutionary pathways to morphological novelty with many modules**. This pipeline allows us to generate a plot like the one shown in Figure 1b but with the incorporation of many morphological modules, including the combination of linearly measured traits and geometric morphometric shapes. **a)** The first step is to create a morphospace of each module using principal components analyses. **b)** An overall morphospace can be created by supplying the primary axes of diversity in the individual module morphospaces as loadings to a new PCA. **c)** Morphological novelty can be estimated as the multi-dimensional distance from the centroid of the overall morphospace, using enough dimensions to cover 95% of the variance in morphospace. **d)** To begin estimating evolutionary novelty, calculate phylogenetic integration between morphological modules. **e)** Then, calculate the residuals for each species from each pairwise axis of integration. **f)** a space of diversity in tendency to evolve off-axis from integration can be generated by supplying the residuals from the previous step as loadings to a PCA (herein "residuals PCA"). **g)** The general evolutionary tendency of a species to evolve in-line with axes of integration or through independent off axis evolution can be obtained by calculating the multidimensional distance from the centroid of the residuals PCA space. **h)**

Finally, creating a plot of the distance from the centroid of the residuals PCA vs the distance from the centroid of the overall morphospace gives a two dimensional space in which a species evolutionary trend and morphological novelty can be compared.

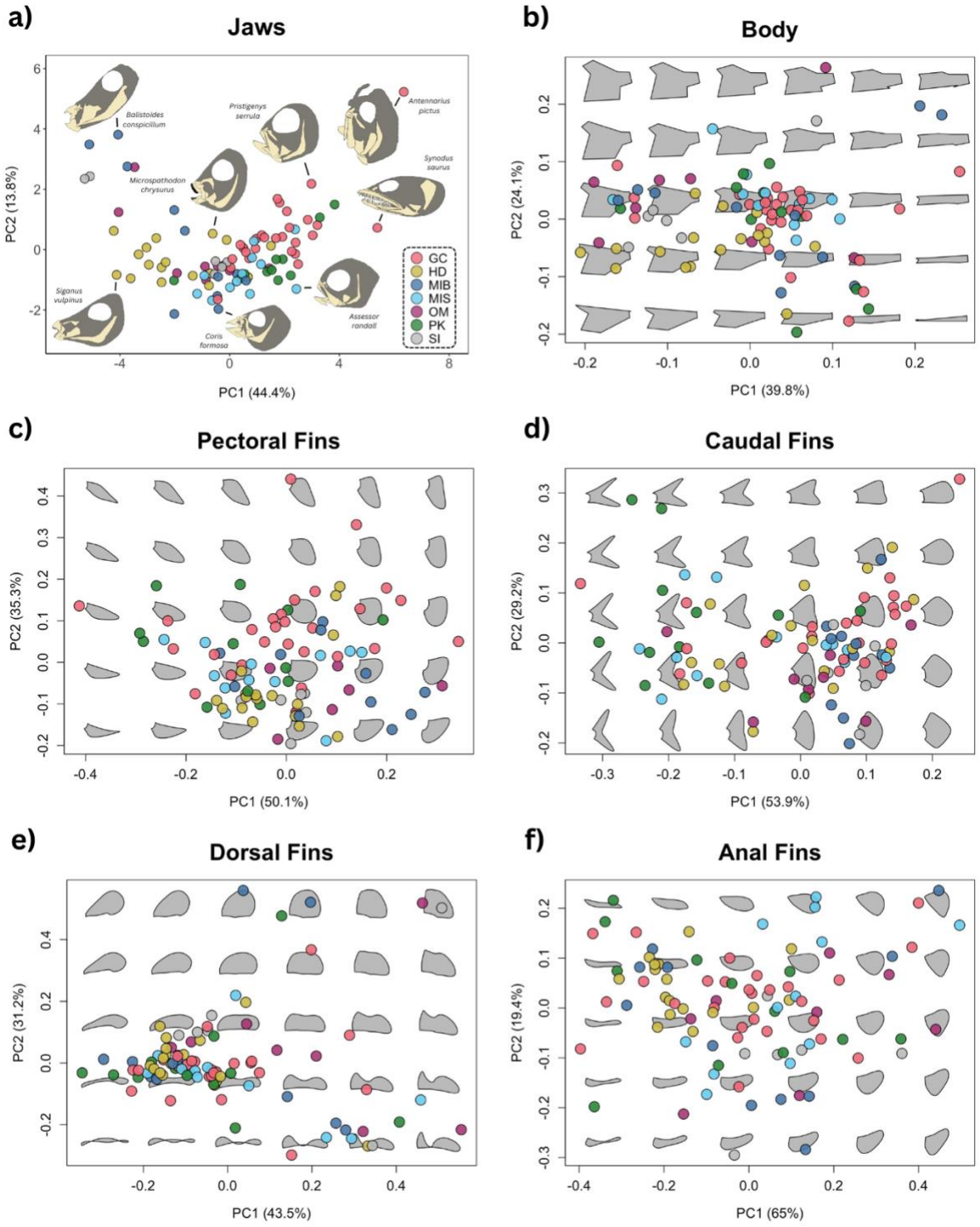

Figure 3. **Reef fish morphospaces for six morphological modules of the functional feeding system.** Each morphospace is constructed from a principal components analysis where, in the case of **a)** jaws, the loadings are the 12 linear dimensions. For **b)** the body **c)** the pectoral fin, **d)** the caudal fin, **e)** the dorsal fin and **f)** the anal fin the loadings are Procrustes superimposed

geometric morphometric landmark coordinates. Each point represents the average morphology for a species (N=93). Species are color coded by diet following Burns et al (In Review). GC = Generalized Carnivore, HD = Herbivore Detritivore, MIB = Mobile Invertivore Biter, MIS = Mobile Invertivore Suction, OM = Omnivore, PK = Planktivore, SI = Sessile Invertivore.

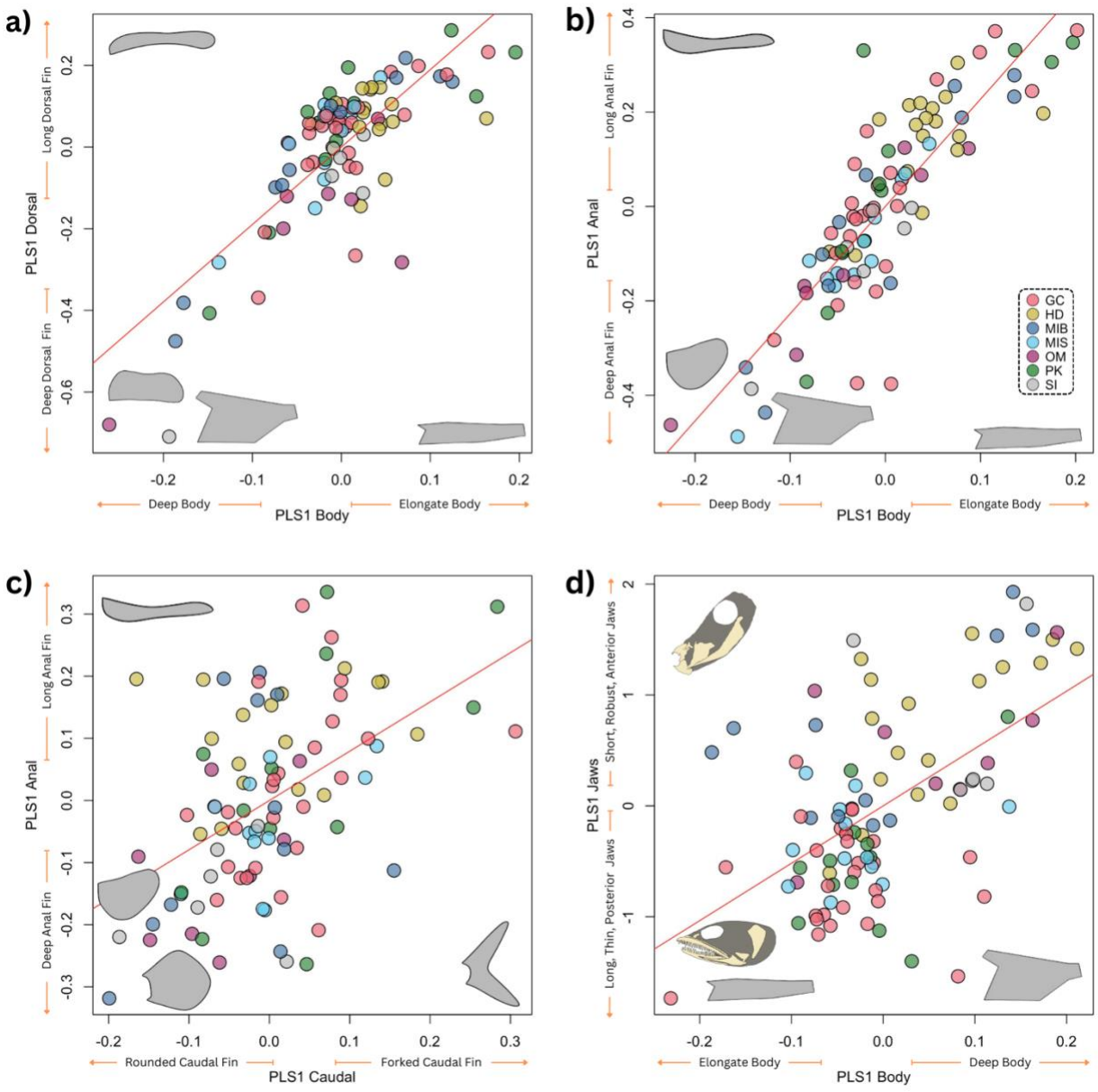

Figure 4. **Modular Integration Examples. a)** The first partial least squares (PLS1) axis of the body and dorsal modules from a two block PLS analysis, **b)** PLS1 of the body and the anal fin, **c)** PLS1 of the caudal fin and the anal fin, **d)** PLS1 of the body and the jaws. The red lines show the axis of integration between the two modules. Each point represents the PLS scores for a species, which are color coded by diet. GC = Generalized Carnivore, HD = Herbivore Detritivore, MIB = Mobile Invertivore Biter, MIS = Mobile Invertivore Suction, OM = Omnivore, PK = Planktivore, SI = Sessile Invertivore.

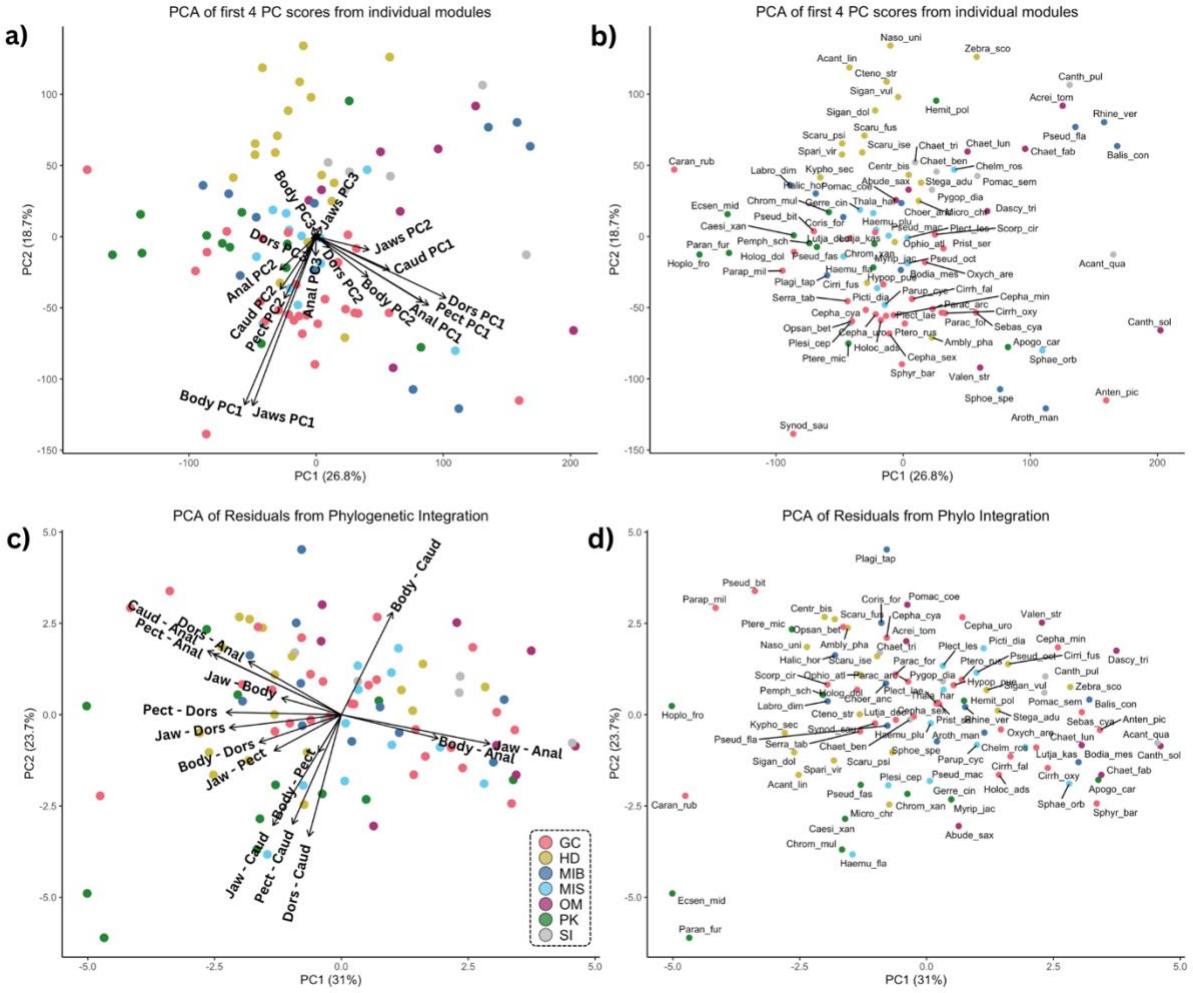

***Figure 5*. Integration residuals PCA and overall morphospace. a)** The 1st and 2nd PC of an overall morphospace where loadings are the weighted first four PCs of the individual morphological morphospaces (overall morphospace). Loading arrows are labeled by the first four letters of the morphological module and the PC axis number. **b)** The overall morphospace with species abbreviations. **c)** The 1st & 2nd principal component (PC) of phylogenetic integration residuals (residuals PCA) with loadings arrows. Loadings are labeled by the two morphological modules in the integration for which residuals were calculated. **d)** The residuals PCA with species abbreviations. Species are abbreviated by the first five letters of the genus and the first three letters of the species separated by an underscore. Species are color coded by diet following Burns et al (In Review). GC = Generalized Carnivore, HD = Herbivore Detritivore, MIB = Mobile Invertivore Biter, MIS = Mobile Invertivore Suction, OM = Omnivore, PK = Planktivore, SI = Sessile Invertivore.

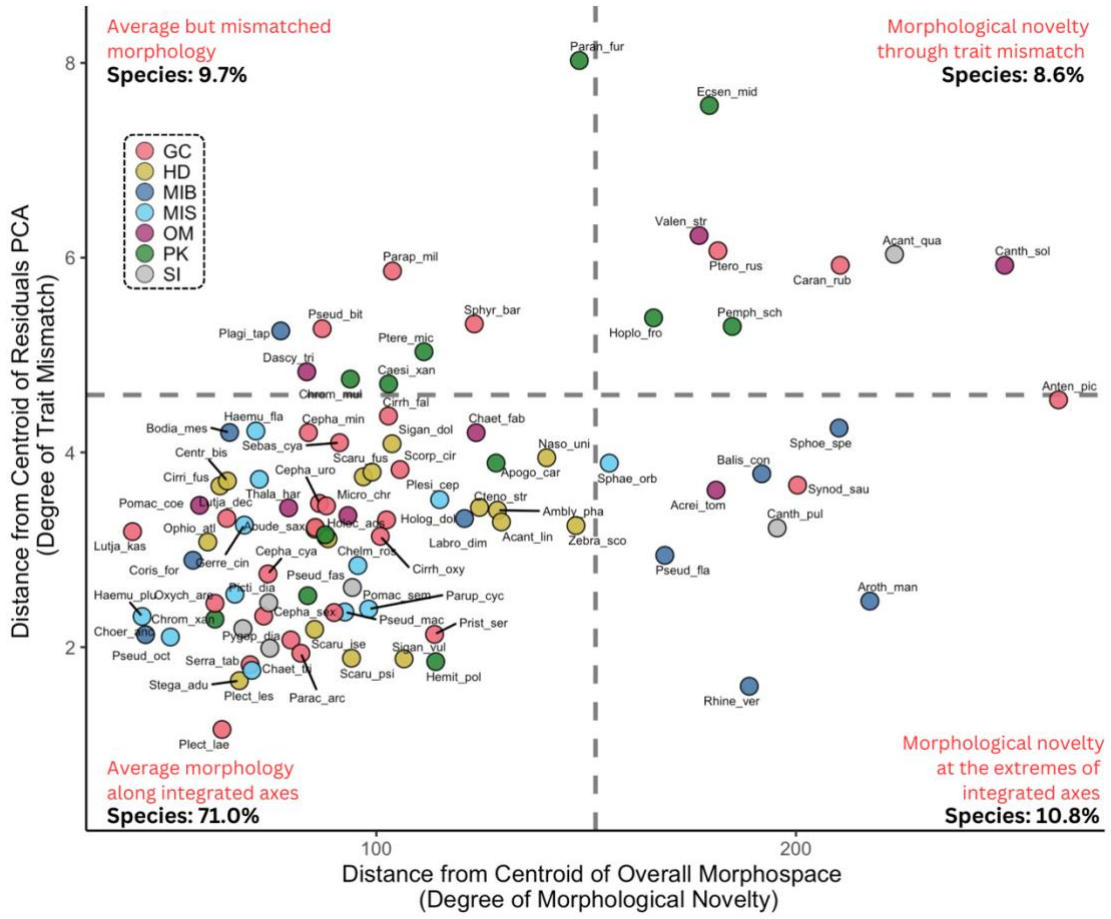

Figure 6. **Evolutionary novelty versus morphological Novelty.** This figure shows the distance from the centroid of the residuals PCA (*Fig. 6 c,d*) versus the distance from the centroid of the overall morphospace (*Fig. 6 a,b*). This framework mirrors Figure 1b but is extended to cover more than two morphological modules. The red lines denote the half-range between the extreme observations on each axis and divide the plot into four quadrants distinguishing evolutionary pathways and morphological outcomes. Each point represents a species (N=93) and percentage of species that fall within each quadrant is provided. Species which have a high distance from the centroid of the residuals PCA are evolving off axis of at least one axis of integration, leading to traits which are evolutionarily mismatched. Species with high distances from the centroid of the overall morphospace have traits which are very different from the average morphology. Species are abbreviated by the first five letters of the genus and the first three letters of the species separated by an underscore. Species are color coded by diet following Burns et al (In Review). GC = Generalized Carnivore, HD = Herbivore Detritivore, MIB = Mobile Invertivore Biter, MIS = Mobile Invertivore Suction, OM = Omnivore, PK = Planktivore, SI = Sessile Invertivore.

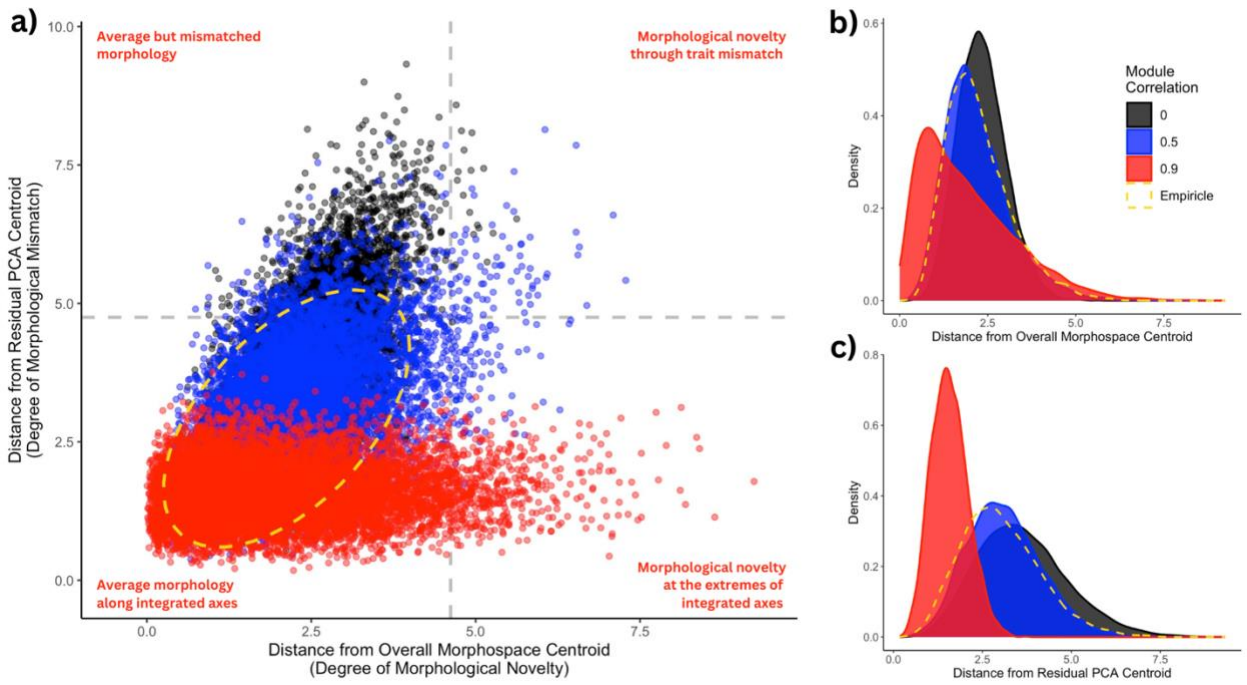

Figure 7. **Simulated morphological evolution under varying degrees of module correlation.** Traits were simulated for a hypothetical system of six morphological modules with a correlation matrix where either all modules are uncorrelated (black), all modules have a correlation of 0.5 (blue), or all modules have a correlation of 0.9 (red). Additionally, I simulated traits using the correlation matrix calculated from my empirical data set of six reef fish morphological modules (yellow dashed lines). Simulations were iterated 100 times for each correlation level. **a)** The distance from the centroid of a PCA of residual values calculated from pairwise integrations among modules (residuals PCA) versus the distance from the centroid of a PCA in which the loadings are the first four PC axes taken from individual module morphospaces (overall morphospace). The yellow dashed ellipse represents the 95% ellipse of the empirical correlation matrix simulation, as plotting the raw values for this simulation obscures the correlation of 0.5 data. Grey dashed lines denote the half-range between the most extreme observations on both axes. **b)** The density distribution of the distance from the centroid of the overall morphospace. **c)** The density distribution of the distance from the centroid of the residuals PCA.

Table 1. **Integration among morphological modules. a)** The strength of integration between morphological modules (or the correlation between modules) is first calculated from a two-block partial least squares (PLS) analysis. **b)** Phylogenetically corrected axes of integration are secondarily calculated using the *phylo.integration* function in the package *geomorph* (v 4.0.7; R). For both the two-block PLS and the phylogenetic integration analyses the pairwise correlation coefficient (*r*) values shown in blue shaded lower regions of the matrices, while the effect sizes (Z) are shown in the yellow shaded upper regions. Asterisks in the superscripts of the r-values represent significant integrations at the levels of one asterisk for $p<0.05$, two for $p<0.01$, three for $p<0.001$.

a) Two-Block PLS	Jaws	Body	Pectoral	Caudal	Dorsal	Anal
Jaws		4.04	3.04	2.57	2.92	1.86
Body	**0.553*****		3.66	3.32	5.41	7.61
Pectoral	**0.443****	**0.520*****		4.02	2.02	2.73
Caudal	**0.397****	**0.483****	**0.556*****		2.14	4.61
Dorsal	**0.444****	**0.782*****	**0.361***	**0.363***		3.56
Anal	**0.332***	**0.852*****	**0.380****	**0.613*****	**0.490*****	
b) Phylo. Integration	Jaws	Body	Pectoral	Caudal	Dorsal	Anal
Jaws		*1.87*	*2.47*	1.47	0.06	2.55
Body	**0.404***		2.11	1.02	4.61	6.39
Pectoral	**0.416****	**0.411***		3.64	0.83	1.95
Caudal	0.351	0.345	**0.523*****		1.53	2.71
Dorsal	0.285	**0.626*****	0.299	0.344		4.42
Anal	**0.407****	**0.771*****	**0.334***	**0.402****	**0.591*****	

References

Adams, D. C., Collyer, M. L., Kaliontzopoulou, A., & Baken, E. K. (2023). *geomorph*: geometric morphometric analyses of 2d and 3d landmark data (4.0.6) [Computer software]. https://cran.r-project.org/web/packages/geomorph/index.html

Adams, D., & Collyer, M. (2019). Phylogenetic comparative methods and the evolution of multivariate phenotypes. Annual Review of Ecology, Evolution, and Systematics, 50, 1–21. https://doi.org/10.1146/annurev-ecolsys-110218-024555

Aguilar-Medrano, R., Frédérich, B., Balart, E. F., & de Luna, E. (2013). Diversification of the pectoral fin shape in damselfishes (Perciformes, Pomacentridae) of the Eastern Pacific. Zoomorphology, 132(2), 197–213. https://doi.org/10.1007/s00435-012-0178-8

Aguilar-Medrano, R., Frédérich, B., & Barber, P. H. (2016). Modular diversification of the locomotor system in damselfishes (Pomacentridae). Journal of Morphology, 277(5), 603–614. https://doi.org/10.1002/jmor.20523

Ahn, D., Kourakis, M. J., Rohde, L. A., Silver, L. M., & Ho, R. K. (2002). T-box gene tbx5 is essential for formation of the pectoral limb bud. Nature, 417(6890), 754–758. https://doi.org/10.1038/nature00814

Akimenko, M.-A., Ekker, M., Wegner, J., Lin, W., & Westerfield, M. (1994). Combinatorial expression of three zebrafish genes related to distal- less: Part of a homeobox gene code for the head. Journal of Neuroscience, 14(6), 3475–3486. https://doi.org/10.1523/JNEUROSCI.14-06-03475.1994

Akimenko, M.-A., Johnson, S. L., Westerfield, M., & Ekker, M. (1995). Differential induction of four msx homeobox genes during fin development and regeneration in zebrafish. Development, 121(2), 347–357. https://doi.org/10.1242/dev.121.2.347

Amundsen, T., & Forsgren, E. (2001). Male mate choice selects for female coloration in a fish. Proceedings of the National Academy of Sciences, 98(23), 13155–13160. https://doi.org/10.1073/pnas.211439298

Astudillo-Clavijo, V., Arbour, J. H., & López-Fernández, H. (2015). Selection towards different adaptive optima drove the early diversification of locomotor phenotypes in the radiation of Neotropical geophagine cichlids. BMC Evolutionary Biology, 15(1), 77. https://doi.org/10.1186/s12862-015-0348-7

Bainbridge, R. (1958). The speed of swimming of fish as related to size and to the frequency and amplitude of the tail beat. Journal of Experimental Biology, 35(1), 109–133. https://doi.org/10.1242/jeb.35.1.109

Baken, E. K., Collyer, M. L., Kaliontzopoulou, A., & Adams, D. C. (2021). geomorph v4.0 and gmShiny: Enhanced analytics and a new graphical interface for a comprehensive morphometric experience. Methods in Ecology and Evolution, 12(12), 2355–2363. https://doi.org/10.1111/2041-210X.13723

Barnett, A., Bellwood, D. R., & Hoey, A. S. (2006). Trophic ecomorphology of cardinalfish. Marine Ecology Progress Series, 322, 249–257. https://doi.org/10.3354/meps322249

Bell, E., Andres, B., & Goswami, A. (2011). Integration and dissociation of limb elements in flying vertebrates: A comparison of pterosaurs, birds and bats. Journal of Evolutionary Biology, 24(12), 2586–2599. https://doi.org/10.1111/j.1420-9101.2011.02381.x

Bellwood, D. R., Klanten, S., Cowman, P. F., Pratchett, M. S., Konow, N., & Van Herwerden, L. (2010). Evolutionary history of the butterflyfishes (f: Chaetodontidae) and the rise of coral feeding fishes. Journal of Evolutionary Biology, 23(2), 335–349. https://doi.org/10.1111/j.1420-9101.2009.01904.x

Bellwood, D. R., & Wainwright, P. C. (2002). The history and biogeography of fishes on coral reefs. In: Sale P.F., editor. Coral Reef Fishes: Dynamics and Diversity in a Complex Ecosystem (pp. 5–32). Academic Press.

Bellwood, D. R., Wainwright, P. C., Fulton, C. J., & Hoey, A. S. (2005). Functional versatility supports coral reef biodiversity. Proceedings of the Royal Society B: Biological Sciences, 273(1582), 101–107. https://doi.org/10.1098/rspb.2005.3276

Bellwood, D., & Wainwright, P. (2001a). Locomotion in labrid fishes: Implications for habitat use and cross-shelf biogeography on the Great Barrier Reef. Coral Reefs, 20(2), 139–150. https://doi.org/10.1007/s003380100156

Bellwood, D., & Wainwright, P. (2001b). Locomotion in labrid fishes: Implications for habitat use and cross-shelf biogeography on the Great Barrier Reef. Coral Reefs, 20(2), 139–150. https://doi.org/10.1007/s003380100156

Berman, S. L. (1985). Convergent evolution in the hindlimb of bipedal rodents. Journal of Zoological Systematics and Evolutionary Research, 23(1), 59–77. https://doi.org/10.1111/j.1439-0469.1985.tb00570.x

Blake, R. W. (2004). Fish functional design and swimming performance. Journal of Fish Biology, 65(5), 1193–1222. https://doi.org/10.1111/j.0022-1112.2004.00568.x

Blake, R. W., Chatters, L. M., & Domenici, P. (1995). Turning radius of yellowfin tuna (Thunnus albacares) in unsteady swimming manoeuvres. Journal of Fish Biology, 46(3), 536–538. https://doi.org/10.1111/j.1095-8649.1995.tb05994.x

Booher, D. B., Gibson, J. C., Liu, C., Longino, J. T., Fisher, B. L., Janda, M., Narula, N., Toulkeridou, E., Mikheyev, A. S., Suarez, A. V., & Economo, E. P. (2021). Functional innovation promotes diversification of form in the evolution of an ultrafast trap-jaw

mechanism in ants. PLOS Biology, 19(3), e3001031. https://doi.org/10.1371/journal.pbio.3001031

Borazjani, I., & Sotiropoulos, F. (2010). On the role of form and kinematics on the hydrodynamics of self-propelled body/caudal fin swimming. Journal of Experimental Biology, 213(1), 89–107. https://doi.org/10.1242/jeb.030932

Bower, L. M., & Piller, K. R. (2015). Shaping up: A geometric morphometric approach to assemblage ecomorphology. Journal of Fish Biology, 87(3), 691–714. https://doi.org/10.1111/jfb.12752

Breder, C. M. (1926). The locomotion of fishes. Zoologica: Scientific Contributions of the New York Zoological Society, 4(5), 159--297. https://doi.org/10.5962/p.203769

Bridge, T. C. L., Luiz, O. J., Coleman, R. R., Kane, C. N., & Kosaki, R. K. (2016). Ecological and morphological traits predict depth-generalist fishes on coral reefs. Proceedings of the Royal Society B: Biological Sciences, 283(1823), 20152332. https://doi.org/10.1098/rspb.2015.2332

Brönmark, C., & Miner, J. G. (1992). Predator-induced phenotypical change in body morphology in crucian carp. Science, 258(5086), 1348–1350. https://doi.org/10.1126/science.258.5086.1348

Burns, M. D., Collyer, M. L., & Sidlauskas, B. L. (2023). Simultaneous integration and modularity underlie the exceptional body shape diversification of characiform fishes. Evolution, 77(3), 746–762. https://doi.org/10.1093/evolut/qpac070

Burns, M. D., Satterfield, D. R., Peoples, N., Chan, H., Barley, A. J., Roberts-Hugghis, A., Russell, K. T., Hess, M., Williamson, S., Corn, K. A., Mihalitsis, M., Wainwright, D. K., & Wainwright, P. C. (In Review). Complexity & weak integration promote the diversity of life: reef fish oral jaw evolution. Nature Communications.

Buttimer, S. M., Stepanova, N., & Womack, M. C. (2020). Evolution of the unique anuran pelvic and hind limb skeleton in relation to microhabitat, locomotor mode, and jump performance. Integrative and Comparative Biology, 60(5), 1330–1345. https://doi.org/10.1093/icb/icaa043

Cannas, M., Schaefer, J., Domenici, P., & Steffensen, J. F. (2006). Gait transition and oxygen consumption in swimming striped surfperch Embiotoca lateralis Agassiz. Journal of Fish Biology, 69(6), 1612–1625. https://doi.org/10.1111/j.1095-8649.2006.01225.x

Chamero, B., Buscalioni, Á. D., & Marugán-Lobón, J. (2013). Pectoral girdle and forelimb variation in extant Crocodylia: The coracoid–humerus pair as an evolutionary module. Biological Journal of the Linnean Society, 108(3), 600–618. https://doi.org/10.1111/j.1095-8312.2012.02037.x

Chang, J., Rabosky, D. L., Smith, S. A., & Alfaro, M. E. (2019). An r package and online resource for macroevolutionary studies using the ray-finned fish tree of life. Methods in Ecology and Evolution, 10(7), 1118–1124. https://doi.org/10.1111/2041-210X.13182

Chivers, D. P., Zhao, X., Brown, G. E., Marchant, T. A., & Ferrari, M. C. O. (2008). Predator-induced changes in morphology of a prey fish: The effects of food level and temporal frequency of predation risk. Evolutionary Ecology, 22(4), 561–574. https://doi.org/10.1007/s10682-007-9182-8

Citadini, J. M., Brandt, R., Williams, C. R., & Gomes, F. R. (2018). Evolution of morphology and locomotor performance in anurans: Relationships with microhabitat diversification. Journal of Evolutionary Biology, 31(3), 371–381. https://doi.org/10.1111/jeb.13228

Claisse, J. T., Clark, T. B., Schumacher, B. D., McTee, S. A., Bushnell, M. E., Callan, C. K., Laidley, C. W., & Parrish, J. D. (2011). Conventional tagging and acoustic telemetry of a small surgeonfish, Zebrasoma flavescens, in a structurally complex coral reef environment.

Environmental Biology of Fishes, 91(2), 185–201. https://doi.org/10.1007/s10641-011-9771-9

Claverie, T., & Wainwright, P. C. (2014). Rrpp: linear model evaluation with randomized residuals in a permutation procedure. PLoS ONE, 9(11), e112732. https://doi.org/10.1371/journal.pone.0112732

Clegg, S. M., Degnan, S. M., Moritz, C., Estoup, A., Kikkawa, J., & Owens, I. P. F. (2002). Rrpp: linear model evaluation with randomized residuals in a permutation procedure. Evolution, 56(10), 2090–2099. https://doi.org/10.1111/j.0014-3820.2002.tb00134.x

Clements, K. D., German, D. P., Piché, J., Tribollet, A., & Choat, J. H. (2016). Integrating ecological roles and trophic diversification on coral reefs: Multiple lines of evidence identify parrotfishes as microphages. Biological Journal of the Linnean Society, 120(4), 729–751. https://doi.org/10.1111/bij.12914

Collar, D. C., Wainwright, P. C., & Alfaro, M. E. (2007). Integrated diversification of locomotion and feeding in labrid fishes. Biology Letters, 4(1), 84–86. https://doi.org/10.1098/rsbl.2007.0509

Collyer, M. L., & Adams, D. C. (2018). RRPP: An r package for fitting linear models to high-dimensional data using residual randomization. Methods in Ecology and Evolution, 9(7), 1772–1779. https://doi.org/10.1111/2041-210X.13029

Collyer, M. L., & Adams, D. C. (2024). RRPP: linear model evaluation with randomized residuals in a permutation procedure (2.0.0) [Computer software]. https://cran.r-project.org/web/packages/RRPP/index.html

Colombo, M., Indermaur, A., Meyer, B. S., & Salzburger, W. (2016). Habitat use and its implications to functional morphology: Niche partitioning and the evolution of locomotory

morphology in Lake Tanganyikan cichlids (Perciformes: Cichlidae). Biological Journal of the Linnean Society, 118(3), 536–550. https://doi.org/10.1111/bij.12754

Conner, J. K., Cooper, I. A., La Rosa, R. J., Pérez, S. G., & Royer, A. M. (2014). Patterns of phenotypic correlations among morphological traits across plants and animals. Philosophical Transactions of the Royal Society B: Biological Sciences, 369(1649), 20130246. https://doi.org/10.1098/rstb.2013.0246

Cooper, W. J., & Westneat, M. W. (2009). Form and function of damselfish skulls: Rapid and repeated evolution into a limited number of trophic niches. BMC Evolutionary Biology, 9(1), 24. https://doi.org/10.1186/1471-2148-9-24

Corn, K. A., Friedman, S. T., Burress, E. D., Martinez, C. M., Larouche, O., Price, S. A., & Wainwright, P. C. (2022). The rise of biting during the Cenozoic fueled reef fish body shape diversification. Proceedings of the National Academy of Sciences, 119(31), e2119828119. https://doi.org/10.1073/pnas.2119828119

Costa, C., & Cataudella, S. (2007). Relationship between shape and trophic ecology of selected species of Sparids of the Caprolace coastal lagoon (Central Tyrrhenian sea). Environmental Biology of Fishes, 78(2), 115–123. https://doi.org/10.1007/s10641-006-9081-9

Crotwell, P. L., Clark, T. G., & Mabee, P. M. (2001). Gdf5 is expressed in the developing skeleton of median fins of late-stage zebrafish, Danio rerio. Development Genes and Evolution, 211(11), 555–558. https://doi.org/10.1007/s00427-001-0186-z

Crotwell, P. L., & Mabee, P. M. (2007). Gene expression patterns underlying proximal–distal skeletal segmentation in late-stage zebrafish, Danio rerio. Developmental Dynamics, 236(11), 3111–3128. https://doi.org/10.1002/dvdy.21352

Crotwell, P. L., Sommervold, A. R., & Mabee, P. M. (2004). Expression of bmp2a and bmp2b in late-stage zebrafish median fin development. Gene Expression Patterns, 5(2), 291–296. https://doi.org/10.1016/j.modgep.2004.07.001

Crumière, A. J. J., Santos, M. E., Sémon, M., Armisén, D., Moreira, F. F. F., & Khila, A. (2016). Diversity in morphology and locomotory behavior is associated with niche expansion in the semi-aquatic bugs. Current Biology, 26(24), 3336–3342. https://doi.org/10.1016/j.cub.2016.09.061

Dahn, R. D., Davis, M. C., Pappano, W. N., & Shubin, N. H. (2007). Sonic hedgehog function in chondrichthyan fins and the evolution of appendage patterning. Nature, 445(7125), 311–314. https://doi.org/10.1038/nature05436

De Barros, T. F., Louvise, J., & Caramaschi, É. P. (2019). Flow gradient drives morphological divergence in an Amazon pelagic stream fish. Hydrobiologia, 833(1), 217–229. https://doi.org/10.1007/s10750-019-3902-2

Denton, J. S. S., & Adams, D. C. (2015). A new phylogenetic test for comparing multiple high-dimensional evolutionary rates suggests interplay of evolutionary rates and modularity in lanternfishes (Myctophiformes; Myctophidae). Evolution, 69(9), 2425–2440. https://doi.org/10.1111/evo.12743

Dewar, H., & Graham, J. B. (1994). Studies of tropical tuna swimming performance in a large water tunnel: I. energetics. Journal of Experimental Biology, 192(1), 13–31. https://doi.org/10.1242/jeb.192.1.13

Di Santo, V., Goerig, E., Wainwright, D. K., Akanyeti, O., Liao, J. C., Castro-Santos, T., & Lauder, G. V. (2021). Convergence of undulatory swimming kinematics across a diversity of fishes.

Proceedings of the National Academy of Sciences, 118(49), e2113206118. https://doi.org/10.1073/pnas.2113206118

Dingerkus, G., & Uhler, L. D. (1977). Enzyme clearing of alcian blue stained whole small vertebrates for demonstration of cartilage. Stain Technology, 52(4), 229–232. https://doi.org/10.3109/10520297709116780

Donley, J. M., Sepulveda, C. A., Konstantinidis, P., Gemballa, S., & Shadwick, R. E. (2004). Convergent evolution in mechanical design of lamnid sharks and tunas. Nature, 429(6987), 61–65. https://doi.org/10.1038/nature02435

Drucker, E. G., & Jensen, J. S. (1996). Pectoral fin locomotion in the striped surfperch: II. Scaling swimming kinematics and performance at a gait transition. Journal of Experimental Biology, 199(10), 2243–2252. https://doi.org/10.1242/jeb.199.10.2243

Du, T. Y., Tissandier, S. C., & Larsson, H. C. E. (2019). Integration and modularity of teleostean pectoral fin shape and its role in the diversification of acanthomorph fishes. Evolution, 73(2), 401–411. https://doi.org/10.1111/evo.13669

Dumont, E. R., Dávalos, L. M., Goldberg, A., Santana, S. E., Rex, K., & Voigt, C. C. (2011a). Morphological innovation, diversification and invasion of a new adaptive zone. Proceedings of the Royal Society B: Biological Sciences, 279(1734), 1797–1805. https://doi.org/10.1098/rspb.2011.2005

Dumont, E. R., Dávalos, L. M., Goldberg, A., Santana, S. E., Rex, K., & Voigt, C. C. (2011b). Morphological innovation, diversification and invasion of a new adaptive zone. Proceedings of the Royal Society B: Biological Sciences, 279(1734), 1797–1805. https://doi.org/10.1098/rspb.2011.2005

Ehlinger, T. J. (1990). Habitat choice and phenotype-limited feeding efficiency in bluegill: individual differences and trophic polymorphism. Ecology, 71(3), 886–896. https://doi.org/10.2307/1937360

Ehlinger, T. J., & Wilson, D. S. (1988). Complex foraging polymorphism in bluegill sunfish. Proceedings of the National Academy of Sciences, 85(6), 1878–1882. https://doi.org/10.1073/pnas.85.6.1878

Eklöv, P., & Jonsson, P. (2007). Pike predators induce morphological changes in young perch and roach. Journal of Fish Biology, 70(1), 155–164. https://doi.org/10.1111/j.1095-8649.2006.01283.x

Eliason, C. M., Proffitt, J. V., & Clarke, J. A. (2023). Early diversification of avian limb morphology and the role of modularity in the locomotor evolution of crown birds. Evolution, 77(2), 342–354. https://doi.org/10.1093/evolut/qpac039

Ellerby, D. J., & Gerry, S. P. (2011). Sympatric divergence and performance trade-offs of bluegill ectomorphs. Evolutionary Biology, 38(4), 422–433. https://doi.org/10.1007/s11692-011-9130-y

Eloy, C. (2013). On the best design for undulatory swimming. Journal of Fluid Mechanics, 717, 48–89. https://doi.org/10.1017/jfm.2012.561

Essner Jr., R. L. (2007). Morphology, locomotor behaviour and microhabitat use in North American squirrels. Journal of Zoology, 272(1), 101–109. https://doi.org/10.1111/j.1469-7998.2006.00247.x

Evans, K. M., Buser, T. J., Larouche, O., & Kolmann, M. A. (2023). Untangling the relationship between developmental and evolutionary integration. Seminars in Cell & Developmental Biology, 145, 22–27. https://doi.org/10.1016/j.semcdb.2022.05.026

Evans, K. M., Larouche, O., Watson, S.-J., Farina, S., Habegger, M. L., & Friedman, M. (2021). Integration drives rapid phenotypic evolution in flatfishes. Proceedings of the National Academy of Sciences, 118(18), e2101330118. https://doi.org/10.1073/pnas.2101330118

Evans, K. M., Waltz, B. T., Tagliacollo, V. A., Sidlauskas, B. L., & Albert, J. S. (2017). Fluctuations in evolutionary integration allow for big brains and disparate faces. Scientific Reports, 7(1), Article 1. https://doi.org/10.1038/srep40431

Fabre, A.-C., Goswami, A., Peigné, S., & Cornette, R. (2014). Morphological integration in the forelimb of musteloid carnivorans. Journal of Anatomy, 225(1), 19–30. https://doi.org/10.1111/joa.12194

Feilich, K. L. (2017). Swimming with multiple propulsors: Measurement and comparison of swimming gaits in three species of neotropical cichlids. Journal of Experimental Biology, jeb.157180. https://doi.org/10.1242/jeb.157180

Felice, R. N., Randau, M., & Goswami, A. (2018). A fly in a tube: Macroevolutionary expectations for integrated phenotypes. Evolution, 72(12), 2580–2594. https://doi.org/10.1111/evo.13608

Fisher, R., & Bellwood, D. (2003). Undisturbed swimming behaviour and nocturnal activity of coral reef fish larvae. Marine Ecology Progress Series, 263, 177–188. https://doi.org/10.3354/meps263177

Foster, K. L., Garland, T., Jr, Schmitz, L., & Higham, T. E. (2018). Skink ecomorphology: Forelimb and hind limb lengths, but not static stability, correlate with habitat use and demonstrate multiple solutions. Biological Journal of the Linnean Society, 125(4), 673–692. https://doi.org/10.1093/biolinnean/bly146

Freitas, R., Zhang, G., & Cohn, M. J. (2006). Evidence that mechanisms of fin development evolved in the midline of early vertebrates. Nature, 442(7106), 1033–1037. https://doi.org/10.1038/nature04984

Friedman, S. T., Price, S. A., Corn, K. A., Larouche, O., Martinez, C. M., & Wainwright, P. C. (2020). Body shape diversification along the benthic–pelagic axis in marine fishes. Proceedings of the Royal Society B: Biological Sciences, 287(1931), 20201053. https://doi.org/10.1098/rspb.2020.1053

Friedman, S. T., Price, S. A., Hoey, A. S., & Wainwright, P. C. (2016). Ecomorphological convergence in planktivorous surgeonfishes. Journal of Evolutionary Biology, 29(5), 965–978. https://doi.org/10.1111/jeb.12837

Friedman, S. T., Price, S. A., & Wainwright, P. C. (2021). The effect of locomotion mode on body shape evolution in teleost fishes. Integrative Organismal Biology, 3(1), obab016. https://doi.org/10.1093/iob/obab016

Fulton, C., Bellwood, D., & Wainwright, P. (2001). The relationship between swimming ability and habitat use in wrasses (Labridae). Marine Biology, 139(1), 25–33. https://doi.org/10.1007/s002270100565

Fulton, C. J. (2007). Swimming speed performance in coral reef fishes: Field validations reveal distinct functional groups. Coral Reefs, 26(2), 217–228. https://doi.org/10.1007/s00338-007-0195-0

Fulton, C. J., Bellwood, D. R., & Wainwright, P. C. (2005). Wave energy and swimming performance shape coral reef fish assemblages. Proceedings of the Royal Society B: Biological Sciences, 272(1565), 827–832. https://doi.org/10.1098/rspb.2004.3029

Fulton, C. J., Johansen, J. L., & Steffensen, J. F. (2013). Energetic Extremes in Aquatic Locomotion by Coral Reef Fishes. PLoS ONE, 8(1), e54033. https://doi.org/10.1371/journal.pone.0054033

Garland, K., Marcy, A., Sherratt, E., & Weisbecker, V. (2017). Out on a limb: Bandicoot limb co-variation suggests complex impacts of development and adaptation on marsupial forelimb evolution. Evolution & Development, 19(2), 69–84. https://doi.org/10.1111/ede.12220

Gatesy, S. M., & Dial, K. P. (1996). Locomotor modules and the evolution of avian flight. Evolution, 50(1), 331–340. https://doi.org/10.1111/j.1558-5646.1996.tb04496.x

Gatesy, S. M., & Middleton, K. M. (1997). Bipedalism, flight, and the evolution of theropod locomotor diversity. Journal of Vertebrate Paleontology, 17(2), 308–329. https://doi.org/10.1080/02724634.1997.10010977

George, A. B., & Westneat, M. W. (2019). Functional morphology of endurance swimming performance and gait transition strategies in balistoid fishes. Journal of Experimental Biology, jeb.194704. https://doi.org/10.1242/jeb.194704

Gerstner, C. L. (1999). Maneuverability of four species of coral-reef fish that differ in body and pectoral-fin morphology. Canadian Journal of Zoology, 77(7), 1102–1110. https://doi.org/10.1139/z99-086

Ghalambor, C. K. (2003). Multi-trait selection, adaptation, and constraints on the evolution of burst swimming performance. Integrative and Comparative Biology, 43(3), 431–438. https://doi.org/10.1093/icb/43.3.431

Ghezelayagh, A., Harrington, R. C., Burress, E. D., Campbell, M. A., Buckner, J. C., Chakrabarty, P., Glass, J. R., McCraney, W. T., Unmack, P. J., Thacker, C. E., Alfaro, M. E., Friedman, S. T., Ludt, W. B., Cowman, P. F., Friedman, M., Price, S. A., Dornburg, A., Faircloth, B. C.,

Wainwright, P. C., & Near, T. J. (2022). Prolonged morphological expansion of spiny-rayed fishes following the end-Cretaceous. Nature Ecology & Evolution, 6(8), 1211–1220. https://doi.org/10.1038/s41559-022-01801-3

Goodrich, E. S. (1906). Notes on the development, structure, and origin of the median and paired fins of fish. Journal of Cell Science, s2-50(198), 333–376. https://doi.org/10.1242/jcs.s2-50.198.333

Goswami, A., & Polly, P. D. (2010). The influence of modularity on cranial morphological disparity in carnivora and primates (Mammalia). PLOS ONE, 5(3), e9517. https://doi.org/10.1371/journal.pone.0009517

Goswami, A., Smaers, J. B., Soligo, C., & Polly, P. D. (2014). The macroevolutionary consequences of phenotypic integration: From development to deep time. Philosophical Transactions of the Royal Society B: Biological Sciences, 369(1649), 20130254. https://doi.org/10.1098/rstb.2013.0254

Granatosky, M. C. (2018). A Review of locomotor diversity in mammals with analyses exploring the influence of substrate use, body mass and intermembral index in primates. Journal of Zoology, 306(4), 207–216. https://doi.org/10.1111/jzo.12608

Hadj-Hammou, J., Mouillot, D., & Graham, N. A. J. (2021). Response and effect traits of coral reef fish. Frontiers in Marine Science, 8. https://doi.org/10.3389/fmars.2021.640619

Hallgrímsson, B., Willmore, K., & Hall, B. K. (2002). Canalization, developmental stability, and morphological integration in primate limbs. American Journal of Physical Anthropology, 119(S35), 131–158. https://doi.org/10.1002/ajpa.10182

Hansen, T. F. (2003). Is modularity necessary for evolvability? Remarks on the relationship between pleiotropy and evolvability. Bio Systems, 69(2–3), 83–94. https://doi.org/10.1016/s0303-2647(02)00132-6

Heude, É., Shaikho, S., & Ekker, M. (2014). The dlx5a/dlx6a Genes Play Essential Roles in the Early Development of Zebrafish Median Fin and Pectoral Structures. PLOS ONE, 9(5), e98505. https://doi.org/10.1371/journal.pone.0098505

Higham, T. E. (2007). Feeding, fins and braking maneuvers: Locomotion during prey capture in centrarchid fishes. Journal of Experimental Biology, 210(1), 107–117. https://doi.org/10.1242/jeb.02634

Higham, T. E., Birn-Jeffery, A. V., Collins, C. E., Hulsey, C. D., & Russell, A. P. (2015). Adaptive simplification and the evolution of gecko locomotion: Morphological and biomechanical consequences of losing adhesion. Proceedings of the National Academy of Sciences, 112(3), 809–814. https://doi.org/10.1073/pnas.1418979112

Hixon, M. A., & Beets, J. P. (1993). Predation, prey refuges, and the structure of coral-reef fish assemblages. Ecological Monographs, 63(1), 77–101. https://doi.org/10.2307/2937124

Hodge, J. R., Alim, C., Bertrand, N. G., Lee, W., Price, S. A., Tran, B., & Wainwright, P. C. (2018). Ecology shapes the evolutionary trade-off between predator avoidance and defence in coral reef butterflyfishes. Ecology Letters, 21(7), 1033–1042. https://doi.org/10.1111/ele.12969

Huertas, V., & Bellwood, D. R. (2020). Trophic separation in planktivorous reef fishes: A new role for mucus? Oecologia, 192(3), 813–822. https://doi.org/10.1007/s00442-020-04608-w

Hulsey, C. D. (2005). Function of a key morphological innovation: Fusion of the cichlid pharyngeal jaw. Proceedings of the Royal Society B: Biological Sciences, 273(1587), 669–675. https://doi.org/10.1098/rspb.2005.3375

Hulsey, C. D., Holzman, R., & Meyer, A. (2018). Dissecting a potential spandrel of adaptive radiation: Body depth and pectoral fin ecomorphology coevolve in Lake Malawi cichlid fishes. Ecology and Evolution, 8(23), 11945–11953. https://doi.org/10.1002/ece3.4651

Jastrebski, C. J., & Robinson, B. W. (n.d.). Natural selection and the evolution of replicated trophic polymorphisms in pumpkinseed sunfish.

Kelly, M. E., & Sears, K. E. (2011). Reduced phenotypic covariation in marsupial limbs and the implications for mammalian evolution. Biological Journal of the Linnean Society, 102(1), 22–36. https://doi.org/10.1111/j.1095-8312.2010.01561.x

Klingenberg, C. P. (2008). Morphological integration and developmental modularity. Annual Review of Ecology, Evolution, and Systematics, 39, 115–132.

Konow, N., & Bellwood, D. R. (2011). Evolution of high trophic diversity based on limited functional disparity in the feeding apparatus of marine angelfishes (f. Pomacanthidae). PLOS ONE, 6(9), e24113. https://doi.org/10.1371/journal.pone.0024113

Konow, N., Bellwood, D. R., Wainwright, P. C., & Kerr, A. M. (2008). Evolution of novel jaw joints promote trophic diversity in coral reef fishes: Novel jaw joints in biting reef fishes. Biological Journal of the Linnean Society, 93(3), 545–555. https://doi.org/10.1111/j.1095-8312.2007.00893.x

Konow, N., & Ferry, L. (2013). Functional morphology of butterflyfishes. In B. Kapoor (Ed.), Biology of Butterflyfishes (pp. 19–47). CRC Press. https://doi.org/10.1201/b15458-3

Konow, N., Price, S. A., Abom, R., Bellwood, D. R., & Wainwright, P. C. (2017). Decoupled diversification dynamics of feeding morphology following a major functional innovation in marine butterflyfishes. Proceedings of the Royal Society B: Biological Sciences, 284(1860), 20170906. https://doi.org/10.1098/rspb.2017.0906

Korsmeyer, K. E., Steffensen, J. F., & Herskin, J. (2002). Energetics of median and paired fin swimming, body and caudal fin swimming, and gait transition in parrotfish (*Scarus schlegeli*) and triggerfish (*Rhinecanthus aculeatus*). Journal of Experimental Biology, 205(9), 1253–1263. https://doi.org/10.1242/jeb.205.9.1253

Kotrschal, K. (1989). Trophic ecomorphology in eastern Pacific blennioid fishes: Character transformation of oral jaws and associated change of their biological roles. Environmental Biology of Fishes, 24(3), 199–218. https://doi.org/10.1007/BF00001224

Langerhans, R. B. (2009). Trade-off between steady and unsteady swimming underlies predator-driven divergence in *Gambusia affinis*. Journal of Evolutionary Biology, 22(5), 1057–1075. https://doi.org/10.1111/j.1420-9101.2009.01716.x

Larouche, O., Benton, B., Corn, K. A., Friedman, S. T., Gross, D., Iwan, M., Kessler, B., Martinez, C. M., Rodriguez, S., Whelpley, H., Wainwright, P. C., & Price, S. A. (2020). Reef-associated fishes have more maneuverable body shapes at a macroevolutionary scale. Coral Reefs, 39(5), 1427–1439. https://doi.org/10.1007/s00338-020-01976-w

Larouche, O., Cloutier, R., & Zelditch, M. L. (2015). Head, body and fins: Patterns of morphological integration and modularity in fishes. Evolutionary Biology, 42(3), 296–311. https://doi.org/10.1007/s11692-015-9324-9

Larouche, O., Zelditch, M. L., & Cloutier, R. (2018). Modularity promotes morphological divergence in ray-finned fishes. Scientific Reports, 8(1), Article 1. https://doi.org/10.1038/s41598-018-25715-y

Lauder, G. V., & Madden, P. G. A. (2007). Fish locomotion: Kinematics and hydrodynamics of flexible foil-like fins. Experiments in Fluids, 43(5), 641–653. https://doi.org/10.1007/s00348-007-0357-4

Lauder, G. V., & Tytell, E. D. (2005). Hydrodynamics of undulatory propulsion. In Fish Physiology (Vol. 23, pp. 425–468). Elsevier. https://doi.org/10.1016/S1546-5098(05)23011-X

Letelier, J., de la Calle-Mustienes, E., Pieretti, J., Naranjo, S., Maeso, I., Nakamura, T., Pascual-Anaya, J., Shubin, N. H., Schneider, I., Martinez-Morales, J. R., & Gómez-Skarmeta, J. L. (2018). A conserved Shh cis-regulatory module highlights a common developmental origin of unpaired and paired fins. Nature Genetics, 50(4), 504–509. https://doi.org/10.1038/s41588-018-0080-5

Letessier, T. B., Juhel, J.-B., Vigliola, L., & Meeuwig, J. J. (2015). Low-cost small action cameras in stereo generates accurate underwater measurements of fish. Journal of Experimental Marine Biology and Ecology, 466, 120–126. https://doi.org/10.1016/j.jembe.2015.02.013

Levis, N. A., Isdaner, A. J., & Pfennig, D. W. (2018). Morphological novelty emerges from pre-existing phenotypic plasticity. Nature Ecology & Evolution, 2(8), Article 8. https://doi.org/10.1038/s41559-018-0601-8

Lighthill, J., & Blake, R. (1990). Biofluiddynamics of balistiform and gymnotiform locomotion. Part 1. Biological background, and analysis by elongated-body theory. Journal of Fluid Mechanics, 212(1), 183. https://doi.org/10.1017/S0022112090001926

Lighthill, M. J. (1969). Hydromechanics of aquatic animal propulsion. Annual Review of Fluid Mechanics, 1(1), 413–446. https://doi.org/10.1146/annurev.fl.01.010169.002213

Lighthill, S. J. (1975). Mathematical Biofluiddynamics. Society for Industrial and Applied Mathematics. https://doi.org/10.1137/1.9781611970517

Lindsey, C. C. (1978). Form, function, and locomotory habits in fish. In W. S. Hoar & D. J. Randall (Eds.), Fish Physiology (Vol. 7, pp. 1–100). Academic Press. https://doi.org/10.1016/S1546-5098(08)60163-6

Long, J. H., & Nipper, K. S. (1996). The Importance of Body Stiffness in Undulatory Propulsion. American Zoologist, 36(6), 678–694. https://doi.org/10.1093/icb/36.6.678

Mabee, P. M., Crotwell, P. L., Bird, N. C., & Burke, A. C. (2002). Evolution of median fin modules in the axial skeleton of fishes. Journal of Experimental Zoology, 294(2), 77–90. https://doi.org/10.1002/jez.10076

Malhotra, A., & Thorpe, R. S. (1991). Experimental detection of rapid evolutionary response in natural lizard populations. Nature, 353(6342), 347–348. https://doi.org/10.1038/353347a0

Mallet, C., Billet, G., Houssaye, A., & Cornette, R. (2020). A first glimpse at the influence of body mass in the morphological integration of the limb long bones: An investigation in modern rhinoceroses. Journal of Anatomy, 237(4), 704–726. https://doi.org/10.1111/joa.13232

Marcoux, T. M., & Korsmeyer, K. E. (2019). Energetics and behavior of coral reef fishes during oscillatory swimming in a simulated wave surge. Journal of Experimental Biology, jeb.191791. https://doi.org/10.1242/jeb.191791

Marroig, G., & Cheverud, J. M. (2005). Size as a line of least evolutionary resistance: Diet and adaptive morphological radiation in new world monkeys. Evolution, 59(5), 1128–1142. https://doi.org/10.1111/j.0014-3820.2005.tb01049.x

Marroig, G., Shirai, L. T., Porto, A., de Oliveira, F. B., & De Conto, V. (2009). The evolution of modularity in the mammalian skull II: Evolutionary consequences. Evolutionary Biology, 36(1), 136–148. https://doi.org/10.1007/s11692-009-9051-1

Martinez, C. M., Friedman, S. T., Corn, K. A., Larouche, O., Price, S. A., & Wainwright, P. C. (2021). The deep sea is a hot spot of fish body shape evolution. Ecology Letters, 24(9), 1788–1799. https://doi.org/10.1111/ele.13785

Martín-Serra, A., Figueirido, B., & Palmqvist, P. (2014). A three-dimensional analysis of morphological evolution and locomotor performance of the carnivoran forelimb. PLOS ONE, 9(1), e85574. https://doi.org/10.1371/journal.pone.0085574

Mchenry, M. J., Pell, C. A., & Long, J. H. (1995). Mechanical control of swimming speed: Stiffness and axial wave form in undulating fish models. Journal of Experimental Biology, 198(11), 2293–2305. https://doi.org/10.1242/jeb.198.11.2293

Meyer, C. G., & Holland, K. N. (2005). Movement patterns, home range size and habitat utilization of the bluespine unicornfish, *Naso unicornis* (Acanthuridae) in a Hawaiian marine reserve. Environmental Biology of Fishes, 73(2), 201–210. https://doi.org/10.1007/s10641-005-0559-7

Meyer, C. G., Papastamatiou, Y. P., & Clark, T. B. (2010). Differential movement patterns and site fidelity among trophic groups of reef fishes in a Hawaiian marine protected area. Marine Biology, 157(7), 1499–1511. https://doi.org/10.1007/s00227-010-1424-6

Mihalitsis, M., & Bellwood, D. R. (2019). Morphological and functional diversity of piscivorous fishes on coral reefs. Coral Reefs, 38(5), 945–954. https://doi.org/10.1007/s00338-019-01820-w

Mihalitsis, M., Morais, R. A., & Bellwood, D. R. (2022). Small predators dominate fish predation in coral reef communities. PLOS Biology, 20(11), e3001898. https://doi.org/10.1371/journal.pbio.3001898

Mittelbach, G. G. (1981). Foraging efficiency and body size: A study of optimal diet and habitat use by bluegills. Ecology, 62(5), 1370–1386. https://doi.org/10.2307/1937300

Mouillot, D., Villéger, S., Parravicini, V., Kulbicki, M., Arias-González, J. E., Bender, M., Chabanet, P., Floeter, S. R., Friedlander, A., Vigliola, L., & Bellwood, D. R. (2014). Functional over-

redundancy and high functional vulnerability in global fish faunas on tropical reefs. Proceedings of the National Academy of Sciences, 111(38), 13757–13762. https://doi.org/10.1073/pnas.1317625111

Neumann, C. J., Grandel, H., Gaffield, W., Schulte-Merker, S., & Nüsslein-Volhard, C. (1999). Transient establishment of anteroposterior polarity in the zebrafish pectoral fin bud in the absence of sonic hedgehog activity. Development, 126(21), 4817–4826. https://doi.org/10.1242/dev.126.21.4817

Neuswanger, J. R., Wipfli, M. S., Rosenberger, A. E., & Hughes, N. F. (2016). Measuring fish and their physical habitats: Versatile 2D and 3D video techniques with user-friendly software. Canadian Journal of Fisheries and Aquatic Sciences, 73(12), 1861–1873. https://doi.org/10.1139/cjfas-2016-0010

Olsen, A. M., & Westneat, M. W. (2015). StereoMorph: An R package for the collection of 3D landmarks and curves using a stereo camera set-up. Methods in Ecology and Evolution, 6(3), 351–356. https://doi.org/10.1111/2041-210X.12326

Orkney, A., Bjarnason, A., Tronrud, B. C., & Benson, R. B. J. (2021). Patterns of skeletal integration in birds reveal that adaptation of element shapes enables coordinated evolution between anatomical modules. Nature Ecology & Evolution, 5(9), Article 9. https://doi.org/10.1038/s41559-021-01509-w

Oufiero, C. E., Walsh, M. R., Reznick, D. N., & Garland, T. (2011). Swimming performance trade-offs across a gradient in community composition in Trinidadian killifish (Rivulus hartii). Ecology, 92(1), 170–179. https://doi.org/10.1890/09-1912.1

Parins-Fukuchi, C. T., & Saulsbury, J. G. (2022). Functional morphological innovation corresponds to shifting lines of genetic least resistance (p. 2022.07.30.502152). bioRxiv. https://doi.org/10.1101/2022.07.30.502152

Perevolotsky, T., Martin, C. H., Rivlin, A., & Holzman, R. (2020). Work that body: Fin and body movements determine herbivore feeding performance within the natural reef environment. Proceedings of the Royal Society B: Biological Sciences, 287(1938), 20201903. https://doi.org/10.1098/rspb.2020.1903

Petit, F., Sears, K. E., & Ahituv, N. (2017). Limb development: A paradigm of gene regulation. Nature Reviews Genetics, 18(4), 245–258. https://doi.org/10.1038/nrg.2016.167

Petrović, T. G., Vukov, T., & Tomašević Kolarov, N. (2021). Patterns of correlations and locomotor specialization in anuran limbs: Association with phylogeny and ecology. Zoology, 144, 125864. https://doi.org/10.1016/j.zool.2020.125864

Pettersson, L. B. (2007). Morphology as a key to behavioural flexibility: Body shape and swimming variability in the dimorphic crucian carp. Web Ecology, 7(1), 113–119. https://doi.org/10.5194/we-7-113-2007

Pettersson, L. B., & Brönmark, C. (1999). Energetic consequences of an inducible morphological defence in crucian carp. Oecologia, 121(1), 12–18. https://doi.org/10.1007/s004420050901

Pink, J. R., & Fulton, C. J. (2014). Right tools for the task: Intraspecific modality in the swimming behaviour of coral reef fishes. Marine Biology, 161(5), 1103–1111. https://doi.org/10.1007/s00227-014-2403-0

Plaut, I. (2001). Critical swimming speed: Its ecological relevance. Comparative Biochemistry and Physiology Part A: Molecular & Integrative Physiology, 131(1), 41–50. https://doi.org/10.1016/S1095-6433(01)00462-7

Porter, H. T., & Motta, P. J. (2004). A comparison of strike and prey capture kinematics of three species of piscivorous fishes: Florida gar (Lepisosteus platyrhincus), redfin needlefish (Strongylura notata), and great barracuda (Sphyraena barracuda). Marine Biology, 145(5), 989–1000. https://doi.org/10.1007/s00227-004-1380-0

Porter, M. E., Roque, C. M., & Long, J. H. (2009). Turning maneuvers in sharks: Predicting body curvature from axial morphology. Journal of Morphology, 270(8), 954–965. https://doi.org/10.1002/jmor.10732

Powell, A. B., & Tucker, John W. (1992). Egg and Larval Development of Laboratory-Reared Nassau Grouper, Epinephelus Striatus (Pisces, Serranidae). Bulletin of Marine Science, 50(1), 171–185.

Price, S. A., Friedman, S. T., Corn, K. A., Larouche, O., Brockelsby, K., Lee, A. J., Nagaraj, M., Bertrand, N. G., Danao, M., Coyne, M. C., Estrada, J. R., Friedman, R., Hoeft, E., Iwan, M., Gross, D., Kao, J. H., Landry, B., Linares, M. J., McGlinn, C., … Wainwright, P. C. (2022). FishShapes v1: Functionally relevant measurements of teleost shape and size on three dimensions. Ecology, 103(12), e3829. https://doi.org/10.1002/ecy.3829

Price, S. A., Friedman, S. T., & Wainwright, P. C. (2015). How predation shaped fish: The impact of fin spines on body form evolution across teleosts. Proceedings of the Royal Society B: Biological Sciences, 282(1819), 20151428. https://doi.org/10.1098/rspb.2015.1428

Price, S. A., Holzman, R., Near, T. J., & Wainwright, P. C. (2011). Coral reefs promote the evolution of morphological diversity and ecological novelty in labrid fishes: Reefs promote fish morphological diversity. Ecology Letters, 14(5), 462–469. https://doi.org/10.1111/j.1461-0248.2011.01607.x

R Core Team. (n.d.). R: A language and environment for statistical computing. [Computer software]. R Foundation for Statistical Computing. https://www.R-project.org/

Rabosky, D. L., Chang, J., Title, P. O., Cowman, P. F., Sallan, L., Friedman, M., Kaschner, K., Garilao, C., Near, T. J., Coll, M., & Alfaro, M. E. (2018). An inverse latitudinal gradient in speciation rate for marine fishes. Nature, 559(7714), 392–395. https://doi.org/10.1038/s41586-018-0273-1

Randall, J. E. (1967). Food habits of reef fishes of the werst indies. Studies in Tropical Oceanography, 66, 665–847.

Revell, L. J. (2012). phytools: An R package for phylogenetic comparative biology (and other things). Methods in Ecology and Evolution, 3(2), 217–223. https://doi.org/10.1111/j.2041-210X.2011.00169.x

Rincón, P. A., Bastir, M., & Grossman, G. D. (2007a). Form and performance: Body shape and prey-capture success in four drift-feeding minnows. Oecologia, 152(2), 345–355. https://doi.org/10.1007/s00442-006-0651-5

Rincón, P. A., Bastir, M., & Grossman, G. D. (2007b). Form and performance: Body shape and prey-capture success in four drift-feeding minnows. Oecologia, 152(2), 345–355. https://doi.org/10.1007/s00442-006-0651-5

Robinson, D. M., Tudor, M. S., & Morris, M. R. (2011). Female preference and the evolution of an exaggerated male ornament: The shape of the preference function matters. Animal Behaviour, 81(5), 1015–1021. https://doi.org/10.1016/j.anbehav.2011.02.005

Rodriguez-Silva, R., Spikes, M., Iturriaga, M., Bennett, K., Josaphat, J., Torres-Pineda, P., Bräger, S., & Schlupp, I. (2022). Feeding strategies and diet variation in livebearing fishes of the

genus Limia (Cyprinodontiformes: Poeciliidae) in the Greater Antilles. Ecology of Freshwater Fish, 31(2), 389–400. https://doi.org/10.1111/eff.12638

Satterfield, D., Claverie, T., & Wainwright, P. (2022). Data from: Body shape and mode of propulsion do not constrain routine swimming in coral reef fishes (Version 3, p. 6931589 bytes) [dataset]. [object Object]. https://doi.org/10.25338/B8R056

Satterfield, D. R., Yin, B., Jung, S., Hodges-Lisk, S., Wainwright, D. K., Burns, M. D., & Wainwright, P. C. (In Review). Weak integration allows novel fin shapes and spurs locomotor diversity in reef fishes. Evolution.

Schaeffer, J., Benton, M. J., Rayfield, E. J., & Stubbs, T. L. (2020). Morphological disparity in theropod jaws: Comparing discrete characters and geometric morphometrics. Palaeontology, 63(2), 283–299. https://doi.org/10.1111/pala.12455

Schluter, D. (1996). Adaptive radiation along genetic lines of least resistance. Evolution, 50(5), 1766–1774. https://doi.org/10.1111/j.1558-5646.1996.tb03563.x

Schmidt, M., & Fischer, M. S. (2009). Morphological integration in mammalian limb proportions: Dissociation between function and development. Evolution, 63(3), 749–766. https://doi.org/10.1111/j.1558-5646.2008.00583.x

Schmitt, R. J., & Coyer, J. A. (1982). The foraging ecology of sympatric marine fish in the genus Embiotoca (Embiotocidae): Importance of foraging behavior in prey size selection. Oecologia, 55(3), 369–378. https://doi.org/10.1007/BF00376925

Schneider, C. A., Rasband, W. S., & Eliceiri, K. W. (2012). NIH Image to ImageJ: 25 years of image analysis. Nature Methods, 9(7), 671–675. https://doi.org/10.1038/nmeth.2089

Schultz, William. W. (2002). Power Requirements of Swimming: Do New Methods Resolve Old Questions? Integrative and Comparative Biology, 42(5), 1018–1025. https://doi.org/10.1093/icb/42.5.1018

Sepulveda, C., & Dickson, K. A. (2000). Maximum Sustainable Speeds and Cost of Swimming in Juvenile Kawakawa Tuna (Euthynnus Affinis) and Chub Mackerel (Scomber Japonicus). Journal of Experimental Biology, 203(20), 3089–3101. https://doi.org/10.1242/jeb.203.20.3089

Sfakiotakis, M., Lane, D. M., & Davies, J. B. C. (1999). Review of fish swimming modes for aquatic locomotion. IEEE Journal of Oceanic Engineering, 24(2), 237–252. https://doi.org/10.1109/48.757275

Shuai, F., Yu, S., Lek, S., & Li, X. (2018). Habitat effects on intra-species variation in functional morphology: Evidence from freshwater fish. Ecology and Evolution, 8(22), 10902–10913. https://doi.org/10.1002/ece3.4555

Siqueira, A. C., Morais, R. A., Bellwood, D. R., & Cowman, P. F. (2020). Trophic innovations fuel reef fish diversification. Nature Communications, 11(1), 2669. https://doi.org/10.1038/s41467-020-16498-w

Sordino, P., van der Hoeven, F., & Duboule, D. (1995). Hox gene expression in teleost fins and the origin of vertebrate digits. Nature, 375(6533), 678–681. https://doi.org/10.1038/375678a0

Stewart, W. J., & Higham, T. E. (2014). Passively stuck: Death does not affect gecko adhesion strength. Biology Letters, 10(12), 20140701. https://doi.org/10.1098/rsbl.2014.0701

Tan, W. C., Vanhooydonck, B., Measey, J., & Herrel, A. (2020). Morphology, locomotor performance and habitat use in southern African agamids. Biological Journal of the Linnean Society, 130(1), 166–177. https://doi.org/10.1093/biolinnean/blaa024

Tebbett, S. B., Goatley, C. H. R., & Bellwood, D. R. (2017). Clarifying functional roles: Algal removal by the surgeonfishes Ctenochaetus striatus and Acanthurus nigrofuscus. Coral Reefs, 36(3), 803–813. https://doi.org/10.1007/s00338-017-1571-z

Tokić, G., & Yue, D. K. P. (2012). Optimal shape and motion of undulatory swimming organisms. Proceedings of the Royal Society B: Biological Sciences, 279(1740), 3065–3074. https://doi.org/10.1098/rspb.2012.0057

Tytell, E. D. (2007). Do trout swim better than eels? Challenges for estimating performance based on the wake of self-propelled bodies. Experiments in Fluids, 43(5), 701–712. https://doi.org/10.1007/s00348-007-0343-x

Tytell, E. D., Borazjani, I., Sotiropoulos, F., Baker, T. V., Anderson, E. J., & Lauder, G. V. (2010). Disentangling the Functional Roles of Morphology and Motion in the Swimming of Fish. Integrative and Comparative Biology, 50(6), 1140–1154. https://doi.org/10.1093/icb/icq057

Tytell, E. D., & Lauder, G. V. (2004). The hydrodynamics of eel swimming. Journal of Experimental Biology, 207(11), 1825–1841. https://doi.org/10.1242/jeb.00968

van Eeden, F. J. M., Granato, M., Schach, U., Brand, M., Furutani-Seiki, M., Haffter, P., Hammerschmidt, M., Heisenberg, C.-P., Jiang, Y.-J., Kane, D. A., Kelsh, R. N., Mullins, M. C., Odenthal, J., Warga, R. M., & Nüsslein-Volhard, C. (1996). Genetic analysis of fin formation in the zebrafish, Danio rerio. Development, 123(1), 255–262. https://doi.org/10.1242/dev.123.1.255

Vidal-García, M., & Scott Keogh, J. (2017). Phylogenetic conservatism in skulls and evolutionary lability in limbs – morphological evolution across an ancient frog radiation is shaped by diet, locomotion and burrowing. BMC Evolutionary Biology, 17(1), 165. https://doi.org/10.1186/s12862-017-0993-0

Videler, J. J. (1993). Fish Swimming. Springer Netherlands. https://doi.org/10.1007/978-94-011-1580-3

Videler, J. J., & Wardle, C. S. (1991). Fish swimming stride by stride: Speed limits and endurance. Reviews in Fish Biology and Fisheries, 1(1), 23–40. https://doi.org/10.1007/BF00042660

Villéger, S., Brosse, S., Mouchet, M., Mouillot, D., & Vanni, M. J. (2017). Functional ecology of fish: Current approaches and future challenges. Aquatic Sciences, 79(4), 783–801. https://doi.org/10.1007/s00027-017-0546-z

Villmoare, B., Fish, J., & Jungers, W. (2011a). Selection, Morphological Integration, and Strepsirrhine Locomotor Adaptations. Evolutionary Biology, 38(1), 88–99. https://doi.org/10.1007/s11692-011-9108-9

Villmoare, B., Fish, J., & Jungers, W. (2011b). Selection, Morphological Integration, and Strepsirrhine Locomotor Adaptations. Evolutionary Biology, 38(1), 88–99. https://doi.org/10.1007/s11692-011-9108-9

Wainwright, P. C. (1987). Biomechanical limits to ecological performance: Mollusc-crushing by the Caribbean hogfish, Lachnolaimus maximus (Labridae). Journal of Zoology, 213(2), 283–297. https://doi.org/10.1111/j.1469-7998.1987.tb03704.x

Wainwright, P. C. (1996). Ecological Explanation through Functional Morphology: The Feeding Biology of Sunfishes. Ecology, 77(5), 1336–1343. https://doi.org/10.2307/2265531

Wainwright, P. C. (2009). Innovation and Diversity in Functional Morphology. In M. Laubichler & J. Maienschein (Eds.), Form and Function in Developmental Evolution (pp. 132–152). Cambridge University Press.

Wainwright, P. C., & Bellwood, D. R. (2002). Ecomorphology of Feeding in Coral Reef Fishes. In In: Sale P.F., editor. Coral Reef Fishes: Dynamics and Diversity in a Complex Ecosystem (pp. 33–55). Academic Press. https://doi.org/10.1016/B978-012615185-5/50004-9

Wainwright, P. C., Bellwood, D. R., & Westneat, M. W. (2002). Ecomorphology of Locomotion in Labrid Fishes. Environmental Biology of Fishes, 65(1), 47–62. https://doi.org/10.1023/A:1019671131001

Wainwright, P. C., Bellwood, D. R., Westneat, M. W., Grubich, J. R., & Hoey, A. S. (2004). A functional morphospace for the skull of labrid fishes: Patterns of diversity in a complex biomechanical system. Biological Journal of the Linnean Society, 82(1), 1–25. https://doi.org/10.1111/j.1095-8312.2004.00313.x

Walker, J. A. (2000). Does a Rigid Body Limit Maneuverability? Journal of Experimental Biology, 203(22), 3391–3396. https://doi.org/10.1242/jeb.203.22.3391

Walker, J. A. (2002). Kinematics, Dynamics, and Energetics of Rowing and Flapping Propulsion in Fishes. Integrative and Comparative Biology, 42(5), 1032–1043. https://doi.org/10.1093/icb/42.5.1032

Walker, J. A., Alfaro, M. E., Noble, M. M., & Fulton, C. J. (2013). Body Fineness Ratio as a Predictor of Maximum Prolonged-Swimming Speed in Coral Reef Fishes. PLoS ONE, 8(10), e75422. https://doi.org/10.1371/journal.pone.0075422

Webb, P. W. (1984a). Body Form, Locomotion and Foraging in Aquatic Vertebrates. American Zoologist, 24(1), 107–120. https://doi.org/10.1093/icb/24.1.107

Webb, P. W. (1984b). Form and Function in Fish Swimming. Scientific American, 251(1), 72–83.

Webb, P. W. (2004). Maneuverability—General Issues. IEEE Journal of Oceanic Engineering, 29(3), 547–555. https://doi.org/10.1109/JOE.2004.833220

Weihs, D. (2002). Stability Versus Maneuverability in Aquatic Locomotion. Integrative and Comparative Biology, 42(1), 127–134. https://doi.org/10.1093/icb/42.1.127

Welsh, J. Q., & Bellwood, D. R. (2012). Spatial ecology of the steephead parrotfish (Chlorurus microrhinos): An evaluation using acoustic telemetry. Coral Reefs, 31(1), 55–65. https://doi.org/10.1007/s00338-011-0813-8

Wikramanayake, E. D. (1990). Ecomorphology and Biogeography of a Tropical Stream Fish Assemblage: Evolution of Assemblage Structure. Ecology, 71(5), 1756–1764. https://doi.org/10.2307/1937583

Wimberly, A. N., Slater, G. J., & Granatosky, M. C. (2021). Evolutionary history of quadrupedal walking gaits shows mammalian release from locomotor constraint. Proceedings of the Royal Society B: Biological Sciences, 288(1957), 20210937. https://doi.org/10.1098/rspb.2021.0937

Winemiller, K. O. (1991). Ecomorphological Diversification in Lowland Freshwater Fish Assemblages from Five Biotic Regions. Ecological Monographs, 61(4), 343–365. https://doi.org/10.2307/2937046

Young, N. M., & Hallgrímsson, B. (2005). Serial Homology and the Evolution of Mammalian Limb Covariation Structure. Evolution, 59(12), 2691–2704. https://doi.org/10.1111/j.0014-3820.2005.tb00980.x

Young, N. M., Wagner, G. P., & Hallgrímsson, B. (2010). Development and the evolvability of human limbs. Proceedings of the National Academy of Sciences, 107(8), 3400–3405. https://doi.org/10.1073/pnas.0911856107

Zelditch, M. L., & Goswami, A. (2021). What does modularity mean? Evolution & Development, 23(5), 377–403. https://doi.org/10.1111/ede.12390

Appendix 1: Chapter 1 Supplementary Materials

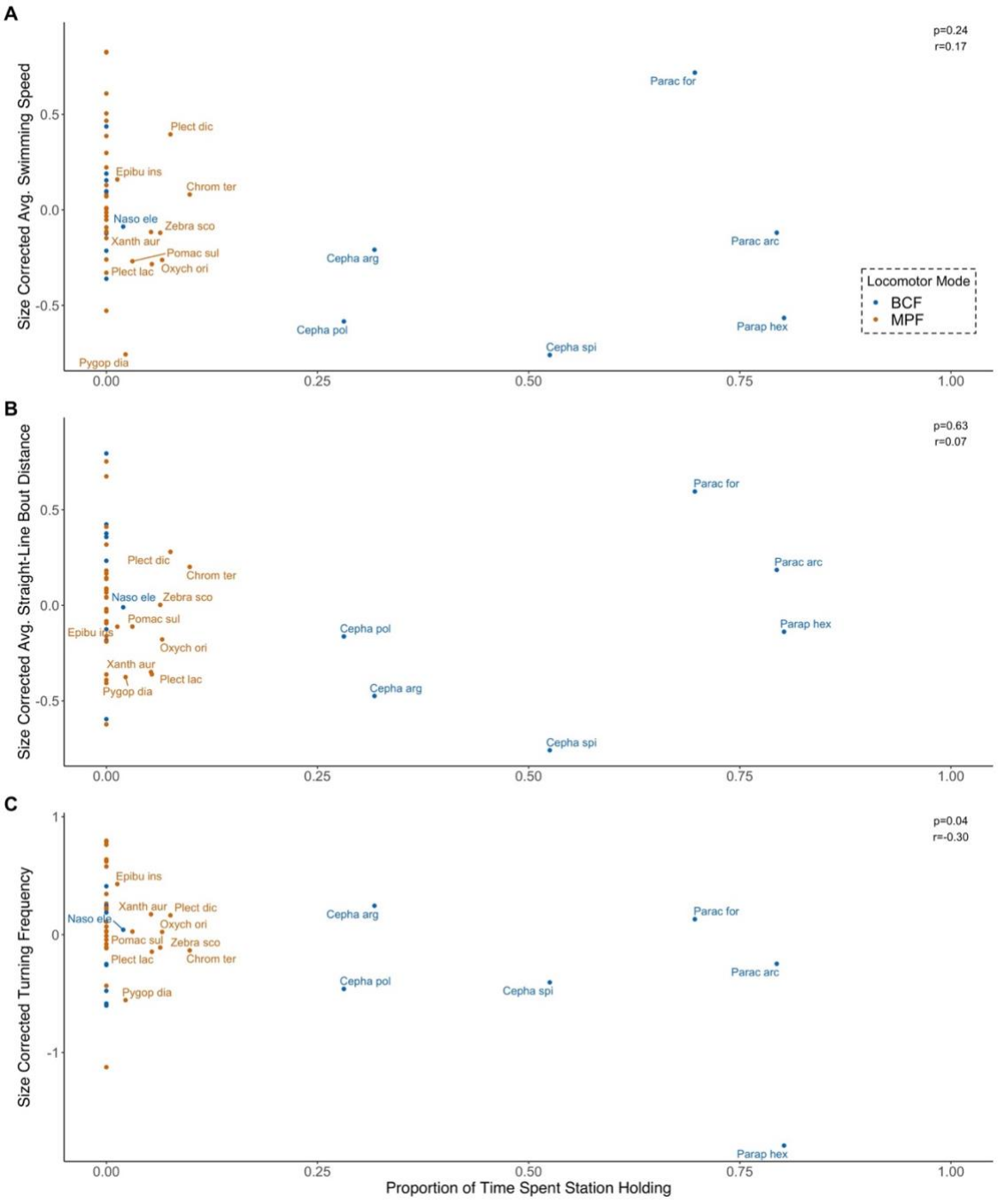

Figure S1. **Relationships between Station Holding and other Behaviors.** Each panel shows the relationship between the proportion of time spent station holding and A) the size corrected average swimming speed, B) the average straight-line swimming bout distance, and C) the turn frequency. Points represent species averages and are labeled by the first 5 letters of the genus and

first 3 letters of the species. For very similar species, the last 3 letters are also provided. Average swimming speed values are the residuals of the relationship between the natural log of a species' average swimming speed during bouts of straight line swimming (cm/s) and the natural log of the average fish body length (cm), shown in Fig. 2A. Turning Frequency values are the residuals of the relationship between the natural log of a species' average number of turns per second and the natural log of the average fish body length (cm), shown in Fig. 2B. Average straight-line swimming bout distance values are the residuals of the relationship between the natural log of a species' average distance traveled during straight line swimming and the natural log of the average fish body length (cm), shown in Fig. 2C. The proportion of time spent station holding is calculated as the proportion of time spent sitting still to the total observation time. Species are color coded by locomotor mode. Blue points and bars represent body caudal fin swimmers (BCF), orange points and bars represent median paired fin swimmers (MPF). P and r values were calculated using phylogenetic general least squares regression.

Table S1. **Species Replacements for Body Shape Data.** The species in this left column of this table are those that behavioral data was collected for but are not sampled in the body shape data set (Price et al., 2022). The species used as replacements are in the right column.

Species in Behavioral Data	Replacement Species From Price et al., (2020)
Anampses meleagrides	*Anampses twistii*
Arothron meleagris	*Arothron nigropunctatus*
Cephalopholis spiloparaea	*Cephalopholis miniata*
Chaetodon mitratus	*Chaetodon fremblii*
Chromis fieldi	*Chromis margaritifer*
Chromis viridis	*Chromis atripectoralis*
Naso elegans	*Naso lituratus*
Oxycheilinus orientalis	*Oxycheilinus unifasciatus*
Parupeneus macronemus	*Parupeneus multifasciatus*
Pomacentrus sulfureus	*Pomacentrus trilineatus*
Scarus caudofasciatus	*Scarus festivus*

Literature Cited:

Price, S. A., Friedman, S. T., Corn, K. A., Larouche, O., Brockelsby, K., Lee, A. J., Nagaraj, M., Bertrand, N. G., Danao, M., Coyne, M. C., Estrada, J. R., Friedman, R., Hoeft, E., Iwan, M., Gross, D., Kao, J. H., Landry, B., Linares, M. J., McGlinn, C., … Wainwright, P. C. (2022). FishShapes v1: Functionally relevant measurements of teleost shape and size on three dimensions. *Ecology*. https://doi.org/10.1002/ECY.3829

Table S2. **Correlations between Swimming Variables and Body Shapes.** The *p* and *r* values are given for the PGLS regressions of each swimming behavior against each body shape ratio. Body shape variables were calculated from Price et al., (2022) data. Body elongation is calculated as body depth divided by standard length (BD/SL). Cross sectional area is the body depth divided by body width (BD/FW). Second moment of area is $((\pi*BD*FW^3)/4)$. Jaw length, mouth width, and head depth were size corrected by dividing by SL. Turning Frequency values are the residuals of the relationship between the natural log of a species' average number of turns per second and the natural log of SL. Average straight-line swimming bout distance values are the residuals of the relationship between the natural log of a species' average distance traveled during straight line swimming and the natural log of SL. The proportion of time spent station holding is calculated as the proportion of time spent sitting still to the total observation time.

Body Shapes	Speed		Turn Frequency		Distance		Station Holding	
	p	*r*	*p*	*r*	*p*	*r*	*p*	*r*
Body Elongation	0.46	0.11	0.05	0.28	0.48	0.10	0.08	0.26
Cross Section Area	0.22	0.18	0.37	0.13	0.47	0.11	0.24	0.17
Jaw Length	0.57	0.08	0.51	0.10	0.52	0.10	0.15	0.20
Mouth Width	0.70	0.06	0.56	0.09	0.57	0.08	0.74	0.05
Head Depth	0.95	0.01	0.54	0.09	0.91	0.02	0.18	0.20
Caudal Peduncle Width	0.10	0.24	0.23	0.18	0.96	0.01	0.27	0.16
Caudal Peduncle Depth	0.30	0.15	0.07	0.27	0.48	0.10	0.97	0.01
Second Moment of Area	0.99	0.00	0.25	0.17	0.23	0.18	0.17	0.20

Literature Cited:

Price, S. A., Friedman, S. T., Corn, K. A., Larouche, O., Brockelsby, K., Lee, A. J., Nagaraj, M., Bertrand, N. G., Danao, M., Coyne, M. C., Estrada, J. R., Friedman, R., Hoeft, E., Iwan, M., Gross, D., Kao, J. H., Landry, B., Linares, M. J., McGlinn, C., … Wainwright, P. C. (2022). FishShapes v1: Functionally relevant measurements of teleost shape and size on three dimensions. *Ecology*. https://doi.org/10.1002/ECY.3829

Appendix 2: Chapter 2 Supplementary Materials

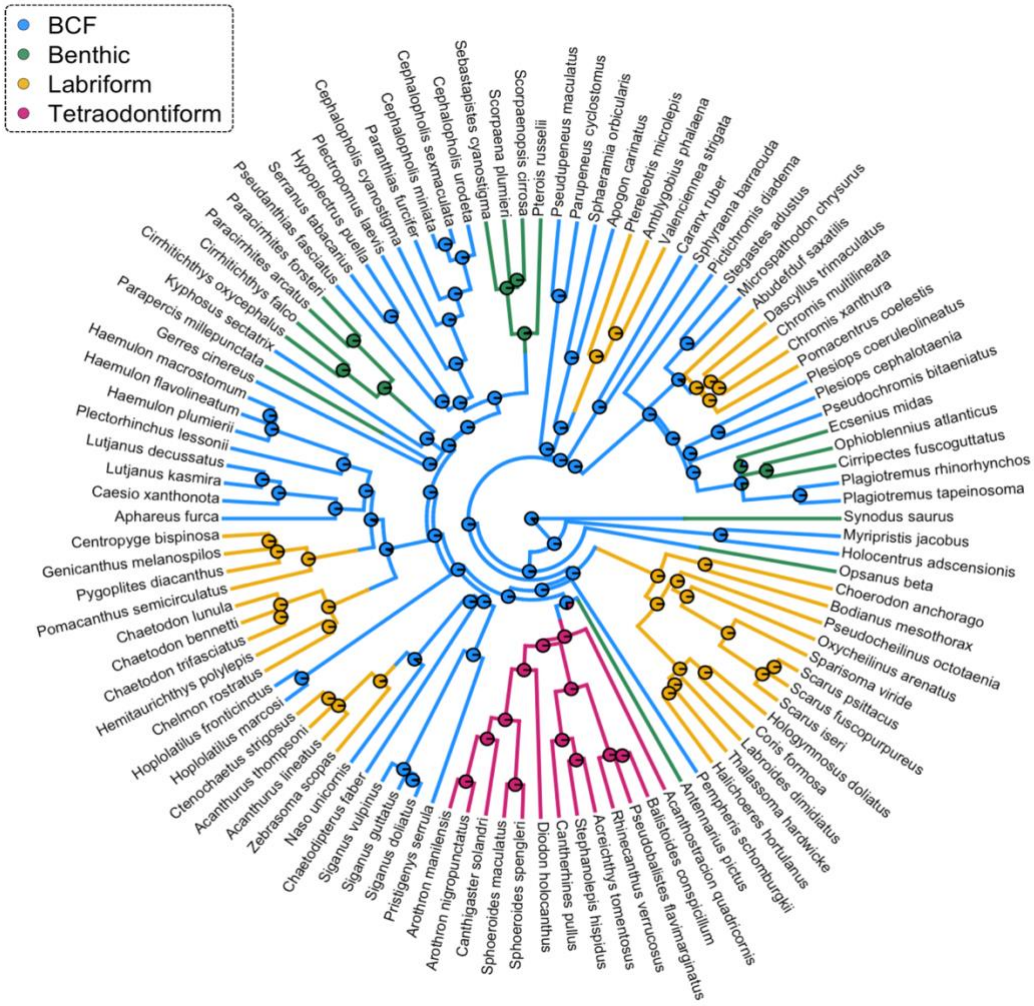

Figure S1. **Stochastic character map of the history of locomotor styles with species tip labels**, with pie charts indicating the node state percentage out of 1000 maps. Blue represents body caudal fin (BCF) swimmers, or those species with use the undulation of their body and caudal to move forward. Yellow lineages are median paired fin (MPF) swimmers that use the pectoral fin as the predominant propulsor (labriform), and in pink are MPF swimmers which use the dorsal and anal fin for propulsion (tetraodontiform). Green represents benthic species.

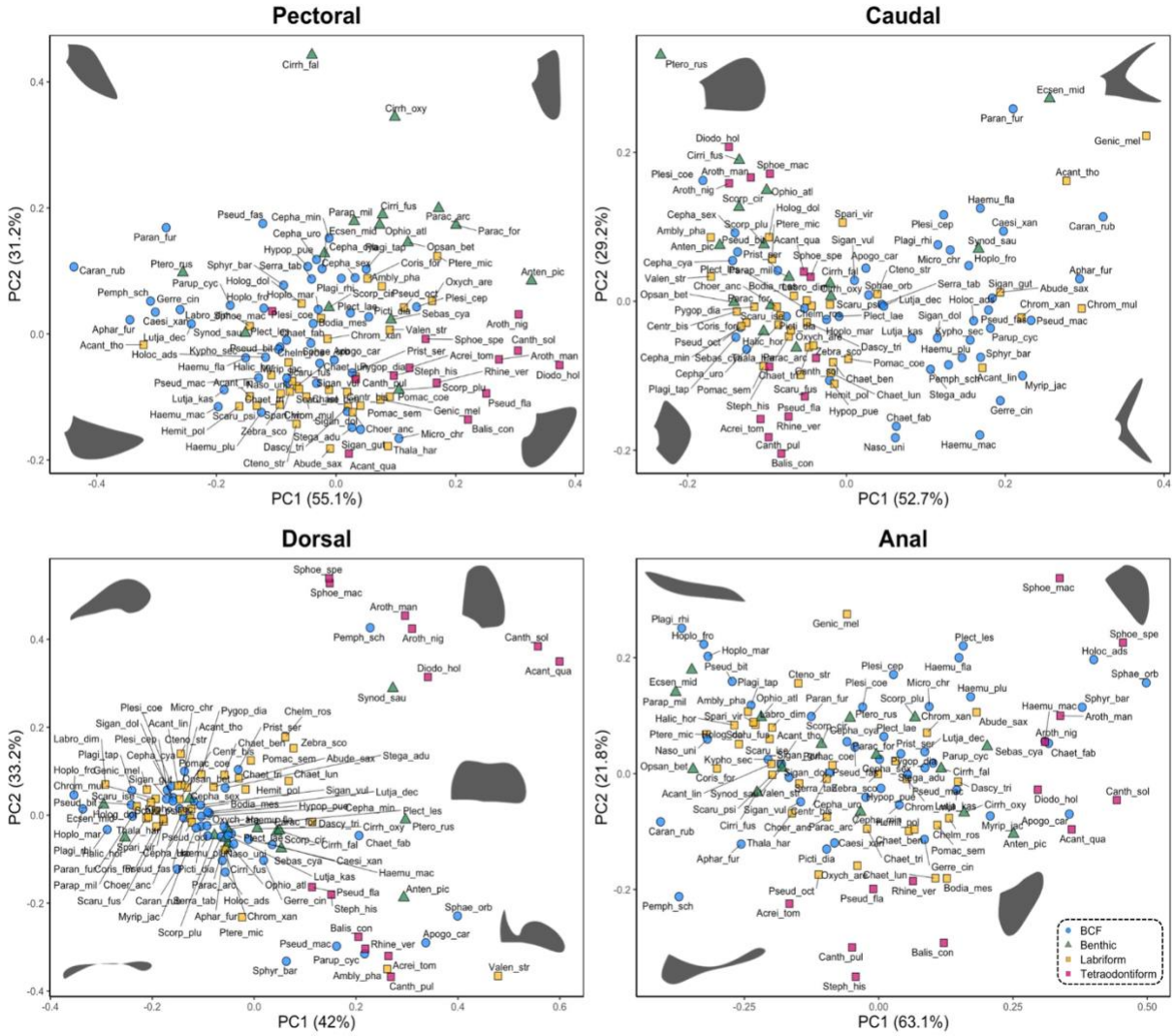

Figure S2. **Fin shape PC2 Vs PC1 plots with species labels.** These plots are the same axes as in figure 2, the fin shape morphospaces for the pectoral, caudal, dorsal, and anal fins. Here abbreviations for species names have been added. The abbreviations are the first 5 letters of the genus and first 3 letters of the species separated by an underscore. Each point represents the average Procrustes superimposed fin shape for a species. Blue circles represent body caudal fin (BCF) swimming species. Green triangles are benthic species. Squares represent median paired fin (MPF) swimming species. MPF Labriform species in yellow, and pink are MPF Tetraodontiform swimmers. A sample of fin shapes have been plotted for each morphospace.

Table S1. Species List. Table includes the name of the species for which fin data was collected, substituted names made to match the Rabosky et al., (2018) phylogeny, the family name, and the locomotor style categorization. Locomotor style classifications were determined from literature review and personal observation (Fulton 2007; Korsmeyer et al., 2002; Webb 1984; PCW; DRS)

Species	Substitution	Family	Locomotor Style
Abudefduf_saxatilis		Pomacentridae	Labriform
Acanthostracion_quadricornis		Ostraciidae	Tetraodontiform
Acanthurus_lineatus		Acanthuridae	Labriform
Acanthurus_thompsoni		Acanthuridae	Labriform
Acreichthys_tomentosus		Monacanthidae	Tetraodontiform
Amblygobius_phalaena		Gobiidae	Labriform
Antennarius_pictus		Antennariidae	Benthic
Aphareus_furca		Lutjanidae	BCF
Apogon_novemfasciatus	*Apogon_carinatus*	Apogonidae	BCF
Arothron_manilensis		Tetraodontidae	Tetraodontiform
Arothron_nigropunctatus		Tetraodontidae	Tetraodontiform
Assessor_randalli	*Plesiops_cephalotaenia*	Plesiopidae	BCF
Balistoides_conspicillum		Balistidae	Tetraodontiform
Bodianus_mesothorax		Labridae	Labriform
Caesio_cuning	*Caesio_xanthonota*	Caesionidae	BCF
Cantherhines_pullus		Monacanthidae	Tetraodontiform
Canthigaster_solandri		Tetraodontidae	Tetraodontiform
Caranx_ruber		Carangidae	BCF
Centropyge_bispinosa		Pomacanthidae	Labriform
Cephalopholis_boenak	*Cephalopholis_sexmaculata*	Serranidae	BCF
Cephalopholis_cyanostigma		Serranidae	BCF
Cephalopholis_miniata		Serranidae	BCF
Cephalopholis_urodeta		Serranidae	BCF
Chaetodipterus_faber		Ephipidae	BCF

Chaetodon_bennetti		Chaetodontidae	Labriform
Chaetodon_lunula		Chaetodontidae	Labriform
Chaetodon_trifasciatus		Chaetodontidae	Labriform
Chelmon_rostratus		Chaetodontidae	Labriform
Choerodon_anchorago		Labridae	Labriform
Chromis_multilineata		Pomacentridae	Labriform
Chromis_xanthura		Pomacentridae	Labriform
Cirrhitichthys_falco		Cirrhitidae	Benthic
Cirrhitichthys_oxycephalus		Cirrhitidae	Benthic
Coris_formosa		Labridae	Labriform
Crossosalarias_macrospilus	*Cirripectes_fuscoguttatus*	Blenniidae	Benthic
Ctenochaetus_strigosus		Acanthuridae	Labriform
Dascyllus_trimaculatus		Pomacentridae	Labriform
Diodon_holacanthus		Diodontidae	Tetraodontiform
Echidna_nebulosa		Muraenidae	BCF
Ecsenius_midas		Blenniidae	Benthic
Exallias_brevis	*Ophioblennius_atlanticus*	Blenniidae	Benthic
Genicanthus_melanospilos		Pomacanthidae	Labriform
Gerres_cinereus		Gerreide	BCF
Haemulon_flavolineatum		Haemulidae	BCF
Haemulon_macrostomum		Haemulidae	BCF
Haemulon_plumierii		Haemulidae	BCF
Halichoeres_hortulanus		Labridae	Labriform
Hemitaurichthys_polylepis		Chaetodontidae	Labriform
Holocentrus_coruscum	*Holocentrus_adscensionis*	Holocentridae	BCF
Hologymnosus_doliatus		Labridae	Labriform
Hoplolatilus_cuniculus	*Hoplolatilus_fronticinctus*	Malacanthidae	BCF
Hoplolatilus_fourmanoiri	*Hoplolatilus_marcosi*	Malacanthidae	BCF
Hypoplectrus_puella		Serranidae	BCF

Kyphosus_sectatrix		Kyphosidae	BCF
Labricinus_cyclophthalmus	*Pseudochromis_bitaeniatus*	Pseudochromidae	BCF
Labroides_dimidiatus		Labridae	Labriform
Lutjanus_decussatus		Lutjanidae	BCF
Lutjanus_kasmira		Lutjanidae	BCF
Meiacanthus_atrodorsalis	*Plagiotremus_tapeinosoma*	Blenniidae	BCF
Microspathodon_chrysurus		Pomacentridae	BCF
Monacanthus_hispidus	*Stephanolepis_hispidus*	Monacanthidae	Tetraodontiform
Myripristis_jacobus		Holocentridae	BCF
Naso_unicornis		Acanthuridae	BCF
Opsanus_beta		Batrachoididae	Benthic
Oxycheilinus_orientalis	*Oxycheilinus_arenatus*	Labridae	Labriform
Paracirrhites_arcatus		Cirrhitidae	Benthic
Paracirrhites_forsteri		Cirrhitidae	Benthic
Paranthias_furcifer		Serranidae	BCF
Parapercis_tetracantha	*Parapercis_millepunctata*	Parapercidae	Benthic
Paraplesiops_poweri	*Plesiops_coeruleolineatus*	Plesiopidae	BCF
Parupeneus_cyclostomus		Mullidae	BCF
Pempheris_schomburgkii		Pempheridae	BCF
Pictichromis_diadema		Pseudochromidae	BCF
Plagiotremus_rhinorhynchos		Blenniidae	BCF
Plectorhinchus_orientalis	*Plectorhinchus_lessonii*	Haemulidae	BCF
Plectropomus_laevis		Serranidae	BCF
Pomacanthus_semicirculatus		Pomacanthidae	Labriform
Pomacentrus_coelestris		Pomacentridae	Labriform
Pristigenys_serrula		Priacanthidae	BCF
Pseudanthias_dispar	*Pseudanthias_fasciatus*	Serranidae	BCF
Pseudobalistes_flavimarginatus		Balistidae	Tetraodontiform
Pseudocheilinus_octotaenia		Labridae	Labriform

Pseudupeneus_maculatus		Mullidae	BCF
Ptereleotris_microlepis		Ptereleotridae	Labriform
Pterois_russelii		Scorpaenidae	Benthic
Pygoplites_diacanthus		Pomacanthidae	Labriform
Rhinecanthus_verrucosus		Balistidae	Tetraodontiform
Scarus_fuscocaudalis	*Scarus_fuscopurpureus*	Scaridae	Labriform
Scarus_iseri		Scaridae	Labriform
Scarus_psittacus		Scaridae	Labriform
Scorpaena_plumieri		Scorpaenidae	Benthic
Sebastapistes_cyanostigma		Scorpaenidae	Benthic
Serranus_tabacarius		Serranidae	BCF
Siganus_doliatus		Siganidae	BCF
Siganus_gutattus		Siganidae	BCF
Siganus_vulpinus		Siganidae	BCF
Sparisoma_viride		Scaridae	Labriform
Sphaeramia_orbicularis		Apogonidae	BCF
Sphoeroides_maculatus		Tetraodontidae	Tetraodontiform
Sphoeroides_spengleri		Tetraodontidae	Tetraodontiform
Sphyraena_barracuda		Sphyraenidae	BCF
Stegastes_adustus		Pomacentridae	BCF
Synodus_saurus		Synodontidae	Benthic
Taenionotus_triacanthus	*Scorpaenopsis_cirrosa*	Scorpaenidae	Benthic
Thalassoma_hardwicke		Labridae	Labriform
Valenciennea_strigata		Gobiidae	Labriform
Zebrasoma_xanthurum	*Zebrasoma_scopas*	Acanthuridae	Labriform

Literature Cited

Fulton, C. J. (2007). Swimming speed performance in coral reef fishes: field validations reveal distinct functional groups. *Coral reefs*, *26*(2), 217-228

Korsmeyer, K. E., Steffensen, J. F., & Herskin, J. (2002). Energetics of median and paired fin swimming, body and caudal fin swimming, and gait transition in parrotfish (Scarus schlegeli) and triggerfish (Rhinecanthus aculeatus). *Journal of experimental biology*, *205*(9), 1253-1263.

Rabosky D.L., Chang J., Title P.O., Cowman P.F., Sallan L., Friedman M., Kaschner K., Garilao C., Near T.J., Coll M., Alfaro M.E. 2018. An inverse latitudinal gradient in speciation rate for marine fishes. Nature 559:392–395.

Webb, P. W. (1984). Form and function in fish swimming. *Scientific American*, *251*(1), 72-83.

Table S2. **Fin Shape Disparity by Locomotor Mode.** Disparities have been corrected for the number of landmarks for each fin. Pairwise *P*-values comparing disparity between locomotor groups are given in the lower half of the table. The p-values associated with disparities which significantly differ by locomotor mode are bolded.

Disparity	Pectoral	Caudal	Dorsal	Anal
BCF	0.031	0.032	0.047	0.053
Bethic	0.052	0.034	0.047	0.041
MPF - Lab.	0.022	0.034	0.043	0.029
MPF - Tet.	0.031	0.031	0.126	0.066
Pairwise Comparison				
BCF : Benthic	**0.014**	0.831	0.982	0.306
BCF : MPF - Lab.	0.227	0.830	0.740	**0.007**
BCF : MPF - Tet.	0.956	0.898	**< 0.001**	0.330
Benthic : MPF - Lab.	**0.002**	0.964	0.828	0.352
Benthic : MPF - Tet.	0.057	0.773	**< 0.001**	0.102
MPF - Lab. : MPF - Tet.	0.357	0.778	**< 0.001**	**0.005**

Table S3. **Hyper Volume Results Pairwise Locomotor Group Comparisons.** Comparisons of the hypervolumes of species within a locomotor group against the hypervolumes of other locomotor groups in a pairwise manner. The table contains the fraction of the hypervolume space which is unique to each hypervolume, and the p-values calculated as the proportion of 10,000 permutations (hypervolume identity was randomly assigned to average fin shape landmarks) in which the unique hypervolume space was more extreme than observed. P-values less that 0.05 (bolded) indicate the real hypervolume occupies more unique space than expected relative to a null distribution. Real hypervolumes and random permutations were generated in *Hypervolume (v 3.1.3; R).*

Hv1	Hv2	unique frac. Hv1	Prop. Of permuted Dist. > unique frac. Hv1	unique frac. Hv2	Prop. Of permuted Dist. > unique frac. Hv2
Pectoral					
BCF	Benthic	0.247	0.7435	0.727	**0.0014**
BCF	Labriform	0.440	0.1252	0.201	0.5879
BCF	Tetraodontiform	0.709	**0.0078**	0.516	0.0890
Benthic	Labriform	0.811	**0.0000**	0.256	0.6627
Benthic	Tetraodontiform	0.847	**0.0000**	0.295	0.4555
Labriform	Tetraodontiform	0.609	0.1000	0.544	0.0573
Caudal					
BCF	Benthic	0.694	0.0315	0.320	0.3942
BCF	Labriform	0.432	0.2589	0.272	0.5061
BCF	Tetraodontiform	0.838	**0.0003**	0.547	0.0465
Benthic	Labriform	0.430	0.3826	0.671	0.2321
Benthic	Tetraodontiform	0.671	0.1902	0.586	0.2611
Labriform	Tetraodontiform	0.808	0.0864	0.582	0.1979
Dorsal					
BCF	Benthic	0.486	0.4759	0.476	0.3738
BCF	Labriform	0.557	0.2351	0.222	0.6717
BCF	Tetraodontiform	0.627	0.1933	0.933	**0.0000**
Benthic	Labriform	0.651	0.2087	0.398	0.5477
Benthic	Tetraodontiform	0.540	0.1809	0.919	**0.0001**
Labriform	Tetraodontiform	0.628	0.2128	0.962	**0.0000**
Anal					
BCF	Benthic	0.556	0.1596	0.173	0.7474
BCF	Labriform	0.758	**0.0002**	0.119	0.9251
BCF	Tetraodontiform	0.752	**0.0207**	0.666	**0.0152**
Benthic	Labriform	0.729	**0.0022**	0.471	0.3370
Benthic	Tetraodontiform	0.763	**0.0022**	0.829	**0.0000**
Labriform	Tetraodontiform	0.454	0.3138	0.798	**0.0003**

Table S4. **Fin by fin comparisons of phylogenetic integration all species included.** This table differs from Table 3 in that here integrations were calculated with all species included. This gives us the overall pattern of evolutionary integration between fins. Table 3 in contrast tells us the integration between fin shapes for species within locomotor groupings. Results generated using *Geomorph (v 4.0.5; R).* Statistically significant integrations were determined based on 1000 iterations and are denoted by p-values (*P)* which are bolded.

Fin By Fin Phylo. Integration	**All Species Included**		
	***r*-PLS**	**Effect (*Z*)**	***P***
Pectoral - Dorsal	0.28	0.82	0.195
Pectoral - Caudal	0.39	2.97	**0.001**
Pectoral - Anal	0.33	2.10	**0.016**
Dorsal - Caudal	0.42	2.95	**0.001**
Dorsal - Anal	0.62	4.92	**0.001**
Caudal - Anal	0.47	3.55	**0.001**

Appendix 3: Chapter 3 Supplementary Materials

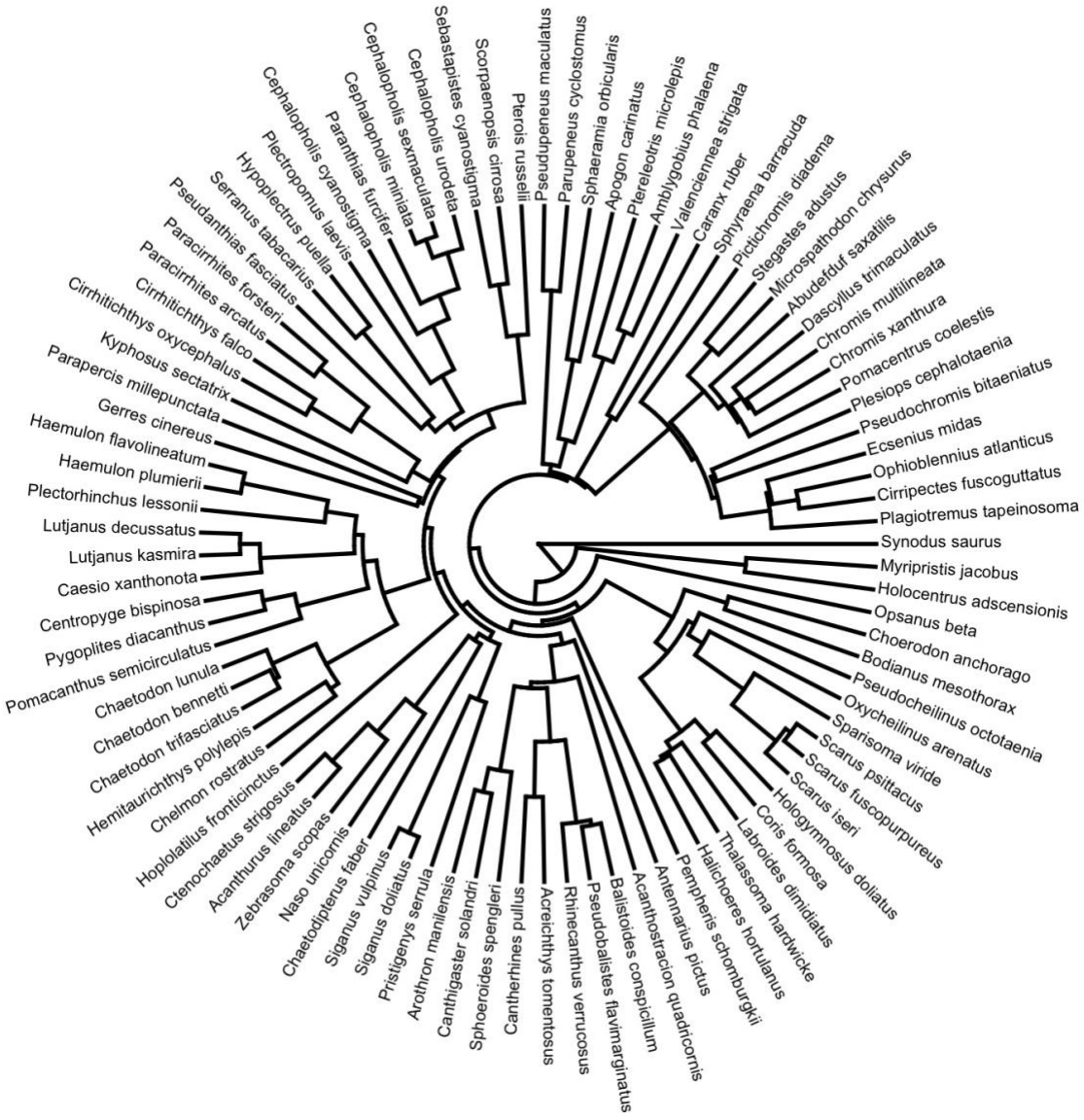

Figure S1. **Reef fish phylogeny.** This phylogeny contains the species (N=93) in my morphological modules data sets and is used in all my phylogenetic analyses. It was pruned from a large time calibrated ray-finned fishes phylogeny from Rabosky et al., (2018) using the associated package *fishtree* (v 0.3.4, R).

Rabosky D.L., Chang J., Title P.O., Cowman P.F., Sallan L., Friedman M., Kaschner K., Garilao C., Near T.J., Coll M., Alfaro M.E. 2018. An inverse latitudinal gradient in speciation rate for marine fishes. Nature 559:392–395.

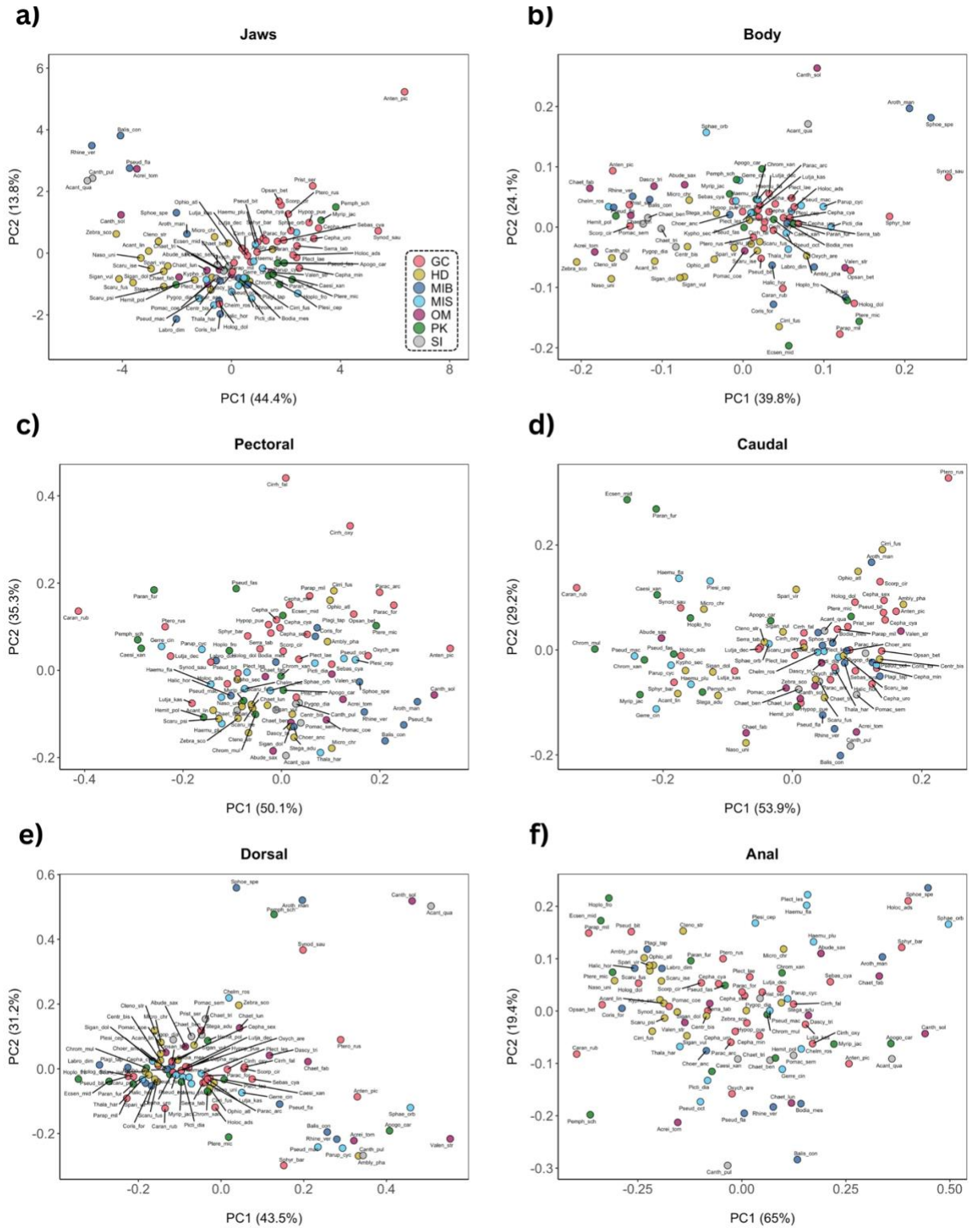

Figure S2. **Reef fish morphospaces for six morphological modules of the functional feeding system with species abbreviations.** Each morphospace is constructed from a principal components analysis where, in the case of **a)** jaws, the loadings are the 12 linear dimensions. For **b)** the body **c)** the pectoral fin, **d)** the caudal fin, **e)** the dorsal fin and **f)** the anal fin the loadings

are Procrustes superimposed geometric morphometric landmark coordinates. Each point represents the average morphology for a species (N=93). Species are abbreviated by the first five letters of the genus and the first three letters of the species separated by an underscore. Species are color coded by diet following Burns et al (In Review). GC = Generalized Carnivore, HD = Herbivore Detritivore, MIB = Mobile Invertivore Biter, MIS = Mobile Invertivore Suction, OM = Omnivore, PK = Planktivore, SI = Sessile Invertivore.

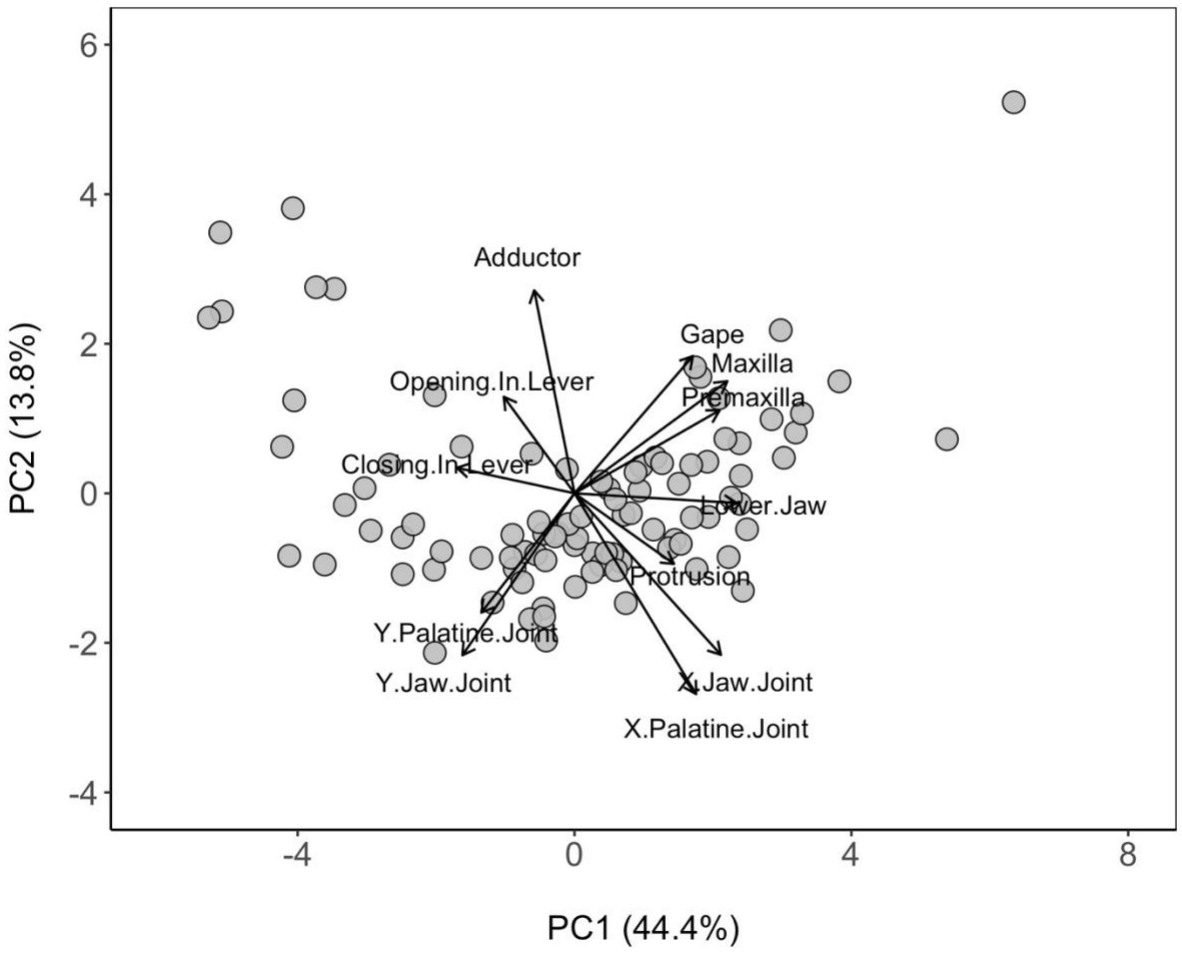

Figure S3. **Jaw morphospace with loadings.** The loadings of the 12 linear measurements used to characterize jaw morphology (see Table S3) are displayed on the first two principal component axes of the jaw morphospace.

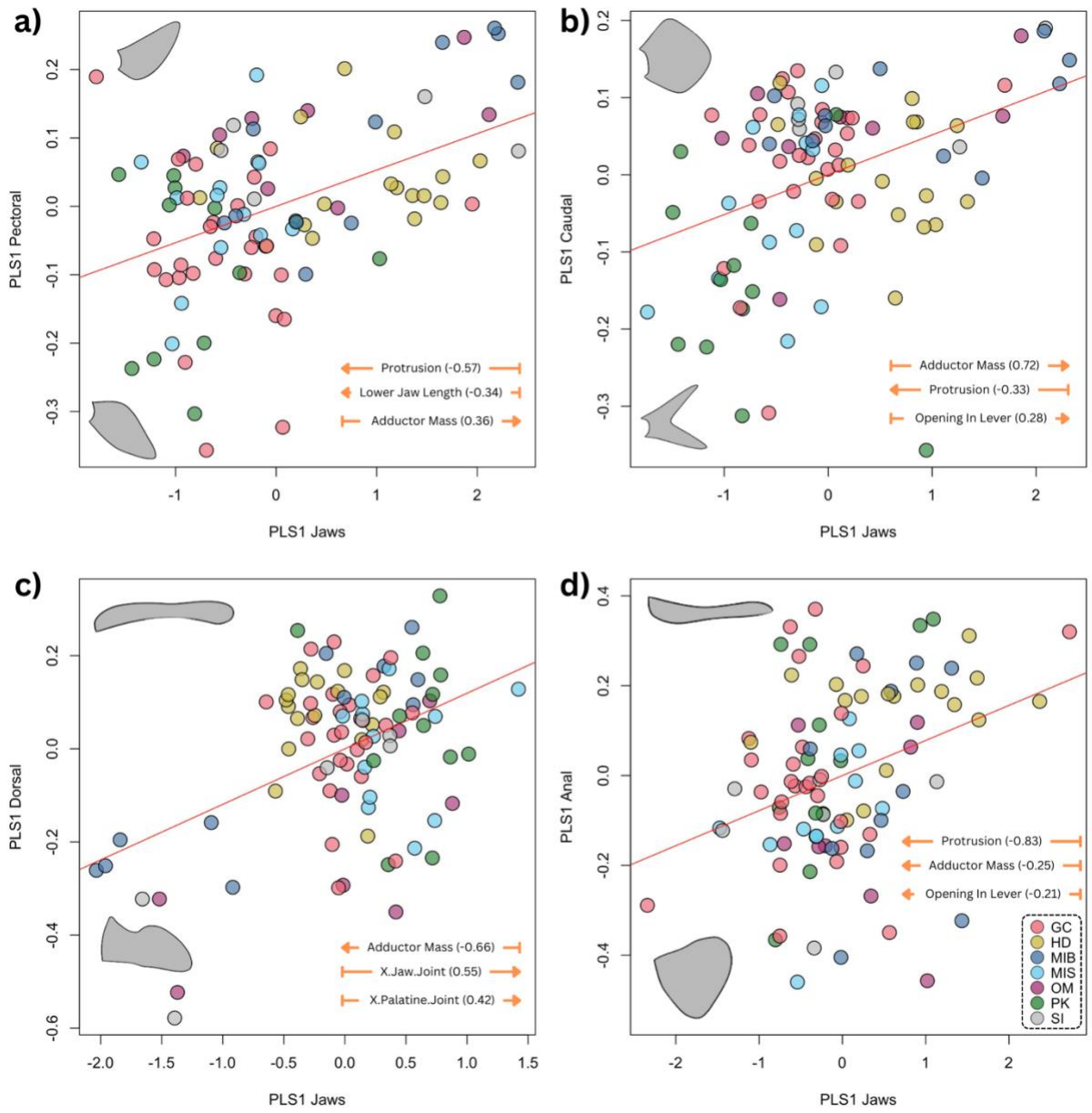

Figure S4. **Integration between the jaws and fins.** The first partial least squares axis (PLS1) of the jaws versus **a**) PLS1 of the pectoral fin, **b)** PLS1 of the caudal fin, **c)** PLS1 of the Dorsal fin, and **d)** PLS1 of the anal fin. The red trendlines represent the best fit integration line. Orange horizontal arrows represent the three jaw traits which load most strongly with PLS1 of the jaws. The numbers inside parentheses within these arrows represent the strength and direction of the loading. Species are color coded by diet following Burns et al (In Review). GC = Generalized Carnivore, HD = Herbivore Detritivore, MIB = Mobile Invertivore Biter, MIS = Mobile Invertivore Suction, OM = Omnivore, PK = Planktivore, SI = Sessile Invertivore.

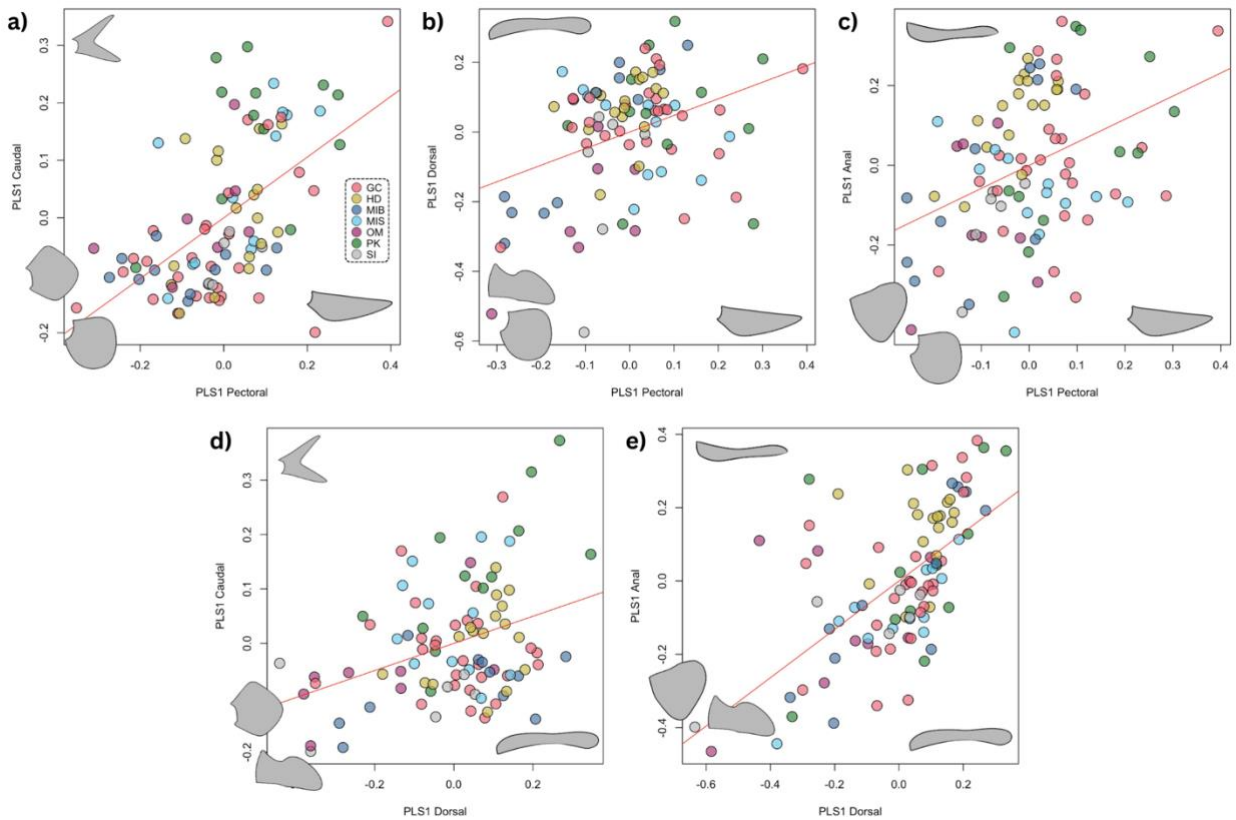

Figure S5. **Integration between fins.** The first partial least squares axis (PLS1) of **a)** the caudal fin versus the pectoral fin, **b)** the dorsal fin versus the pectoral fin, **c)** the anal fin versus the pectoral fin, **d)** the caudal fin versus the dorsal fin, **e)** the anal fin versus the dorsal fin. Red trendlines represent the best fit integration line. The plot for the dorsal versus the anal is included in Figure 5 in the main text. Species are color coded by diet following Burns et al (In Review). GC = Generalized Carnivore, HD = Herbivore Detritivore, MIB = Mobile Invertivore Biter, MIS = Mobile Invertivore Suction, OM = Omnivore, PK = Planktivore, SI = Sessile Invertivore.

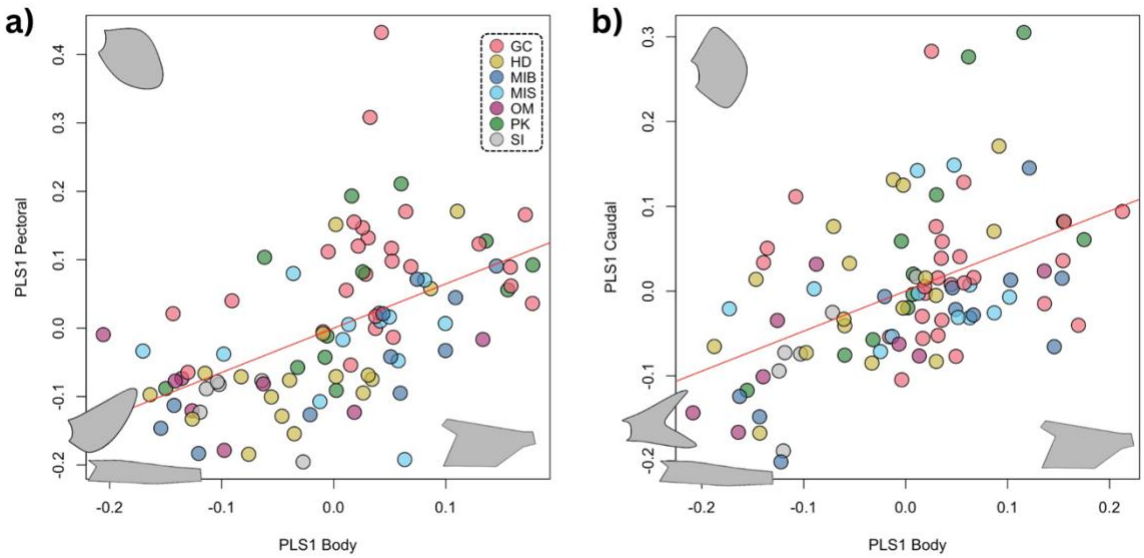

Figure S6. **Integration between the body and fins.** The first partial least squares axis (PLS1) of the body and **a)** the pectoral fin, and **b)** the caudal fin. Red trendlines represent the best fit integration line. The plots for the body integration with the dorsal and anal fin are included in Figure 5 in the main text. Species are color coded by diet following Burns et al (In Review). GC = Generalized Carnivore, HD = Herbivore Detritivore, MIB = Mobile Invertivore Biter, MIS = Mobile Invertivore Suction, OM = Omnivore, PK = Planktivore, SI = Sessile Invertivore.

Table S1. **Species list**. Table includes the name of the species for which morphological data was available or collected, substituted names made to match the Rabosky et al., (2018) phylogeny, the family name, and the diet categorization. Diet classifications follow definitions in Burns et al., (in Review) which were modified from Siqueira et al. (2020). GC = Generalized Carnivore, HD = Herbivore Detritivore, MIB = Mobile Invertivore Biter, MIS = Mobile Invertivore Suction, OM = Omnivore, PK = Planktivore, SI = Sessile Invertivore.

Species	Substitution	Family	Diet
Abudefduf_saxatilis		Pomacentridae	OM
Acanthostracion_quadricornis		Ostraciidae	SI
Acanthurus_lineatus		Acanthuridae	HD
Acreichthys_tomentosus		Monacanthidae	OM
Amblygobius_phalaena		Gobiidae	HD
Antennarius_pictus		Antennariidae	GC
Apogon_novemfasciatus	*Apogon_carinatus*	Apogonidae	PK
Arothron_manilensis		Tetraodontidae	MIB
Assessor_randalli	*Plesiops_cephalotaenia*	Plesiopidae	MIS
Balistoides_conspicillum		Balistidae	MIB
Bodianus_mesothorax		Labridae	MIB
Caesio_cuning	*Caesio_xanthonota*	Caesionidae	PK
Cantherhines_pullus		Monacanthidae	SI
Canthigaster_solandri		Tetraodontidae	OM
Caranx_ruber		Carangidae	GC
Centropyge_bispinosa		Pomacanthidae	HD
Cephalopholis_boenak	*Cephalopholis_sexmaculata*	Serranidae	GC
Cephalopholis_cyanostigma		Serranidae	GC
Cephalopholis_miniata		Serranidae	GC
Cephalopholis_urodeta		Serranidae	GC
Chaetodipterus_faber		Ephipidae	OM

Chaetodon_bennetti		Chaetodontidae	SI
Chaetodon_lunula		Chaetodontidae	OM
Chaetodon_trifasciatus		Chaetodontidae	SI
Chelmon_rostratus		Chaetodontidae	MIS
Choerodon_anchorago		Labridae	MIB
Chromis_multilineata		Pomacentridae	PK
Chromis_xanthura		Pomacentridae	PK
Cirrhitichthys_falco		Cirrhitidae	GC
Cirrhitichthys_oxycephalus		Cirrhitidae	GC
Coris_formosa		Labridae	MIB
Crossosalarias_macrospilus	*Cirripectes_fuscoguttatus*	Blenniidae	HD
Ctenochaetus_strigosus		Acanthuridae	HD
Dascyllus_trimaculatus		Pomacentridae	OM
Ecsenius_midas		Blenniidae	PK
Exallias_brevis	*Ophioblennius_atlanticus*	Blenniidae	HD
Gerres_cinereus		Gerreide	MIS
Haemulon_flavolineatum		Haemulidae	MIS
Haemulon_plumierii		Haemulidae	MIS
Halichoeres_hortulanus		Labridae	MIB
Hemitaurichthys_polylepis		Chaetodontidae	PK
Holocentrus_coruscum	*Holocentrus_adscensionis*	Holocentridae	GC
Hologymnosus_doliatus		Labridae	GC
Hoplolatilus_cuniculus	*Hoplolatilus_fronticinctus*	Malacanthidae	PK
Hypoplectrus_puella		Serranidae	GC
Kyphosus_sectatrix		Kyphosidae	HD
Labricinus_cyclophthalmus	*Pseudochromis_bitaeniatus*	Pseudochromidae	GC
Labroides_dimidiatus		Labridae	MIB
Lutjanus_decussatus		Lutjanidae	GC

Lutjanus_kasmira		Lutjanidae	GC
Meiacanthus_atrodorsalis	*Plagiotremus_tapeinosoma*	Blenniidae	MIB
Microspathodon_chrysurus		Pomacentridae	HD
Myripristis_jacobus		Holocentridae	PK
Naso_unicornis		Acanthuridae	HD
Opsanus_beta		Batrachoididae	GC
Oxycheilinus_orientalis	*Oxycheilinus_arenatus*	Labridae	GC
Paracirrhites_arcatus		Cirrhitidae	GC
Paracirrhites_forsteri		Cirrhitidae	GC
Paranthias_furcifer		Serranidae	PK
Parapercis_tetracantha	*Parapercis_millepunctata*	Parapercidae	GC
Parupeneus_cyclostomus		Mullidae	MIS
Pempheris_schomburgkii		Pempheridae	PK
Pictichromis_diadema		Pseudochromidae	MIS
Plectorhinchus_orientalis	*Plectorhinchus_lessonii*	Haemulidae	MIS
Plectropomus_laevis		Serranidae	GC
Pomacanthus_semicirculatus		Pomacanthidae	SI
Pomacentrus_coelestris		Pomacentridae	OM
Pristigenys_serrula		Priacanthidae	GC
Pseudanthias_dispar	*Pseudanthias_fasciatus*	Serranidae	PK
Pseudobalistes_flavimarginatus		Balistidae	MIB
Pseudocheilinus_octotaenia		Labridae	MIS
Pseudupeneus_maculatus		Mullidae	MIS
Ptereleotris_microlepis		Ptereleotridae	PK
Pterois_russelii		Scorpaenidae	GC
Pygoplites_diacanthus		Pomacanthidae	SI
Rhinecanthus_verrucosus		Balistidae	MIB
Scarus_fuscocaudalis	*Scarus_fuscopurpureus*	Scaridae	HD

Scarus_iseri		Scaridae	HD
Scarus_psittacus		Scaridae	HD
Sebastapistes_cyanostigma		Scorpaenidae	GC
Serranus_tabacarius		Serranidae	GC
Siganus_doliatus		Siganidae	HD
Siganus_vulpinus		Siganidae	HD
Sparisoma_viride		Scaridae	HD
Sphaeramia_orbicularis		Apogonidae	MIS
Sphoeroides_spengleri		Tetraodontidae	MIB
Sphyraena_barracuda		Sphyraenidae	GC
Stegastes_adustus		Pomacentridae	HD
Synodus_saurus		Synodontidae	GC
Taenionotus_triacanthus	*Scorpaenopsis_cirrosa*	Scorpaenidae	GC
Thalassoma_hardwicke		Labridae	MIS
Valenciennea_strigata		Gobiidae	OM
Zebrasoma_xanthurum	*Zebrasoma_scopas*	Acanthuridae	HD

Rabosky D.L., Chang J., Title P.O., Cowman P.F., Sallan L., Friedman M., Kaschner K., Garilao C., Near T.J., Coll M., Alfaro M.E. 2018. An inverse latitudinal gradient in speciation rate for marine fishes. Nature 559:392–395.

Table S2. **Body Shape Landmarks**. Landmarks were placed on homologous locations on the reef fish body which are defined in this table. Landmarks were digitized onto lateral images of cleared and stained specimen.

Landmarks	Definitions
Anal Fin Anterior Insertion	Insertion of the last ray of the anal fin into the body
Anal Fin Posterior Insertion	Insertion of the first spine of the anal fin into the body
Caudal Fin Dorsal Insertion	Insertion of the dorsal-most ray of the caudal fin into the body
Caudal Fin Ventral Insertion	Insertion of the ventral-most ray of the anal fin into the body
Dorsal Fin Anterior Insertion	Insertion of the last ray of the dorsal fin into the body
Dorsal Fin Posterior Insertion	Insertion of the first spine (or ray in the absence of spines) of the anal fin into the body
Orbit Anterior	Anterior limit of the orbit
Orbit Dorsal	Dorsal limit of the orbit
Orbit Posterior	Posterior limit of the orbit
Orbit Ventral	Ventral limit of the orbit
Pectoral Fin Dorsal Insertion	Insertion of the dorsal-most ray of the pectoral fin into the body
Pectoral Fin Ventral Insertion	Insertion of the ventral-most ray of the caudal fin into the body
Pectoral Girdle Ventral Tip	Ventral limit of the cleithrum
Skull Dorsal-Anterior Limit	Dorsal-Anterior limit of the skull, where the head meets the body
Skull-Spine Joint	Joint between the skull and the first vertebrae of the spinal column

Table S3. **Oral Jaw Measurements**. This is the list of measurements I retained from a larger set of measurements collected in Burns et al., (In Review). The short-hand abbreviations are used in Figure S? which shows the loadings of the jaw morphospace. Measurements are separated by those that were physically measured on fresh specimen and those that were digitally measured from images of cleared and stained specimen. Measurements were size corrected as ratios of body mass, head length, or lower jaw length.

Shorthand	Definitions
Fresh Specimen	
Adductor	Mass of the adductor mandibulae / Body mass
Gape	Length of mouth gape / Head length
Protrusion	Length of jaw protrusion / Head length
Cleared & Stained Images	
Closing.In.Lever	Length from joint between the quadrate and articular (herein "lower jaw joint") to dorsal tip of the articular / Lower jaw length
Lower.Jaw	Length from the lower jaw joint to the distal tip of the dentary / Head legth
Maxilla	Length from the dorsal tip to ventral tip of the maxilla / Head Length
Premaxilla	Length from the distal tip to the proximal tip of the dentigerous premaxilla / Head length
Opening.In.Lever	Length from the lower jaw joint to the ventral anterior tip of the articular / Lower jaw length
X.Jaw.Joint	Horizontal distance of the lower jaw joint from coordinate origin* / Head length
X.Palatine.Joint	Horizontal distance from the joint between the palatine and the maxilla (herein "palatine joint") and the coordinate origin* / Head length
Y.Jaw.Joint	Verticle distance of the lower jaw joint from coordinate origin* / Head length
Y.Palatine.Joint	Verticle distance of the palatine joint from coordinate origin* / Head length
***Coordinate space was established by centering an origin on the intersection of a verticle line passing through the center of the orbit and a horizontal line from the tip of the dentary and the last vertebrae centra.*	

Burns, M. D., Satterfield, D. R., Peoples, N., Chan, H., Barley, A. J., Roberts-Hugghis, A., Russell, K. T., Hess, M., Williamson, S., Corn, K. A., Mihalitsis, M., Wainwright, D. K., & Wainwright, P. C. (In Review). Complexity & Weak Integration Promote the Diversity of Life: Reef Fish Oral Jaw Evolution. Nature Communications.

Table S4. **Statistical properties of the distributions of distances from the morphological centroid under simulated correlation matrices.** Basic statistics were calculated on the distributions of the simulated species distances from the centroid of the overall morphospace under a correlation matrix where all modules have a correlation of r=0, r=0.5, and r=0.9, and under the empirically observed module correlations for reef fishes. For r=0, r=0.5, and r=0.9 means of the distributions were compared using an ANOVA, variances were compared using a Levene's test, and Anderson-Darling test was used to evaluate differences in the skew of the distributions.

Statistics	***r = 0***	***r = 0.5***	***r = 0.9***	**empiricle *r* matrix**	**Test**	**Result**
Mean	2.34	2.20	1.94	2.25	ANOVA	*p < 0.0001, F: 356.6*
Variance	0.47	0.84	1.82	0.87	Levene's	*p < 0.0001, F: 1422.7*
Skew	0.37	0.99	1.03	0.96	Anderson-Darling	*p < 0.0001, AD: 1486.5*
Median	2.30	2.04	1.65	2.09		
Min	0.41	0.24	0.00	0.24		
Max	5.63	7.28	9.23	7.81		
Range	5.21	7.04	9.23	7.57		

Table S5. **Morphological Module phylogenetic ANOVAs by Diet.** Phylogenetic ANOVAs were calculated using the *procD.pgls* function in the package *geomorph* (v 4.0.7; R). The *pairwise* function in the package *RRPP* (v 4.0.7; R) was used for pairwise comparisons of diet groups. P-values and *F* statistics where mean morphology significantly differs by diet are bolded. For modules with different mean morphology by diet the pairwise least squares comparisons are provided to indicate which diet differ in morphology from each other.

Phylo. ANOVA	Jaws	Body	Pectoral	Caudal	Dorsal	Anal	Overall	Residuals
p	**0.001**	**0.017**	0.077	**0.001**	**0.013**	0.060	**0.001**	**0.003**
F	**2.549**	**1.757**	1.472	**2.893**	**1.769**	1.639	**3.119**	**2.522**
Pairwise Comparison								
GC:HD	**0.029**	0.411		0.888	0.949		**0.002**	0.478
GC:MIB	0.244	0.934		0.897	0.772		0.594	0.975
GC:MIS	0.140	0.590		0.340	0.899		0.110	0.442
GC:OM	**0.031**	0.157		0.640	**0.015**		**0.003**	**0.031**
GC:PK	**0.024**	0.777		**0.001**	0.890		**0.001**	**0.001**
GC:SI	0.138	0.689		0.974	0.628		**0.040**	0.929
HD:MIB	0.665	0.471		0.860	0.666		0.177	0.494
HD:MIS	0.056	0.294		0.823	0.980		**0.031**	0.378
HD:OM	0.719	0.727		0.691	**0.010**		0.104	**0.049**
HD:PK	**0.041**	0.418		**0.010**	0.772		**0.003**	**0.024**
HD:SI	0.705	0.918		0.938	0.449		0.658	0.643
MIB:MIS	0.251	0.808		0.381	0.438		0.309	0.200
MIB:OM	0.505	0.221		0.875	**0.003**		**0.010**	**0.010**
MIB:PK	0.232	0.884		**0.001**	0.931		**0.003**	**0.005**
MIB:SI	0.587	0.738		0.979	0.355		0.340	0.628
MIS:OM	0.293	0.317		0.574	0.148		0.062	0.155
MIS:PK	0.931	0.416		0.091	0.560		**0.008**	**0.015**
MIS:SI	0.349	0.608		0.822	0.881		0.326	0.919
OM:PK	0.290	0.125		**0.003**	**0.001**		**0.001**	**0.001**
OM:SI	0.995	0.848		0.990	0.506		0.934	0.325
PK:SI	0.459	0.693		**0.026**	0.205		**0.003**	**0.012**